

**EMPIRICAL STUDIES OF LAMINAR FLOW IN  
POROUS CONSOLIDATED MEDIA**

by

**Jay Herbert Lehr**

---

**A Dissertation Submitted to the Faculty of the**

**DEPARTMENT OF HYDROLOGY**

**In Partial Fulfillment of the Requirements  
For the Degree of**

**DOCTOR OF PHILOSOPHY**

**In the Graduate College**

**THE UNIVERSITY OF ARIZONA**

**1 9 6 2**

THE UNIVERSITY OF ARIZONA

GRADUATE COLLEGE

I hereby recommend that this dissertation prepared under my direction by Jay Herbert Lehr entitled EMPIRICAL STUDIES OF LAMINAR FLOW IN POROUS CONSOLIDATED MEDIA be accepted as fulfilling the dissertation requirement of the degree of Doctor of Philosophy

John H. Hesterman  
Dissertation Director

May 11, 1962  
Date

After inspection of the dissertation, the following members of the Final Examination Committee concur in its approval and recommend its acceptance:\*

<u>Henry J. Miles</u>	<u>May 8, 1962</u>
<u>John G. Ferris</u>	<u>May 8, 1962</u>
<u>Herbert F. Shultz</u>	<u>May 8, 1962</u>
<u>Lee Resnick</u>	<u>May 9, 1962</u>
<u>John H. Hesterman</u>	<u>May 11, 1962</u>

\*This approval and acceptance is contingent on the candidate's adequate performance and defense of this dissertation at the final oral examination. The inclusion of this sheet bound into the library copy of the dissertation is evidence of satisfactory performance at the final examination.

STATEMENT BY AUTHOR

This dissertation has been submitted in partial fulfillment of requirements for an advanced degree at The University of Arizona and is deposited in The University Library to be made available to borrowers under rules of the Library.

Brief quotations from this thesis are allowable without special permission, provided that accurate acknowledgment of source is made. Requests for permission for extended quotation from or reproduction of this manuscript in whole or in part may be granted by the head of the major department or the Dean of the Graduate College when in their judgment the proposed use of the material is in the interests of scholarship. In all other instances, however, permission must be obtained from the author.

SIGNED: \_\_\_\_\_

*Jay Herbert Lehr*

## ABSTRACT

### EMPIRICAL STUDIES OF LAMINAR FLOW IN POROUS CONSOLIDATED MEDIA

by

Jay Herbert Lehr

The influence of geologic factors in controlling flow patterns in hydraulic systems is evaluated by hydraulic models which are constructed as a porous consolidated media that simulates the interstitial geometry of consolidated rocks. Colored inks are injected into the flow system and are observed through the transparent sides of the model case. Visual analysis of the flow system, leads to salient conclusions concerning fundamental aspects of complex flow systems.

Empirical experiments were conducted on the following aspects:

- (1) Refraction of flow lines across lithologic interfaces: The law of streamline refraction, as described by King Hubbert, was found to be correct where boundary conditions do not interfere.
- (2) Continuity of flow around and through highly permeable and impermeable lenses of different lithologies: The flow system around impermeable lenses indicates the nonexistence of stagnant areas where a hydraulic gradient is imposed on a saturated ground water system.
- (3) Flow net system caused by a single pumping well: Transient changes of individual flow vectors, within the immediate

area of influence, were analyzed at the moment pumping began. The absence of a transition phase indicates a rapid adjustment of the flow system to the pumping condition.

- (4) Flow net system of mutual interference of depression cones caused by pumping multiple wells: This permitted an analysis of the ground water divide. Flow bands divided into flow paths which moved in opposite directions.
- (5) Effects of emplacing pumping wells in highly permeable media: The increased area of influence of water movement to wells was clearly illustrated. This analysis demonstrates the capture of partially confined flow from great depths.
- (6) The relation of the shape of artificial recharge pits to infiltration rate: Variations of flow net systems of rectangular and wedge-shaped pits were analyzed. When all other factors were held constant, the shape of the recharge pit was found to have no important effect upon recharge rate.
- (7) Flow toward an effluent stream: The potential head of ground water beneath the stream was found to increase with depth.
- (8) The relationship between hydraulic gradient and flow net configuration: The hydraulic gradient was found to have no effect on the flow net of a confined system, but a definite effect upon unconfined flow systems, in as much as it alters the water table which is the upper flow boundary.
- (9) Flow pattern through tilted and faulted sedimentary structures: The geometric convergence of the aquifer boundaries caused the convergence of flow lines through a

brecciated fault zone. A possible genesis of a hydrothermal vein ore was suggested by this flow pattern.

- (10) Formation of perched water tables: The mechanisms by which saturated ground water mounds can be formed on a low permeability lens was demonstrated. Evidence was found which indicates that perched ground water probably escapes through the perching body as well as around its extremities.
- (11) Confluence of gravity water and saturated flow: Unsaturated flow arriving at the water table of the saturated ground water body becomes an integral part of that body which acts as a single hydrodynamic system.
- (12) Artesian ground water systems: A model illustrating the classic artesian aquifer situation was constructed, and flowing and non-flowing artesian wells were studied. A ground water mound was formed in the water table aquifer by water discharging naturally from the artesian aquifer through a fault in the confining layer.
- (13) Subsidence around a pumping well: Water was pumped from a simulated artesian well, the piezometric surface in the vicinity of the well was lowered and the overburden was observed to subside while compressing the artesian aquifer.
- (14) Cone of depression formed around single and multiple well systems: The drawdown at any point within the area of influence of a multiple well system was shown to be equal to the sum of the individual drawdowns of each well in the multiple well system, provided recharge and evaporation are

neglected.

Information resulting from these studies will provide guides for scientific development and exploitation of ground water supplies. Contributions were made that will advance the use of hydraulic models as exploratory tools in scientific hydrology. Further, this work brought into focus the importance of hydraulic models as communication media for interpreting cause-effect relationships in highly complex flow systems, of the type that so often are involved in regional problems of water resource development and management.

## ACKNOWLEDGMENTS

Grateful acknowledgment is made to H. E. Skibitzke and H. T. Chapman of the Water Resource Division, United States Geological Survey, for their ideas on the formation of a consolidated medium for use in hydraulic models, and to H. E. Skibitzke for his help in defining the hydrodynamic theory involved in this work. I wish to thank Dr. John W. Harshbarger for his help and advice throughout the project.

## TABLE OF CONTENTS

<u>CHAPTER</u>	<u>PAGE</u>
I. INTRODUCTION . . . . .	1
II. REVIEW OF LITERATURE . . . . .	5
III. THE HYDRODYNAMIC ANALOGY . . . . .	18
IV. METHODOLOGY. . . . .	33
V. MODEL EXPERIMENTS AND RESULTS. . . . .	47
VI. CONCLUSIONS. . . . .	145
BIBLIOGRAPHY . . . . .	148

## TABLE OF FIGURES

FIGURE	PAGE
1.	Photograph of a horizontal type model containing ink reservoir cups . . . . . 42
2.	Photograph of a small vertical type model containing ink injection tubes. . . . . 42
3.	Photographic history of a horizontal refraction model. The pictures were taken at the following times after the entrance of ink: A at 6 min., B at 16 min., and C at 32 min. . . . . 51
4.	Flow net diagram of the horizontal refraction model shown in Figure 3. . . . . 52
5.	Photographs of an arcuate refraction model taken before and after the movement of ink flow bands through the system. . . 61
6.	Flow net diagram of the arcuate refraction model in Figure 5 64
7.	Photographic history of a horizontal lens model. The pictures were taken at the following times after the entrance of ink: A at 6 min., B at 18 min., C at 34 min., D at 44 min. . . . . 67
8.	Flow net diagram of the horizontal lens model in Figure 7. . 70
9.	Photographic history of a small vertical well model. The pictures were taken at the following times: A at 23 min. after the entrance of ink, B at 2 min. after pumping began which was 24 min. after entrance of ink, C at 10 min. after pumping. . . . . 72

FIGURE	PAGE
9. (continued) Photographic history of a small vertical well model. The pictures were taken at the following times: D at 6 min. after pumping stopped, pumping had continued for 11 min., E at 25 min. after pumping stopped. . . . .	73
10. Flow net diagram of the small vertical well model in Figure 9 . . . . .	76
11. Photographic history of a large vertical double well model. The pictures were taken at the following times after the entrance of ink: A at 6 min., B at 16 min., C at 26 min., and D at 28 min. . . . .	79
12. Flow net diagram of the large vertical double well model in Figure 11. . . . .	80
13. Flow net diagram illustrating an incorrect representation of a hypothetical ground water divide. . . . .	82
14. Photographic history of a large vertical layer model. The pictures were taken at the following times: A at 0 min., B at 7 min., and C at 51 min. after entrance of ink, D at 10 min. after the start of pumping in the two wells. Pumping began 52 min. after the entrance of ink. . . . .	85
15. Flow net diagram of the large vertical layer model under non-pumping conditions as shown in Figure 14 . . . . .	87
16. Graph of $Q/Q_0$ versus $K_1/K_2$ for various values of $r_0$ . . . . .	89
17. Photograph of an effluent stream model showing flow bands moving through a porous medium of isotropic permeability . . . . .	92
18. Flow net diagram of effluent stream model shown in Figure 17 . . . . .	94
19. Photographic history of an effluent stream model containing a porous medium of anisotropic permeability. . . . .	95

FIGURE	PAGE
20. Photographic history of a fault model illustrating the movement of ink flow bands under a hydraulic gradient of 3.3%. The pictures were taken at the following times: A at 1.5 min., B at 14.2 min., C at 25.6 min., and D at 55 min . . . . .	99
21. Flow net diagram of the fault model shown in Figure 20 . .	100
22. Photographic history of the fault model illustrating the movement of flow bands under a hydraulic gradient. The pictures were taken at the following times: A at 120 min., B at 130 min., and C at 140 min. . . . .	102
23. Photographic history of a recharge model containing a wedge shaped pit. The pictures were taken at the following times after the entrance of ink: A at 0 min., B at 1-1/2 min., C at 2-3/4 min., and D at 18-3/4 min . . . . .	107
24. Photographic history of a recharge model containing a rectangular shaped pit. The pictures were taken at the following times after the entrance of ink: A at 0 min., B at 1-1/2 min., C at 3 min., and D at 26 min. . . . .	108
25. Flow net diagram of the recharge model containing a wedge shaped pit as shown in Figure 23 . . . . .	111
26. Flow net diagram of the recharge model containing a rectangular shaped pit as shown in Figure 24 . . . . .	112
27. Photographic history of an infiltration model as clear water infiltrates into the dry porous medium. The pictures were taken at the times shown in the photographs . . . . .	114
28. Continuation of photographic history shown in Figure 27 of an infiltration model as clear water infiltrates into the dry porous medium. The pictures were taken at the times shown in the photographs . . . . .	115

FIGURE

PAGE

29.	Photographic history of the infiltration model as ink is injected into the unsaturated zone in the fine grained medium and the saturated zone in the lower coarse grained medium. The pictures were taken at the times shown in the photographs. . . . .	117
30.	Photographic history of the infiltration model as ink is injected into unsaturated zone of the coarse grained medium. This is a continuation of Figure 29. The pictures were taken at the times shown in the photographs . . . . .	118
31.	Photograph of the infiltration model showing a perched water body on the uppermost clay lens, being recharged by water from the saturated zone . . . . .	122
32.	Photograph of an artesian well model showing water levels in three wells under static water level conditions . . . . .	126
33.	Photograph of an artesian well model showing ink flow bands, while well C <sub>5</sub> is being pumped. . . . .	126
34.	Photographic history of an artesian subsidence model before and after pumping in Well A. The white line represents the bottom of the overburden before pumping. . . . .	131
35.	Photograph of a cone of depression model with its static water level drawn in white . . . . .	134
36.	Photograph of the cone of depression model after pumping in well B had reached a steady state. The cone of depression is drawn in black . . . . .	135
37.	Photograph of the cone of depression model after pumping in well A had reached a steady state. The cone of depression is drawn in yellow. . . . .	135
38.	Photograph of the cone of depression model after pumping in wells A and B had reached a steady state. The existing multiple cone of depression is drawn in red, while the individual cones of depression of wells A and B (as shown	

**FIGURE**

**PAGE**

in Figures 36 and 27) are drawn in yellow and black, respectively . . . . . 135

39. Photographs of the cone of depression model (a) under static water level conditions, (b) after pumping in well B reached a steady state, and (c) after recharging into well B reached a steady state. . . . . 138

40. Photograph of the cone of depression model with well B recharging and well A discharging. The resultant water level is drawn in red. . . . . 140

41. Photographic history of the cone of depression model, as green runoff water infiltrated into the subsurface of the porous medium. . . . . 142

## CHAPTER I

### INTRODUCTION

Statement of Problem. Hydrologists have been describing the characteristics of laminar flow in saturated rock with very little aid from empirical experimentation. A great deal of literature is lacking in clarity and validity due to this fact. There is a need for a hydrodynamic analogy to achieve a better understanding of the affects of geologic factors on ground water flow. Models utilizing viscous fluid, electric circuits, rubber membranes, and unconsolidated sand to study ground water flow have been useful, but have not permitted a broad understanding of the hydrodynamic system within the geologic framework. The problems of boundary conditions and capillary forces have impeded the development of a clear hydrodynamic analogy. There is also a difficulty in proving the future accuracy of any ground water flow models due to the lack of adequate instrumentation for the purpose of measuring the physical parameters within the prototype hydrogeologic structure. The models themselves represent only a small slice or element from an infinite aquifer, and the water moves at greatly magnified speeds. The extremely long periods of time needed to make similar tests within the prototype complicate the analogous studies.

Scope of the Problem. As ground water flow takes place beneath the land surface, it is difficult for the student to envision actual movement in the true space and time dimensions. Further, it

has become apparent that realistic understanding and solution of ground water movement requires basic knowledge of flow net analysis of ground water systems. The development of hydraulic models simulating common geological skeletons in consolidated media, instituted in this study, offers an opportunity for live demonstrations of actual ground water movement. The effects of grain size, various lithologies, boundary conditions, recharge and discharge and well development on ground water movement can be readily observed in the models. The problem is treated within an empirical framework, but the author attempts to analyze each of these physical factors theoretically.

Objectives of Research. The ultimate objective of this research is to achieve a better understanding of ground water movement. The classical, mathematical descriptions of laminar ground water flow are not only difficult for the average student to understand, but they are limited to particular geologic conditions based on assumptions that do not commonly occur. The movement of ground water has long been considered to be somewhat mysterious, however, empirical observations coupled with a thorough analysis of the physical principles involved shall provide a basic understanding to the layman and student. This shall eventually lead to better development, production and conservation of ground water supplies. The immediate objective of this study, which will hopefully bring about a better understanding of ground water movement, is the development of an easily observed hydraulic model which will be an accurate hydrodynamic analogy to natural ground water systems.

Method of Treatment. In order to develop a good hydrodynamically analogous ground water model with which to study the characteristics of laminar flow in saturated rock, the author executed the following research plan:

1. Construction techniques were developed for producing models that could be studied empirically. Experiments were performed to determine the best formulation for a consolidated porous media. Materials such as glass and plexiglass were tested for their competence as an outer casing. Recharge, discharge and ink injection systems were developed by extensive experimentation.

2. Preliminary test models were constructed. Several model designs were tested in order to achieve flow patterns which were analogous to those known to occur in nature.

3. Each individual hydrodynamic parameter was analyzed in order to test the validity of the analogy.

4. Models analogous to true geologic and hydrologic situations were constructed. The following ground water flow phenomena were studied by means of these models:

- (a) The refraction of water as it moved across interfaces between materials of different permeability.
- (b) The relationship between hydraulic gradient and flow net configuration.
- (c) Flow around and through lenses of different lithology and permeability.
- (d) Flow nets surrounding a single pumping well.
- (e) Flow nets surrounding multiple pumping wells.

- (f) Flow net displacement caused by wells pumping in the vicinity of layers varying in permeability and situated at different depths.
- (g) Flow toward an effluent stream.
- (h) Flow pattern through tilted and faulted sedimentary structures.
- (i) Open pit recharge, and its relation to pit shapes.
- (j) Formation of perched water tables.
- (k) Confluence of gravity water and saturated flow.
- (l) Artesian ground water systems.
- (m) Subsidence around a pumping artesian well.
- (n) Cones of depression formed around single and multiple well systems.

Each individual model experiment was studied in terms of the specific phenomena observed. The flow nets of the various ground water systems were analyzed in order to synthesize the broad pattern of ground water flow, as controlled by geologic factors. Such a synthesis provides a coherent set of basic physical concepts regarding the controls on the ground water flow systems.

## CHAPTER II

### REVIEW OF LITERATURE

The use of models for the study of physical phenomenon has an appeal for everyone endowed with natural curiosity. M. K. Hubbert (16) has accurately described the pertinence and value of model studies as follows:

Many of the phenomena of physical science are simple enough and well enough understood that they are amenable to complete mathematical analysis without recourse to auxiliary experimentation. There are other phenomena, however, which though being made up of well-understood simple systems, are so complicated as a whole as to render complete mathematical analysis difficult or impossible. The distribution of stress in a complicated machine part, or the flow of water in an irregularly shaped vessel, constitute examples of the latter kind.

When something must be known about one of these complicated problems it is usual, whenever possible, to obtain the desired information empirically by direct experimentation. Often, however, the thing studied is too large to be experimented with. Or as in the case of large engineering structures, the information on a bridge, dam or building is needed in advance of designing the structure.

Under these conditions, where mathematical analysis is inadequate, and where for one reason or another direct experimentation is precluded, the best remaining alternative is to construct and study a scale model.

The first ground water flow model ever built is credited to P. Forchheimer, who in 1898 at Graz, Austria, constructed an unconsolidated sand model for the purpose of studying radial flow to a pumping well. Since that time sand models have been improved, and in

addition to them three other types of ground water models have been developed; namely viscous fluid models, electrical models, and membrane models.

Discussions of these various models follow, along with a thorough historical review of the development of hydraulic sand models up to the author's present experiments on porous consolidated models.

### Viscous Fluid Models

Viscous fluid models were originally developed in England in 1899 by H. S. Hele-Shaw (14) (after whom they are often called Hele-Shaw models) as a tool for naval architects. The models consisted of two closely spaced parallel glass plates with a viscous fluid, namely glycerin, flowing between them. Hele-Shaw placed various solid geometric objects between the plates and by injecting dye streams into the flowing glycerin he was able to observe the flow pattern around the objects and make observations as to what might be the optimum shape for the hulls of ships.

It has since been shown by hydrodynamicists that laminar flow between two parallel plates forms a two dimensional potential flow field which can be made analogous to steady and unsteady flow in confined and unconfined aquifers. Varying the separation between the parallel plates by the insertion of thin laminated sheets, will give desired variations in permeability within the models. The quantity  $\frac{1}{P\theta}$ , where  $P$  = permeability and  $\theta$  = porosity, varies directly with the plate separation. The major advantage of this type of model is that the free surface of the flowing viscous fluid, which is analogous to a free surface in ground water flow, is clearly visible and can be studied in

great detail. D. K. Todd (36) used viscous-fluid models to good advantage in studying unsteady flow, and was able to check his results successfully with numerical solutions of non-linear differential equations. This type of model, however, does not lend itself well to the construction of complex internal boundary conditions.

### Electrical Models

The ability to substitute a study of the flow of electricity in a homogeneous isotropic conductor, for a study of the flow of water through a homogeneous isotropic porous media is brought about by the similarity in physical laws governing their flow.

Ohm's law:

$$I = \frac{E}{R} \quad (1)$$

governs the flow of electricity, where I is the current flowing through a unit of area of a section whose resistivity is R and across which there is a voltage E.

Darcy's law:

$$Q = P I A \quad (2)$$

governs water flow through a porous media where Q is the volume rate of flow of water through an area of cross section A, whose permeability (the inverse of resistivity) is P, across which there is a hydraulic gradient I. Therefore the following proportionalities exist.

$$I \propto Q, \quad E \propto I, \quad \frac{1}{R} \propto P$$

A complete mathematical analysis of this analogy is given by Horner and Bruce (15).

Electrical models can be divided into two general classes. The first class contains models depending on electronic conduction, and the second class contains models which depend on ionic conduction.

Examples of electronic conductors are thin metal sheets, carbon paper, graphite and other solid conductors, all of which depend upon the movement of electrons through the solids. Electrons are introduced at one boundary displacing free electrons within the model which causes electrons to move out through another boundary, thus producing a flowing current which in turn produces a potential drop in accordance with Ohm's law. The ionic type model utilizing electrolytic solutions such as salt water or salt solutions in gelatins depend upon the mobility of ions through the medium. Ions are moved into, through and out of the model once again setting up an electric current and a potential drop.

The advantage of electrical models is that the potential drop which is analogous to head loss can be accurately measured at any point on the model with a galvanometer probe, thus facilitating the construction of a flow net. This flow net is used to study the flow of electricity through the media which can be considered analogous to the flow of water through a porous media, such as a permeable rock. The major limitation of electrical models is the difficulty in setting up a free surface analogous to the water table, since there is no analogous force of gravity to produce it.

#### Membrane Models

When a rubber membrane is stretched over a frame representing boundary conditions in an aquifer and probes are pushed into the membrane

representing drawdowns in wells, the resulting deformation of the rubber membrane is closely analogous to the deformation of the water table caused by pumping wells. This type of model study is excellently described and mathematically analyzed by Hansen (11). The membrane analogy is extremely well suited for the study of the free water surface around a multiple well system within a complexly bounded aquifer. This type of model, however, does not offer adequate information about the flow within the aquifer itself.

### Sand Models

Sand models are the only true ground water flow models inasmuch as both the model and the aquifer represent a porous media. Experiments performed upon them most often utilize the flow of water through the porous media which again is the actual situation in nature. A sand model is a scale model of an actual aquifer in which the boundaries have been scaled down and the permeability normally modified. In the past, models utilized unconsolidated sand packed into water tight containers having a variety of shapes such as rectangles, columns and radial sectors.

The majority of the early sand model investigations concerned themselves with the position of the interface between fresh and salt water beneath the surface of the ground. The first of these experiments was performed by R. d'Andrimont (7) between 1902 and 1905. d'Andrimont used a glass tank 60 cm x 60 cm x 30 cm filled with loose sand intended to represent the Belgian coast. He poured a yellow solution of potassium bichromate having the same density as salt water, into the bottom of the tank. He then poured clean fresh water onto the sand so that he would

be able to visually study the interface between the two liquids. He imbedded potassium permanganate crystals in the sand, in order that the color train emanating from them would give some precise indication of the path traveled by the water within the aquifer. R. d'Andrimont observed in his experiments that, when the liquid of salt water density was placed in the tank prior to the fresh water, no mixing of the two liquids took place. However, when the liquid of salt water density was placed in the tank after the fresh water, he found that a very thorough mixing occurred as the higher density liquid settled slowly to the bottom of the tank. This last observation proved to be of importance when studies were made of salt water tides moving up fresh water rivers during intense storm periods. In these cases the river may change from an effluent stage to an influent stage and salt water will be superimposed onto the fresh ground water body.

d'Andrimont (8) also performed an experiment where he studied ground water flow in a geologic cross section simulating a valley fill. He attempted in this experiment to gain a better understanding of the different levels of ground water movement. It had been a common belief at that time that ground water at depth was stagnant and in fact that the upper level of stagnation was at the level of the lowest position of natural discharge in the valley. d'Andrimont discovered in his valley fill problem, that water, well below the lowest discharge point in the ground, was in motion; he did, however, still believe that there was a stagnant zone at some lower depth.

During 1905-1906 J. M. K. Pennink (29) experimented with glass tanks, filled with sand, varying in dimensions from 1 to 3 feet in height,

1 to 3 feet in width and usually 1 inch thick. With the exception of one experiment in which he injected dye streams into the model in order to study flow as it moved down gradient, all of his work involved the salt water fresh water interface. He used either a combination of clear salt water at the bottom with colored fresh water at the top or milk at the bottom with clear fresh water at the top. Pennink varied the placement of fresh water intakes and outlets along with actual pumping wells in order to study the variations in the configuration of the interface. Pennink's pictorial monograph (29) on his experiments has become a classic.

Pennink did theorize, from a combination of field study and model study, an excellent flow net depicting the effluent stream situation. It was evident from his flow net that the entire ground water system was in motion. However, the importance of this fact was not recognized at that time, and the stagnation theory as held by R. d'Andrimont continued in vogue.

Following these experiments, the petroleum industry took the lead in the construction of sand models. In 1920-1921 Mills (23, 24) constructed two steel tanks with plate glass fronts. The dimensions of the smaller model were (92 x 48 x 9 cm) while the dimensions of the larger model were approximately twice those of the smaller. Within the tanks he packed a variety of sands into configurations simulating sedimentary beds and lenses. Once the model was completely packed with sand it was tightly sealed on all sides and various layers of gas, water and oil were pumped into the models under pressure. Mills then studied their movements relative to one another and the various sand layers in the model.

Through these experimental studies Mills was able to draw the following conclusions. (1) Variations in the textures and bedding of oil and water bearing sands cause corresponding variations in the movements of the fluids through the sands. (2) Movements of oil and water through sands tends to follow the paths of least resistance generally through the relatively coarse, open textured parts of the beds. (3) Frictional and capillary resistances to the movements of oil and water through saturated sands increases as the size of the interstices decrease. (4) Rapid flow of oil and water through sands may cause oil to be trapped behind when the rock texture is very fine. Mills demonstrated that, as a result of this last phenomenon, there are enormous underground losses of oil. Due to this work a logical step was made toward the more intelligent development and application of improved methods of oil recovery.

In 1932, Wyckoff, Botset and Muskat (38) utilized a radial sector of sand to show that the old Dupuit formula of 1863 (stating that the fluid outflow is proportional to the square of the differences in the fluid heights in the sand) is exact within experimental error, provided the fluid heights are replaced by fluid heads measured at the sand bottom.

Potter and Baker (30) built a sand model in 1938 for the purpose of studying the behavior of perched water tables. They used a glass tank 17" x 12" x 4" into which they placed unconsolidated sand in the form of a hill with two impermeable clay layers set at different depths within the hill. Water was sprinkled onto the hill, in order to simulate rain, and water level observations were made at various points within the

model by means of observation wells set in the sand. They were able to study the rise and fall of the perched ground water mound, which provided an explanation for the wide range of ground water fluctuations observed among wells in the same ground water horizon.

Kirkham (20) used a sand model 29" x 19.5" x 2.5" to study artificial drainage of land in 1939. He forced water in the bottom and allowed it to drain at a point near the top. Dye streams were pumped into the model at numerous points along the bottom and an excellent picture of the flow paths into the drains was obtained. In the same year Mavis and Tsui (23) experimented with a glass walled flume 41" long 18" deep and 3" wide, in order to study the movement of water in the capillary fringe. Dye was injected into the flow moving across the model. A study of the resulting flow bands uncovered the fact that the water in the capillary fringe moved in the same direction as the phreatic water in the main body of the permeable material but with an average velocity of approximately two-thirds the velocity of the phreatic water.

Kellogg (19) utilized sand models in 1948 for the purpose of studying the effects of drainage rates on the stability of earth dams. This is one of the few studies in which the use of unconsolidated material was a distinct advantage. Kellogg tested materials of varying permeability which he shaped in the form of small earth dams. The models were then saturated and allowed to drain at various rates which were controlled by the rate of drawdown of the water behind the dam. He concluded from his investigation that the possibility of mass slides resulting from rapid reservoir drawdown has been somewhat exaggerated.

In 1952, Baumann (3) made a study of ground water movement controlled through spreading operations. He utilized a sloping glass tank 46" x 12" x 12" filled with unconsolidated sand. Water was introduced upstream and formed a mound which moved down stream. Piezometer tubes and dye lines were used to plot the flow net produced by the spreading operation. Baumann showed in his experiment that the height of the mound produced by spreading depends on: (1) rate of infiltration, (2) duration of spreading, (3) permeability of sediment, (4) depth to the water table, (5) thickness of the aquifer, (6) slope of the lower impervious surface, (7) distance downstream to control boundaries.

Harder and others (13), working in 1953 on the sea water intrusion problem, constructed a plexiglass model composed of a middle section 6" high and 4' long closed at the top with steel bracing along the sides. This section was bolted to end tanks bounded by bronze screens. A 3" inside thickness was used and subsequent experience with this model indicated that no information of any importance could be gained from increasing the width. The middle section was filled with unconsolidated sand, and one end tank was fed at a constant level with fresh water and the other tank with sea water. Injection wells 1/4" in diameter penetrating the entire aquifer were placed along the face of the model. These wells were used to study the effects of fresh water injection upon an intruding body of salt water. Harder found that if fresh water recharge was maintained at a sufficient rate, a fresh water pressure ridge resulted which reversed the intrusive movement of the salt water. Experiments proved that it is necessary to form the ridge

inland of the salt water wedge in order to prevent any salt water inland of the ridge from being driven still further inland. As a result of this research, extensive investigations were conducted along the coast of California, which have now proved this method to be quite successful.

Hansen (12) made an excellent study of unconfined ground water flow to multiple wells in 1953. He built a model composed of a 90 degree sector of a circle having a 120" radius and a depth of 36". It was normally filled with 30" of sand while the water saturated zone was 24" thick. The model contained three wells, one at the apex and one each 36" from the apex along the sides. The sides of the model were plexiglass with wooden bracing. Hansen utilized 174 piezometer tubes to show the position of the free surface around the wells. The piezometer tubes were flexible plastic containing a dye solution used as a water level indicator. The piezometer tubes were arranged so that when they were squeezed a slug of dye solution was injected into the flow system of the model along the plexiglass face making possible visual study of the flow net. Among the many excellent observations Hansen made in this experiment are the following: (1) The water table intersects a well above the level of the water in the well because the water is pumped out more rapidly than the water level can be maintained. Therefore, there is a seepage zone along the side of the well, and the length of it is proportional to the efficiency of the well. (2) The atmospheric pressure surface or free water surface is lowered slightly as a result of upward movement of water into the capillary zone. (3) Trapped air reduces permeability.

Hansen also discovered that the Dupuit equation is not valid in the area immediately adjacent to a well where the slope of the free

surface becomes very steep. Hall (9) arrived at this same conclusion in 1955 as the result of a model study he performed using a  $15^{\circ}$  sector of radius 76.8", filled with unconsolidated sand, surrounding a fully penetrating gravity well. The sector was made with plexiglass sides completely supported by steel bracing. Piezometer tubes were used to observe free water levels.

Emphasis on ground water elevations has in some instances tended to obscure the importance of ground water movement. Nemeth (27), in his model studies in 1956 attempted to correct this situation. He performed an extensive series of experiments using a glass tank 4 feet long, 1 foot high and 1 inch wide. He placed various layers of unconsolidated sands into the model simulating many different sedimentary cross sections. Two vertical, impermeable strips 4" long were placed as barriers 1 foot apart in the middle of the model. A hydraulic gradient was created in the model by maintaining a higher water level in front of the first barrier than that maintained behind the second barrier. He injected dye at the top of the model at the upper end of the hydraulic gradient and observed flow lines as they encountered variations in lithology.

The most recent important contribution to hydraulic model studies was made by Skibitzke (31) in 1960 when he designed the first permanently consolidated hydraulic model. He combined unconsolidated sand with a small amount of epoxy resin and produced a consolidated porous media. Skibitzke studied the ion-exchange and absorption characteristics of a porous solid as a means of determining in detail how liquids flowed through the solid. The experiment utilized a vertical rectangular block of sand mixed with epoxy resin and sealed on all sides by another epoxy

resin. Radioactive tracers were injected into the vertical flow system and allowed to move through for certain time periods. The blocks were then cut up in thin horizontal sections which were photographed using radiographic film. The spread of the radioactivity in the block was clearly visible on the film.

A review of hydraulic literature has been presented in this chapter because it is of the utmost importance in the performance of any research study to preface the investigation with a thorough review of the work that has preceded it. The earlier work must normally serve as a foundation for all the experimenters who follow after it. The study conducted by this author into previous model work has guided him in the refinement of construction materials and techniques as well as experimental procedures which have led to what is hoped to be an improved ground water flow model.

## CHAPTER III

### THE HYDRODYNAMIC ANALOGY

#### Hydrodynamic Theory

It is important to the study and solution of problems in fluid flow to understand the general formulation of the hydrodynamics governing the flow. There are essentially three physical conditions, which when specified for the fluid flow system, will completely describe that system. The first condition is that it obey some equation of continuity, second that it be describable by an equation of state, and finally, its dynamical reactions to pressure gradients and external forces must be specified. These conditions for the flow of a homogeneous incompressible liquid through a porous medium are discussed briefly in the following paragraphs.

All systems of fluid flow are subject to the law of conservation of matter. This law states that the fluid mass in any closed system can be neither created nor destroyed. When referring to fluid in motion this law has been more conveniently stated by Muskat (26) for analytical purposes to read:

"The net excess of mass flux per unit of time, into or out of any infinitesimal volume element in the fluid system is exactly equal to the change per unit of time of the fluid density in that element

multiplied by the free volume of the element."

$$\frac{d\rho}{dt} + \rho \left( \frac{du}{dx} + \frac{dv}{dy} + \frac{dw}{dz} \right) = 0 \quad (1)$$

Equation (1), commonly called the "equation of continuity" represents this law, where  $u$ ,  $v$  and  $w$  are the velocity components in the  $x$ ,  $y$  and  $z$  directions, respectively, and  $\rho$  is the fluid density at  $(x, y, z)$ .

When the fluid of the system is an essentially incompressible liquid such as water, its equation of state pertinent to ground water hydrology is

$$\rho = \text{constant} \quad (2)$$

$$\therefore \frac{D\rho}{Dt} = 0 \quad (3)$$

When the equation of continuity (2.1) is combined with the equation of state (2.2) the result is a specialized continuity equation (2.4) for an incompressible liquid.

$$\frac{du}{dx} + \frac{dv}{dy} + \frac{dw}{dz} = 0 \quad (4)$$

The equation of continuity for steady state systems can be more simply written as

$$Q = A \theta V \quad (5)$$

where  $Q$  is the rate of flow in volume/time units,  $A$  is the cross sectional area through which flow occurs and  $V$  is the average of flow. This equation applies only when the variables  $A$ ,  $\theta$  and  $V$  are defined to be space integrals of their respective functions.

It has been proved that the Stokes-Navier equation

$$\rho \frac{dV}{dt} = -\rho \vec{g} + \nabla p + \mu \nabla^2 V \quad (6)$$

where  $g$  = acceleration of gravity and  $p$  = fluid pressure and  $\mu$  = viscosity, accurately describes the hydrodynamics of viscous flow of incompressible fluids. One hundred years ago Lamb (22) used the following notation to state the potential energy forces in the Stokes-Navier equation

$$\begin{aligned} \rho X &= -\frac{dP}{dX} \\ \rho Y &= -\frac{dP}{dY} \\ \rho Z &= -\frac{dP}{dZ} \end{aligned} \quad (7)$$

In more modern vector notation this has become

$$\rho \vec{g} = -\nabla P, \quad (8)$$

which has been further simplified in ground water hydrology to be

$$\rho \vec{g} - \nabla P = \nabla h \quad (9)$$

This equation states that the term hydraulic head ( $\nabla h$ ) is the resultant of the gravity head and pressure head. It is now used almost universally in saturated flow problems because of its simplifying effects on flow calculations, and also because of the ease with which it can be measured when  $\rho$  is constant. It should be pointed out however that this is still a complex function when  $\rho$  is variable. Due to the difficulty in applying Stokes-Navier equation to the many fine channels of a porous medium, more attention has been focused on the macroscopic reactions in a porous medium. Dynamical reactions of a fluid passing through the fine channels of a porous medium, may, from a macroscopic

point of view, appear in quite different form than when analyzed microscopically.

Darcy studied these reactions and originated the law which states that macroscopically, the velocity of a fluid flowing through a porous media is directly proportional to the pressure gradient acting on the fluid. The word macroscopically, used here, means that the volume elements to which the velocity and pressure refer contain a large number of small pores within which the actual dynamic variables may vary greatly on a microscopic scale. Darcy's law is essentially a statistical result giving the empirical equivalent to the Stokes-Navier equation for each individual pore as averaged over very large numbers of individual pores. His law forms the dynamical basis for the hydrodynamic solution of the viscous flow of homogeneous fluids through porous media. It is superior to the Stokes-Navier equation, because the latter equation presents insurmountable mathematical difficulties when applied to any thing as involved as the flow through the labyrinth of passages in a porous medium.

Darcy's law can be written in general terms as follows

$$V = \frac{K}{\mu} (\rho g - \nabla p) \quad (10)$$

where K is a constant of proportionality known as conductivity,  $\mu$  = viscosity, p = fluid pressure and g is the acceleration of gravity.

Darcy's law can be written as

$$Q = P I A \quad (11)$$

for steady state conditions of incompressible liquids, such as water, flowing through a porous medium. Here P is the permeability of the

medium normally expressed in USGS units (gal/day/ft<sup>2</sup>/1:1 gradient at 60°F),  
 I is the hydraulic gradient  $\frac{h}{L}$  where h is the difference in hydraulic  
 head between two points and L is the distance a water particle must  
 travel between the two points, A is the cross sectional area through  
 which flow is being considered.

The dynamical laws characterizing the flow of incompressible  
 liquid through a porous medium have now been described by Darcy's equation.  
 By combining this equation with the equation of continuity and the  
 equation of state for an incompressible liquid, we arrive at the  
 equation of motion for this system represented by the Laplace equation.

$$\nabla P \text{ grad } h = 0 \quad (12)$$

When P is constant in all directions the Laplace equation can be written  
 as follows:

$$\nabla^2 h = 0 \quad (13)$$

### Scaling and Similitude

Prior to the presentation of the model experiments performed in this study it is desirable to appraise the merits and values of the experiments by showing the hydrodynamic analogy which exists between the models and the prototypes.

Sand models are normally intended to be small scale reproductions of actual flow systems. The objective of utilizing a scale model is to enable a particular physical system or class of systems to be analyzed in terms of the observed behavior of a laboratory model. To accomplish this objective the model must be designed and its behavior analyzed in a manner that will permit an extrapolation of the analysis to the prototype.

As previously mentioned the Stokes-Navier equation

$$\rho \frac{dV}{dt} = -\nabla h + \mu \nabla^2 \vec{V} \quad (14)$$

accurately describes viscous flow of incompressible fluids. For most practical application involving flow in porous solids it is possible to assume that the total acceleration is negligible. Therefore equation (10) becomes

$$0 = \nabla h + \mu \nabla^2 \vec{V} \quad (15)$$

$$\therefore \nabla h \propto \mu \nabla^2 \vec{V} \quad (16)$$

This states that the drag resulting from viscosity is balanced by the potential gradient. Darcy demonstrated this empirically and M. K. Hubbert demonstrated it theoretically.

$$\text{Since } \mu \nabla^2 \vec{V} \propto \vec{V} \quad (17)$$

and if porosity ( $\theta$ ) is constant

$$\vec{V} \propto \vec{Q} \quad (18)$$

or

$$\vec{V} = \frac{\vec{Q}}{\theta} \quad (19)$$

$$\text{then } \nabla h \propto \vec{V} \quad (20)$$

$$\text{or } \nabla h \propto \frac{Q}{\theta} \quad (21)$$

By removing the varies as ( $\propto$ ) by the integration of the Stokes-Navier equation, and replacing it with a constant of proportionality (permeability) the equation becomes

$$\nabla h = \frac{\vec{Q}}{P\theta} \quad (22)$$

This is a non-dimensional equation which can be used to show the similitude between a model and its prototype.

It is absolutely necessary for the model and the original flow system to have geometrically similar boundaries if the results obtained within the model are to be applicable to the physical flow problem. Only if this is so, will the potential and streamline distribution in the model be equivalent to those in the actual flow system. The internal geometry of the pore spaces of the model, however, can have any geometry without effecting the gross similitude of the flow patterns.

The potential and streamline distributions depend only on the shape of the model and not upon its absolute dimensions, which may be chosen on the basis of convenience and accuracy.

Having now discussed the analytical theory of scaling let us mention the actual problems involved in the physical construction of the scale models. Considering the physical makeup of the models alone, we are primarily concerned with two variables. The first variable is the material used to simulate natural rock, the second variable is the boundary condition imposed upon the material. Unlike geologic models constructed to show how structural deformations in the earth's crust are formed, hydraulic models are not concerned with the strength of materials being used. This greatly simplifies the model problem because when one must deal with strength, it becomes a complex problem to scale down strength which is manifested in large scale bodies to an analogous strength on a small scale. It is not uncommon to utilize soft putty in a structural model to represent solid granite in the prototype. In a hydraulic model the medium representing natural rock need only simulate the hydraulic conduction properties of the prototype. These conduction properties are best expressed by the term permeability which is a measure of the capacity of a porous medium to transmit water.

Ultimately, permeability is an inverse measure of the frictional resistance which a rock offers to water flowing laminaarly through it. The second physical variable, boundary conditions, must be set up in the model in a direct linear proportion to the prototype. In other words, as it has been previously stated the two must be geometrically similar. The models can be considered as non-dimensional models since a model 2 feet long, 1 foot high and 1/4 foot wide can be considered to represent a prototype having any desirable dimension as long as the ratio of length to height to width remains similar at 8:4:1.

Hydraulic models can be utilized for two purposes, namely qualitative and quantitative studies. In qualitative studies we are primarily interested in a vectorial flow net analysis of the system and are not concerned with quantitative flow determinations. Conversely quantitative studies as the name implies are concerned with quantitative flow determinations.

The experiments carried out by this author have been primarily concerned with qualitative determinations of laminar flow in porous consolidated media. Emphasis was not placed on quantitative determinations since the models were not constructed to represent any specific geologic prototypes, but intended to represent general geologic and hydrologic situations.

In terms of qualitative studies it is best at this point to expand our discussion of the hydrodynamic analogy in regard to its adequacy in portraying the correct flow net, the correct two dimensional view and the infinite aquifer concept.

The flow nets observed in these models will accurately portray the flow net occurring in nature when all the boundary conditions in the model are proportionate to those occurring in the natural situation. Where two or more geologic formations are present in the model and prototype the ratio of the permeability of each formation to each other, formation must be the same in both, although the absolute values of the permeabilities need not be the same in qualitative studies. To further illustrate this fact, the following example is offered. Assume three formations occur in a prototype having permeabilities of 1500, 1000, and 500 USGS units respectively. These formations can be represented in a

scale model by formations having permeabilities of 3000, 2000 and 1000 USGS units and that model will yield a flow net identical to the prototype, since the relative permeabilities in both the model and the prototype are 3:2:1.

For the purpose of solving many ground water problems, the permeability of the porous medium is assumed to be isotropic, or in other words equal in all directions. In actual fact, the permeability within most rocks is greater parallel to the bedding plane, than it is perpendicular to the bedding plane. This is due primarily to the manner in which the individual grains were packed upon deposition. However, the assumption of isotropic permeability will yield an accurate representation of flow systems which may be considered as two dimensional with the planes of flow parallel to the bedding planes. Under these circumstances there is no component of flow perpendicular to the bedding planes, and therefore the permeability in that direction does not enter into the problem. If, however, the problem does involve components of flow in more than one direction of an anisotropic medium, this fact should be taken into account. In scale models of aquifer systems, the anisotropic permeability can be accounted for by actually constructing the porous medium with unequal permeabilities in the X and Z directions. This can be accomplished by specialized packing procedures, though a certain amount of trial and error may be necessary in order to arrive at the desired permeability ratios.

The hydraulic models used in this study represent a two dimensional view of the ground water flow system. All fluid systems actually extend in three dimensions, however, there are cases where all

the features of motion may be observed in a single plane since the motion is identical in all other planes parallel to it. This occurs in situations of similar recharge and discharge when the velocity distribution vector  $V$  varies only with two rectangular coordinates and is independent of the third. There are two types of problems that may take this form. The first type occurs when the porous medium is constant with depth along the  $Z$  axis, thus producing a flow net in the  $XY$  plain which does not vary along the  $Z$  axis.

If, for instance, we have a homogeneous sand of uniform thickness, completely saturated with water and entirely penetrated by a well, the resulting flow pattern would be constant in all horizontal planes. There would be no vertical component of motion of the water moving toward the well. This system could be studied as a two dimensional system in the horizontal plane. If, however, the well is only partially penetrating, the water beneath the well would be drawn up to it, thereby attaining a component of vertical velocity, disrupting the two dimensional system. This would represent a three dimensional system, however a great deal could still be learned about it by studying various two dimensional planes intersecting the system. The aforementioned situation with the completely saturated sand layer normally occurs under conditions of confinement. Here the entire aquifer is saturated leaving no doubt as to the boundaries of the saturated aquifer body.

Under normal circumstances when the aquifer is not confined, a gravity flow system will occur. In this system the upper boundary is represented by the capillary fringe which occurs at some finite distance above the water table. The height of capillary rise depends primarily

upon the mean grain size of the aquifer. The capillary rise produced in the models used in this study is very small due to the coarse grained texture of the porous media. Movement of water in this zone is quite complex, but fortunately it can be disregarded for most qualitative studies. For practical purposes the free water table can be considered as the upper flow boundary. The water table is also the potential energy gradient which, of necessity, must decline in elevation as energy is dissipated against friction during the fluid flow through the porous medium. This sloping surface gives rise to a vertical component of velocity which causes the flow net in the XY plane to vary with the Z axis.

The second type of problem which may be studied strictly in two dimensions, occurs when the porous medium or geologic frame work is constant in one horizontal direction (X or Y). The flow net in this situation is the same in all vertical planes perpendicular to the axis having the constant hydrologic conditions. This is true for both gravity flow and confined flow systems, as long as the vertical component of velocity is constant along the one horizontal axis.

One of the most important concepts in hydraulic model work is that of the infinite aquifer. Generally we attempt to study a finite lamina from the infinite aquifer without disturbing the overall relationship of this lamina to the infinite aquifer system. The basic flow direction of an infinite aquifer is approximately horizontal, the average gradient being only a few feet per mile. In order to represent a lamina of this, it is necessary to have the water enter and leave in this same horizontal direction. This concept is produced in the models

by the use of open end tanks at each end of the model, which serve as recharge and discharge reservoirs. These end tanks are infinitely permeable, consequently, these boundaries represent equipotential surfaces across which the water must flow perpendicularly. All water enters and leaves the model in the same direction regardless of its activity while within the actual synthetic geology of the model.

The hydraulic models employed in this study can be used for quantitative determinations, but great care must be taken in applying these values to the prototype situation. It is possible to use materials in the models having the exact permeability as those in the prototype. If ground water gradients are then produced in the models to match those in the prototype, the resulting flow velocity ( $V$ ) and flow rate ( $Q$ ) in the model will equal the velocity and flow rate in the prototype. Under normal circumstances it is desirable to increase model permeabilities or gradients for the purpose of speeding up the experiments beyond the normal rate of ground water flow. These changes can be done to scale so that the resultant quantitative determinations are directly proportional to those occurring in nature.

One of the most common arguments against sand models in the past has been the belief that the close proximity of the boundary walls has a distorting effect on quantitative studies. A number of investigators have studied the effects of confining walls upon the resistance to flow of the porous medium within a container. They are nearly in unanimous agreement that generally these boundary effects are very small. In cases of laminar flow, all energy losses are due to viscous forces in the fluid working against friction. They are proportionate to the

velocity gradient and the surface area over which the forces act. Rose (33) has shown that the porosity of a confined porous medium is larger near the walls of the container than in the interior. He has also concluded that the tortuosity is greater in the interior of the medium than at the walls. This is because the packing at the walls has only two degrees of freedom, since the wall provides a constraint, whereas in the interior three degrees of freedom exist. These factors may tend to decrease the resistance to flow along the walls due to the decreased surface area present. Rose has compared the resistance of small cross sections of confined porous media to the resistance of the same material in an essentially infinite bed. He classified the confined medium by means of the  $D/d$  ratio where "D" is the distance between the walls of the container, and "d" is the diameter of the grains. The results of his experiments showed that in beds having a  $D/d$  ratio greater than 50 the "wall effect" can be entirely neglected. Since all of the models used in this study have a  $D/d$  ratio of 50 or more, the wall effect will not interfere with the hydrodynamic analogy. This author has added further evidence of this last fact by proving that there is no appreciable difference between the resistance to flow along the wall of the models and the average resistance to flow of the entire cross section of the model. This was accomplished by measuring the velocity of flow along the wall of the models by means of an ink tracer, and calculating the average velocity of flow through the model by the equation

$$V = \frac{Q}{A\theta}$$

(another form of equation 2.5)

and then comparing the two values of velocity. All of the models used produced an equality between these values, which substantiates the accuracy of these models quantitatively as well as qualitatively.

## CHAPTER IV

### METHODOLOGY

Nearly all previous hydraulic models developed for studying laminar flow utilized unconsolidated sand. Unconsolidated sand models have the following major disadvantages:

1. They limit studies to nearly homogeneous media.
2. Hydrologic characteristics cannot be identically reproduced in order to exactly repeat an experiment.
3. Hydrologic characteristics may not remain constant during experimentation due to the possibility of the occurrence of such things as channelling and the changing of the packing arrangement.

These objectionable features were overcome in this study by using models which utilize consolidated media simulating natural sedimentary rock. The consolidated medium consists of grains bound together by epoxy resin. This admixture allows itself to be molded easily and will solidify in any desired form. The fabric of the media can be positioned in glass or plexiglass cases under various structural and heterogeneous lithological conditions. The consolidated media will allow continuous experimentation under stable simulated geologic conditions. The hydrologic characteristics of the model will remain constant throughout the life of the model which should be many years. Ground water systems can be established and controlled in the model by

the use of hydraulic pumps, simulating recharge and discharge into and out of the model. Colored inks can be inserted into the flow system forming visible flow lines which can be analyzed in order to synthesize the broad pattern of ground water flow as controlled by geologic factors.

#### A. Model Types

Three types of glass models have been used in this study. The first type is referred to as the "small horizontal model" which is 18 in. long, 12 in. wide and the inside thickness is 1-5/8 in. It has a 3/8 in. plate glass top and the back and sides are sealed with opaque epoxy resin. Aluminum reservoir tanks are attached at each end extending 2 in. from the ends of the model and are 3 in. deep. A 12 in. strip of 1 in. aluminum angle bar is bonded to the glass top at each end so that the water levels in the reservoir tanks can be maintained above the level of the model. In a few of the "small horizontal models" a plexiglass top was used instead of a glass top in order to facilitate the drilling of observation wells. The second type of glass model is the "small vertical model" which is 18 in. long, 12 in. high and 1-5/8 in. thick inside with 3/8 in. plate glass covers on the front and back. The bottom is sealed with epoxy resin and the top is open. At each end is an aluminum reservoir tank extending 1 in. from the model. The third type glass model is the "large vertical model" which is 30 in. long, 12 in. high and 1 in. thick inside. It has 3/8 in. plate glass covers on the front and back and is sealed with resin at the bottom while being open at the top. The aluminum reservoir tanks extend 1 in. from the model at each end.

Models utilizing entirely plexiglass cases have been built having dimensions ranging from 12 in. to 36 in. in height, 18 in. to 36 in. in length and 1/2 in. to 4 in. in thickness. This type of model has been extremely successful. They consist essentially of a rectangular case made of 1/2 in. thick plexiglass. When the sand and resin mixture is formed into the case, a wooden dummy 1 in. x 1 in. x height of case is placed in each end of the case. When the sand mixture is hardened the wood dummies are removed leaving what are essentially built-in end tanks. This model is nearly a one piece construction.

The overall size of a model may be chosen according to convenience, however, the relative dimensions will depend on the prototype to which the model is being made geometrically similar. Models should be thick enough to produce a negligible wall effect, but there is no apparent advantage in increasing the thickness beyond this point, since only two dimensions of the model are actually being studied.

## B. Formation of Consolidated Media

### 1. Selection of Sand

The first step in forming the consolidated media was to select the proper unconsolidated material for the skeleton. The grain size chosen was dependent upon the permeability desired. If a high permeability was desired, a coarse grain size was chosen and if a low permeability was desired, a fine grain size was chosen. In all cases the sand used was very nearly white in color, so that the colored dye bands would show up very clearly. It is possible to wash plain brown sand in warm hydrochloric acid and thereby obtain white sand, but the

author found that in the long run this was quite uneconomical. Therefore, graded white sand was purchased from the Crystal Silica Company for use in most of the experiments. This sand was separated into various size fractions and then used separately or combined with other fractions in order to obtain the wide range of permeabilities which were used in the models.

Commercial glass beads were also tried in the models, but offer no particular advantage over sand, except that they appear pure white in color and can be purchased in finer sizes than sand.

## 2. Selection of Resin

The second step in the formation of the consolidated media was to choose the proper resin. The properties which were desired were as follows:

- (1) clear color
- (2) low viscosity
- (3) high adhesive properties
- (4) long working time
- (5) ability to cure at room temperature
- (6) ability to bond with glass and plexiglass
- (7) complete stability in the presence of water at normal room temperatures.

After testing many different resins the author decided upon Epocast 202, produced by the Furane Plastic Company.

### 3. Selection of Sand to Resin Ratio

A method was then devised by which one could calculate the proper proportions of sand and resin in order to obtain a consolidated media of high strength and high permeability for the particular grain size being used. It is undesirable to attempt to adjust the permeability by means of varying the proportion of resin used. It is much too expensive a material to be used in excess in order to decrease the permeability, and secondly, any volume used in excess of a thin film on the grains will not be evenly distributed, but will collect at the bottom of the rock due to gravity. If the quantity of resin is decreased too much it will have little or no effect on the permeability, but will decrease the strength of the media and may ultimately allow the consolidated media to disintegrate.

For the purpose of calculating the proper amount of resin to be used with a given amount of sand let us assume that we are using spherical grains. Given a volume  $V$ , the number of grains needed to fill the volume  $V$  will vary as the cube of the radius (or diameter) of the grains, since the volume of a sphere equals  $\frac{4}{3} \pi R^3$ . In other words, if it takes  $X$  number of 1 mm diameter grains to fill the volume  $V$ , then it would take  $8X$  grains of 1/2 mm diameter to fill the same volume. The surface area of a sphere is equal to  $\pi D^2$ , therefore a 1/2 mm grain has a surface area 1/4 as large as a 1 mm grain. By halving the size of the grains, 8 times as many grains are needed, each measuring 1/4 the surface area, resulting in a doubled total surface area. This would infer that twice as much cement would be needed. However, since there are more grain contacts per volume with smaller grains, each contact need not be as

strong as the contacts in the larger grained rocks which have fewer contacts. The strength of the total contacts of all the rocks should be equal. Therefore, as the grain size is halved, slightly less than twice as much resin is needed.

Since the amount of resin used in a sand is partly dependent on the shape and surface texture of the grains, a different sand to resin ratio will have to be obtained for different sand types. However, if all the sand used has approximately the same grain shape and texture, it is necessary only to find the proper resin ratio for one size increment by trial and error and all other ratios can be computed. A good criteria for trial and error experiment is to slowly add resin to the sand, while mixing, until the sand grains all appear shiny, due to the resin film around them. The proportion of resin to sand mixed at this point will be quite close to the optimum. Once a satisfactory ratio for the first grain size increment is obtained, let this ratio be called  $R_1$ . From the following semi-empirical equation all other ratios can be computed.

$$R_2 = \frac{A_2 + b_2}{A_1 + b_2} \times R_1 - \left[ \frac{\left( \frac{A_2 + b_2}{A_1 + b_1} \right) R_1 - R_1}{5} \right]$$

where

$R_2$  = ratio of sand to resin by weight for sand size increment number 2

$R_1$  = ratio of sand to resin by weight for sand size increment number 1 found by trial and error

$A_1$  = maximum grain diameter of sand #1 in MM

$b_1$  = minimum grain diameter of sand #1 in MM

$A_2$  = maximum grain diameter of sand #2 in MM

$b_2$  = minimum grain diameter of sand #2 in MM

$$\left[ \frac{\left( \frac{A_2 + b_2}{A_1 + b_1} \right) R_1 - R_1}{5} \right] = \text{the factor which accounts for the}$$

decrease or increase of grain contacts as sand size changes. The number 5 in the divider may be called the "contact factor" and may be varied as the experimenter sees fit. If the contact factor is decreased the sand to resin ratio will decrease and vice versa.

When using a sand with a mixture of size increments, a weighted average of their sand to resin ratios will give the correct ratio for the mixture.

The following ratios were computed for sand fraction used in this investigation.

<u>Sand Fraction</u>	<u>Sand to Resin Ratio</u>
.25 mm - .4 mm	17.8
.4 mm - .6 mm	28.1
.6 mm - 1.0 mm	38.2
1.0 mm - 2.0 mm	68

#### 4. Consolidated Sand and Resin Mixture

Once the sand and resin is thoroughly mixed it is packed tightly into the mold or case in thin layers until it is full. Care must be taken to pack the sand evenly and to eliminate all air pockets. Careful even packing will produce a medium of isotropic permeability. In cases where an anisotropic permeability is desired, the packing can be adjusted to achieve the desired permeability arrangement. The densest packing arrangements produce the lowest permeabilities.

An infinite variety of structural and lithologic patterns can be carefully built into the models. The procedure for accomplishing complex structures is as follows. A piece of wood is cut to conform exactly to the inside dimensions of the model. The geologic structure desired in the model is then traced onto the wood, after which the wood is cut up along the pattern lines into what is essentially a jigsaw puzzle. Each piece of the puzzle is the proper shape and size of the lithologic unit within the model. The pieces are then assembled into the complete geologic pattern within the mold. Having accomplished this, one piece of wood at a time is removed from the mold and replaced with the proper sand and resin mixture which will yield the correct permeability for the lithologic unit at that position in the geologic structure. Care must be taken to pack each succeeding section tightly against those sections surrounding it in order to avoid any excessive permeabilities along lithologic interfaces. When each piece of wood has been removed from the mold and replaced by a sand and resin mixture, the model is allowed to cure for forty-eight hours. At the end of this time the sand and resin mixture is a stable, permanent consolidated porous medium.

### C. Construction of Glass Type Models

Glass type models are constructed with the use of an aluminum bar stock mold having the dimensions of the desired synthetic rock. The mold is thoroughly waxed to prevent sand and resin from sticking to it. A glass plate, which will become the transparent face of the model, is placed in the bottom of the mold with a thin coat of epoxy resin upon it. The sand and resin mixture is then placed into the mold as previously

described. The top of the sand is made perfectly flat by striking off the upper surface after it has been built up to a slightly excessive height. After forty-eight hours when the sand has hardened, and is firmly bonded to the glass face plate, it is removed from the mold by disassembling the mold from around it. The sides of the rock which need to be sealed are then coated with Epocoat 19A, a very viscous opaque epoxy resin used for sealing. While the resin on the back is still soft, a glass plate is bonded to the back of the rock for added strength. The resin will harden in eight hours, at which time the aluminum end tanks can be bonded to the model with Epocoat 19A. The "small horizontal models" utilize open horizontal end tanks and supply ink to the model through ink reservoir cups bonded to the end of the rock within the end tank, as shown in Figure 1. The small and large vertical models utilize vertical open end tanks and supply ink to the model through 1/8" brass tubes driven 1/4" into the rock and extending out through the sides of the end tank, as shown in Figure 2.

#### D. Construction of Plexiglass Models

The first step in constructing a plexiglass model is to build a plexiglass case of 1/2" thick plexiglass having the desired inside dimensions. The necessity of using exceptionally thick plexiglass is to avoid any warping or bending. The sides, bottom, and top of the case, are permanently bonded to the front plate of the model with plexiglass cement, while the back is screwed onto the case with #6 sheet metal screws. All holes are predrilled. The top of the case is perforated when water table conditions are desired in the model, but it



Figure 1. Photograph of a horizontal type model containing ink reservoir cups.

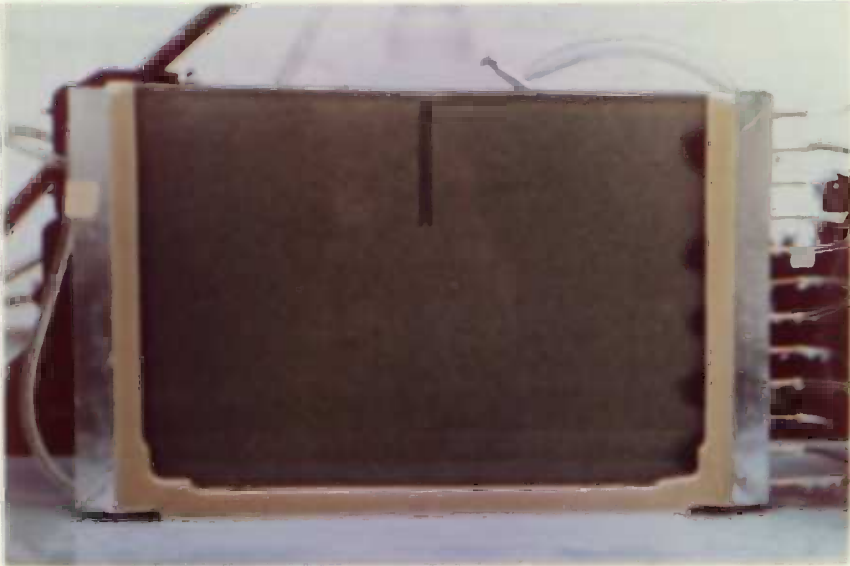


Figure 2. Photograph of a small vertical type model containing ink injection tubes.

is not perforated if confined aquifer conditions are desired. When plexiglass is used, the case itself is used as the mold. Wooden dummies coated with wax are used in all positions, such as the end areas, where the experimenter does not wish to deposit any sand. The front surface which is not covered by the wooden dummies is first coated with a thin layer of resin, after which the sand and resin mixture is packed into the case. The upper surface is struck off evenly after the level of the sand is built up slightly above the plexiglass case. When the model has cured for forty-eight hours the wooden dummies are removed leaving the desired open areas. This construction results in built-in end tanks, which have the advantage of eliminating the necessity of attaching external end tanks which increase the possibility of leakage through poorly bonded seams.

Once the dummies are removed a 1/8" foam plastic gasket is placed on the back of the rock and then the plexiglass back is screwed onto the model. The gasket allows the back to be form fitted to the rock, and is essentially impermeable, allowing no water to pass behind the rock. The model is made water tight by placing a bead of plexiglass cement on all the seams.

The plexiglass models have proved to be superior to the glass models for the following reasons:

- (1) They are light in weight.
- (2) They are easily fabricated.
- (3) They are permanently water tight.
- (4) They are nearly unbreakable.
- (5) Holes may be easily drilled through the plexiglass permitting

the attachment of external fittings such as recharge tubes, discharge tubes, ink injection tubes and wells.

## E. Construction of Model Fittings

### 1. Ink injection systems

As previously mentioned, the glass type models employed ink reservoir cups and ink injection tubes. Each cup or tube represents the source for one single ink flow band. The plexiglass models, however, use an improved ink injection system, where a single 1/8" ID brass tube is imbedded in the sand mixture prior to its consolidation, at any desired position close to the inside face of the model. The tube is perforated at desired intervals and at one end it protrudes from the side or top of the model. Ink is pumped into this tube through flexible plastic tubing and will discharge in nearly equal amounts through all the perforations beneath the water level in the model, due to an equal hydraulic head at each of these points. Differences in gradients leading away from the perforations may cause small inequalities in ink discharge. This system eliminates the necessity for individual control of each ink flow band, and decreases the number of external connections.

### 2. Discharge and Recharge Connections

Water is recharged into models and discharged from the models through plastic tubing connected to the end tanks. The plastic tubing can either be connected directly into a hole in the end tanks or connected to a brass tube protruding from the end tank. Water levels are maintained at desired elevations by drain tubes attached at those elevations. Water is supplied at such a rate that the water level

reaches the drain elevation, but cannot exceed it due to the ability of the drain tube to carry off all excess water.

### 3. Wells

Wells are simulated in the models by 1/4" open holes at the face of the models or by holes containing perforated plexiglass tubing. The open holes are formed by embedding a waxed tube in the sand prior to consolidation, and removing it through a hole in the top of the model after consolidation. When a plexiglass screen is desired, it is imbedded in the sand prior to consolidation and then allowed to remain there. These wells can be recharged and discharged through plastic tubing attached to a brass tube simulating the pump column.

#### F. Setting Models in Operation with Proper Use of Hydraulic Pumps

Operation of the hydraulic models is carried on with the use of two Sigmamotor hydraulic pumps. These pumps produce a kneading action on flexible plastic tubing which is connected to a water source, causing water to move at regulated speeds through the tubing. A large Sigmamotor pump is used to supply water to the recharge tank of the model through 1/4" ID tubing, and also to recharge and discharge wells with the same size tubing. A small Sigmamotor pump is employed to pump ink to the various types of ink injection tubes and reservoir cups. The ink used in this study was green Esterlane Angus ink diluted in 100 parts of water in order to make the density difference negligible.

The first step in setting the model in operation is to saturate the consolidated media by slowly pumping water into the model until the

water level rises to the desired height. When a dry model is saturated slowly, little or no air will be trapped in the consolidated media. However, when a model is being reused and is still damp air will be trapped in the consolidated media no matter how slowly it is saturated. Allowing air to become trapped has two main disadvantages: first, it decreases the permeability of the model, and secondly, if the air is trapped along the face of the model it will break up the ink flow bands reducing their visibility. The problem of trapped air can be eliminated in the plexiglass models by evacuating the models with a small vacuum pump prior to the entrance of water. The models are made air tight by placing vinyl tape over all the openings in the model, and placing plastic cups on all the protruding brass tubes. A tube from the vacuum pump is connected to the highest outlet in the model and a tube from the water pump is connected to the lowest outlet. The model is first evacuated by the vacuum pump and then saturated by the water pump. By following this procedure the author was able to obtain constant permeability and excellent visibility in all the model experiments.

Once the model is saturated, the recharge and discharge tubes can be set at the proper positions, and the pumps can be regulated in such a manner as to allow the model to operate automatically.

## CHAPTER V

### MODEL EXPERIMENTS AND RESULTS

This chapter deals specifically with the model experiments performed by the author. A wide variety of ground water flow phenomena have been examined in this work. The experiments are presented as independent studies of particular ground water flow systems, all of which obey the basic potential theory of hydrodynamics. It is the hope of the author that the following treatment and discussion of these specialized cases will help to clarify them in terms of basic ground water flow theory.

Experiments are presented in the order in which they were performed. Discussion of each experiment includes a description of the models utilized, the objectives of the model study, and the observations and measurements made by the author, as well as any pertinent conclusions which were drawn from the study.

#### EXPERIMENT 1

The first models built in this study were three "small horizontal models" each having a homogeneous media of a different porosity and permeability. They were built slightly different from later small horizontal models inasmuch as their end tanks were completely sealed by an aluminum cover plate. There was only a single outlet in each end

tank, one end being used for recharge and the other for discharge. The models were built with three basic objectives, (1) to study the permeability of the consolidated media, (2) to study the effects of operating the models under pressure and (3) to attempt to achieve turbulent flow in a saturated porous consolidated medium.

The models were found to be capable of fulfilling only the first stated objective. They proved to be excellent self contained permeameters with which one could measure the permeability of the enclosed consolidated media under a variety of hydraulic gradients. When attempts were made to operate the models under hydraulic pressures of greater than 2 psi (pounds per square inch) at the recharge outlet, the models separated along the seams and began to leak. When the discharge outlet was closed on one of the models and the water pressure was maintained at the intake, an almost instantaneous explosion of the model occurred. Having observed this experiment, the author became quite impressed with the almost negligible compressibility of water. These experiments utilizing excessive pressures within the models tended to show that this type of inexpensive portable laboratory model is not adequate for studies of fluids under pressure.

Experiments were made upon the models attempting to produce turbulent flow. Ink was injected into the model through a brass tube driven through the end tank and into the rock. Water was pumped into the model under as great a pressure as could be produced which was only 2 psi, but the velocity of flow obtained was not within the turbulent range and laminar flow continued. Velocities of up to 2500 feet per day were achieved in the models without turbulent flow occurring. This fact

infers that very little turbulence will occur in ground water flow since normal ground water velocities are many times slower than those achieved in the models. Exceptions, however, most likely do occur in fractured basalts and limestone solution channels where the physics of the open channel flow predominate. Turbulent flow has also been known to occur in the immediate vicinity of pumping wells where ground water gradients are exceedingly steep.

## EXPERIMENT 2

It is common in nature to find a multitude of inhomogeneties within the geologic framework of the ground water system. These variations in the geologic structure have an enormous effect on the ground water flow. When water moves through a homogeneous porous media, it can be expected to flow in nearly parallel straight line paths down the hydraulic gradient. In areas where frequent changes in lithology, and consequently permeability, occur, these straight flow paths may be disrupted into an exceedingly complex tortuous pattern. It is of value to have a basic understanding of the effects of changing permeability upon ground water flow direction.

The objective of the second set of experiments was to study the refraction of water as it flows from one medium into another medium having a different coefficient of permeability. The small horizontal model shown in Figure 3 consists of three consolidated members. Members "a" and "c" have the same permeability being 1500 USGS units (gal/day/ft<sup>2</sup>/1:1 gradient) while member "b" has a permeability of

9000 USGS units. The rock units were completely saturated in a closed system and a hydraulic gradient was maintained by keeping the water level in the recharge tank at the right end of the model higher than the water level in the discharge tank at the left end of the model. The results of the many experiments performed by passing ink flow bands (a flow band is a finite group of contiguous flow lines) through this model are best illustrated by the photographic history in Figure 3. Figure 3C shows the ink flow bands after they refracted across both the first and second interfaces.

The flow net diagram of this refraction experiment appears in Figure 4. The path which a particle of water follows in its course through a saturated porous medium is called a flow line. These are represented by green lines in Figure 4. Along each flow line there must be a point where the water has dissipated any given specific portion of its potential. A line connecting all such points of equal head is called an equipotential line. These are represented by red lines in Figure 4. There are actually an unlimited number of flow lines and equipotentials in any system, however, in drawing a flow net, only a finite number of lines are drawn which best illustrate the general flow picture.

Flow must follow paths of steepest gradient, much the same as a ball will take the steepest path when rolling down a hill. Since the gradients are maximum along paths normal to the equipotentials, the flow lines must cross the equipotentials at right angles, thus forming a conjugate system.

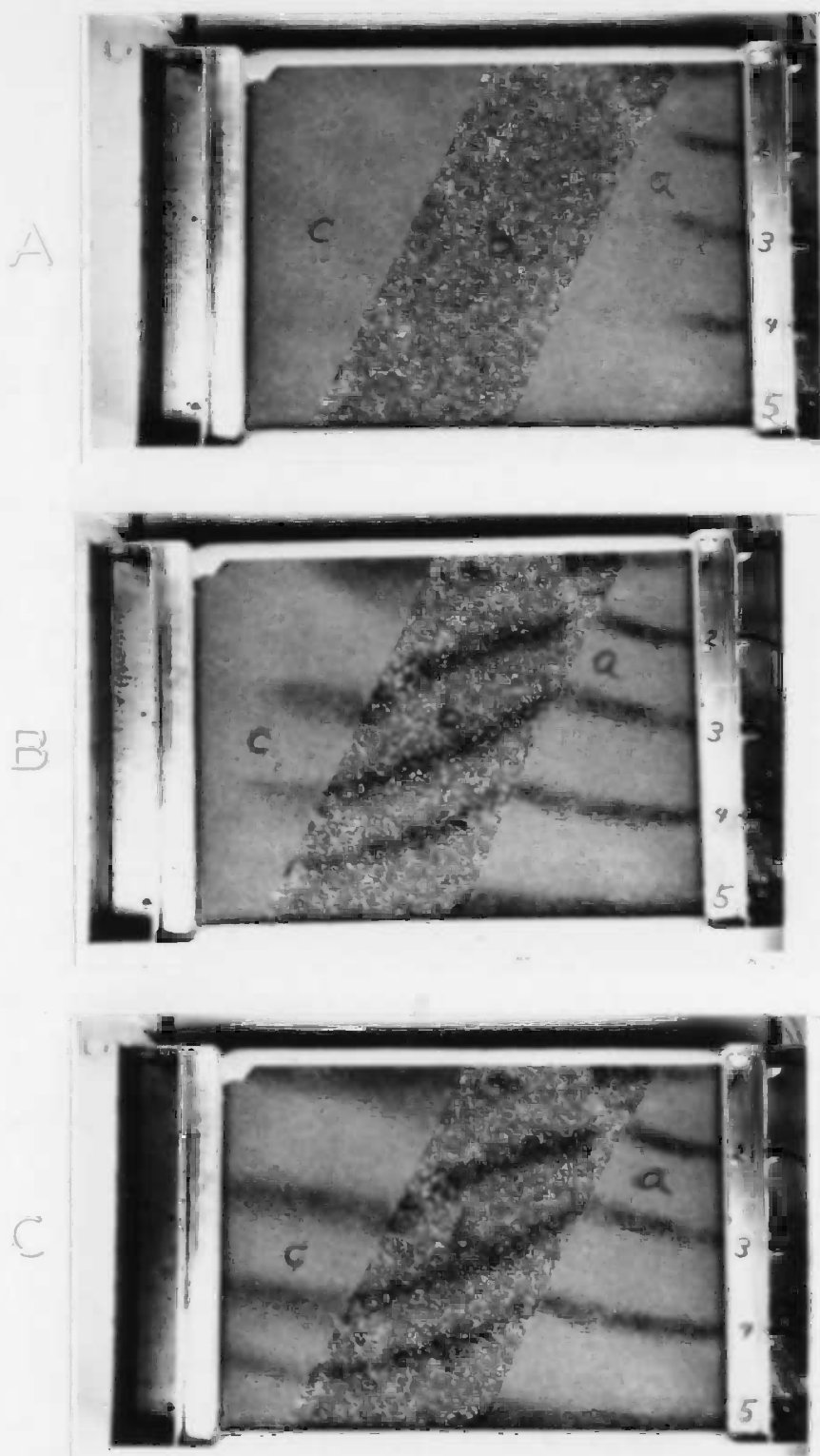


Figure 3. Photographic history of a horizontal refraction model. The pictures were taken at the following times after the entrance of ink: A at 6 min., B at 16 min. and C at 32 min.

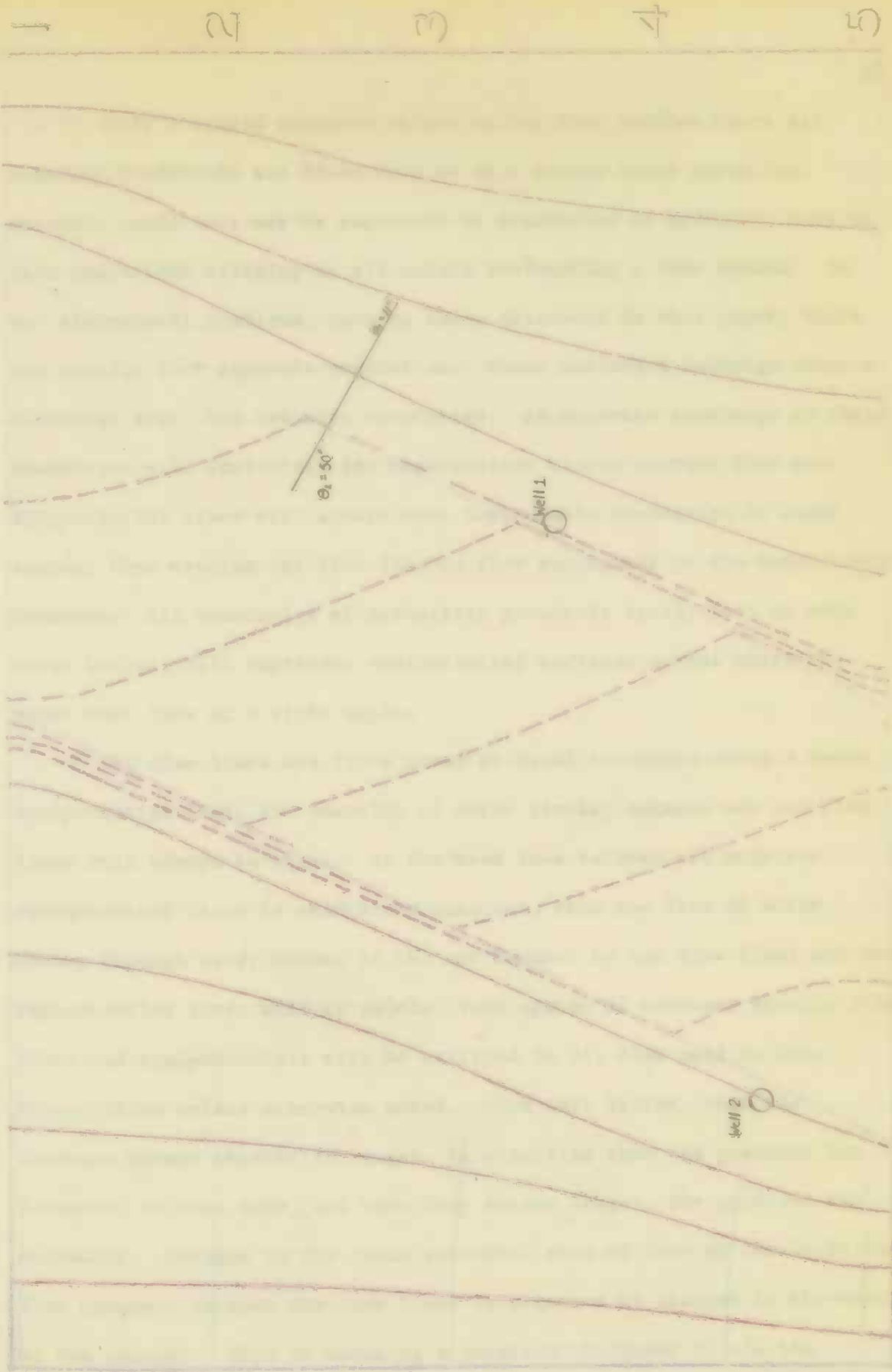


Figure 4. Flow net diagram of the horizontal refraction model shown in Figure 3.

Model Boundary Line  
 Equipotential Line  
 Flow Line  
 Supplemental Equipotential Line  
 Scale = 1/2

Only a single solution exists to any flow problem where all boundary conditions are fixed such as in a steady state situation. Boundary conditions may be expressed as statements of hydraulic head or flow conditions existing at all points surrounding a flow system. In two dimensional problems, such as those discussed in this paper, there are usually four separate boundaries. These include a recharge area, a discharge area, and two side boundaries. An accurate knowledge of these boundaries will facilitate the construction of the correct flow net. Equipotential lines will always meet impermeable boundaries at right angles, thus causing one flow line to flow contiguous to the impermeable boundary. All boundaries of infinitely permeable areas, such as open water bodies, will represent equipotential surfaces across which the water must flow at a right angle.

If flow lines are first drawn at equal intervals along a known equipotential line, the quantity of water flowing between any two flow lines will always be equal. If the head loss between all adjacent equipotential lines is maintained constant, then the flux of water moving through every element of the net bounded by two flow lines and two equipotential lines will be equal. This system of constant density flow lines and equipotentials will be utilized in all flow nets in this dissertation unless otherwise noted. With this system, when the elements become shorter in length, it signifies that the gradient has increased in that area, and when they become longer, the gradient has decreased. Changes in the cross sectional area of flow of the individual flow channels between the flow lines is signaled by changes in the width of the channel. This is assuming a constant thickness of all the

elements in the third dimension. By applying these concepts to the continuity equation

$$Q = A \theta V \quad (2.5)$$

and to the Darcy equation

$$Q = P I A \quad (2.11)$$

one can ascertain any changes which must be occurring in permeabilities or velocities; for instance, when elements become narrower in width with no accompanying change in length (gradient) it means that the permeability must have increased.

The positions of the equipotential lines in Figure 4 were determined by solving the equation

$$h = \frac{\theta V L}{P} \quad (1)$$

for various positions along the flow lines, where  $h$  = head difference,  $\theta$  = porosity of media,  $V$  = velocity of flow,  $L$  = length of flow path and  $P$  = permeability of the medium.  $P$  and  $\theta$  were constants of the members within the model, and  $V$  and  $L$  were measured from observations of the ink flow bands.

The above equation is derived from the steady state equations 3-4 and 3-8 as follows:

$$A \theta V = P I A = P \frac{h}{L} A \quad (2)$$

$$\theta V = P \frac{h}{L} \quad (3)$$

$$h = \frac{\theta V L}{P} \quad (1)$$

Care must be taken in using this equation to use the proper constants applied to  $P$ , which is in gals/day/ft<sup>2</sup>/1:1 gradient, in order to convert it into cubic feet.  $V$  must then be measured in feet per day. It was possible to check some of these calculations by water level measurements in the recharge tank, discharge tank and in Wells 1 and 2 shown in Figure 4, but not in Figure 3. The wells were installed after the pictures were taken in order to obtain the water level measurements. The wells were 1/4 in. in diameter with open holes penetrating the entire member. They contained a plexiglass tube extending from the top of the hold to a point 2 inches above the top so that no water could flow out of the well.

It should be noticed in Figure 4 that the contours are more closely spaced in members "a" and "c" than in member "b". This signifies that the hydraulic gradient is steeper in members "a" and "c" than in member "b", which is undoubtedly a result of the fact that the permeability in "a" and "c" is lower than that in "b". The slope of the hydraulic gradient in a medium varies inversely as the permeability of that medium when the flow rate and cross sectional area are kept constant. This follows logically from equation (2.11).

Since the contrast in permeability of members "a" and "c" and member "b" was great, member "b" closely represented an equipotential surface. The open water in the recharge tank is an equipotential surface, therefore the difference in hydraulic head between any position on the two equipotential surfaces must be nearly equal. This means that the gradient between two points on a flow line connecting these areas is inversely proportionate to the path length between them. This is clearly

illustrated in the flow net (Figure 4).

When the law of refraction as described by Hubbert (16) was applied to the refraction of the flow bands crossing the first and second interfaces, it was found that flow bands 2, 3 and 4 obeyed the law while flow bands 1 and 5 did not obey the law. The equation for the law of refraction is

$$\frac{\tan \theta_1}{\tan \theta_2} = \frac{P_1}{P_2} \quad (4)$$

Where  $\theta_1$  is the angle between the flow band in the incident medium and the line normal to the interface, and where  $\theta_2$  is the angle between the same flow band in the refraction medium and the line normal to the interface. These angles are shown for flow band 3 (Figure 4).  $P_1$  is the permeability of the incident medium, and  $P_2$  is the permeability of the refraction medium. The following calculations illustrate the correctness of the law of refraction for flow band 3 crossing the first interface.

$$\begin{array}{lll} \theta_1 = 11^\circ & \tan \theta_1 = 0.1944 & P_1 = 1500 \\ \theta_2 = 50^\circ & \tan \theta_2 = 1.1918 & P_2 = 9000 \end{array}$$

$$\frac{\tan \theta_1}{\tan \theta_2} = .1632 = \frac{P_1}{P_2} = .1667$$

This is less than 3% error which is within the range of permissible experimental error.

Where boundary conditions interfere, as in bands No. 1 and 5 which are contiguous to the right and left boundaries of the model, the law of refraction does not hold true because the equation of continuity (2.1) must first be satisfied. This law states that in saturated flow

the volume of flow leaving a given volume of media must be equalled by the volume of flow entering that same volume of media. If flow band No. 1 was allowed to refract the full amount, there would be no flow moving along the boundary, and this is not possible in saturated flow. The refraction of flow band No. 5 is physically retarded by the left impermeable boundary of the model. Both of these particular situations of flow bands 1 and 5 are ultimately controlled by the continuity equation.

During the time experiments were being performed upon this model, it became evident that although the model was made up of three members having specific permeabilities, the model as a whole had a different permeability than any of the members. There seemed to be no obvious relationship between the permeability of the parts and the permeability of the whole. However, a search of the petroleum industries literature uncovered some information on this problem which has enabled the author to adapt an equation by which the permeability of the entire media can be calculated, when the permeability of the parts are known. The equation has value in practical hydrology when it is desired to test an aquifer containing many lateral variations in permeability as a single aquifer with one effective permeability. This type of treatment saves multiple computations when calculating regional hydrologic characteristics.

The equation is derived as follows:

Assume an aquifer having lateral facies changes. The facies are designated 1, 2 and 3 etc., all of which have approximately the same average saturated cross section (this is most likely to occur in confined aquifers). In such a situation the total discharge  $Q_t$  which passes through the whole aquifer is the same as the  $Q_1$ ,  $Q_2$  and  $Q_3$  passing through

the different facies of the aquifer. The total headloss  $h_t$  is equal to the sum of the individual headlosses  $h_1$ ,  $h_2$  and  $h_3$ . Therefore,

$$Q_t = P_t \frac{h_t}{L_t} A_t \quad (5)$$

$$h_t = \frac{Q_t L_t}{P_t A_t} = h_1 + h_2 + h_3 + \dots \quad (6)$$

$$\frac{Q_t L_t}{P_t A_t} = \frac{Q_1 L_1}{P_1 A_1} + \frac{Q_2 L_2}{P_2 A_2} + \frac{Q_3 L_3}{P_3 A_3} + \dots \quad (7)$$

since  $Q_t = Q_1 = Q_2 = Q_3$  and  $A_t = A_1 = A_2 = A_3$  (8)

therefore  $\frac{L_t}{P_t} = \frac{L_1}{P_1} + \frac{L_2}{P_2} + \frac{L_3}{P_3} + \dots$  (9)

and the final equation becomes

$$P_t = \frac{L_t}{\sum_i \frac{L_i}{P_i}} \quad (10)$$

This equation was used to calculate the specific permeability of the small horizontal refraction model as shown below.

$$L_t = 18 \text{ in.} \quad L_a \text{ average} = L_b \text{ average} = L_c \text{ average} = 6 \text{ in.}$$

$$P_a = 1500 \text{ USGS units} = P_c, P_b = 9000 \text{ USGS units}$$

$$P_t = \frac{18}{\frac{6}{1500} + \frac{6}{9000} + \frac{6}{1500}} = \frac{18}{\frac{78}{9000}} = \frac{27000}{13} = 2077 \text{ USGS}$$

The accuracy of this equation was checked with the model by solving for  $P_t$  of the model using the equation...  $Q_t = P_t I_t A_t$ .  $Q_t$ ,  $I_t$  and  $A_t$  were measured directly and then the equation was solved for  $P_t$ . The resultant permeability was 2100 USGS units which agrees with the value calculated above.

The refraction of flowlines across members of contrasting permeability is extremely important to the problem of waste disposal. The highly permeable member "b" in this model may represent a buried stream channel, or a brecciated fault zone which can radically change the direction of fluid flow within the ground water body. An increasingly complex spectrum of wastes are being discharged into the ground water body through disposal pits or wells. Looming on the horizon is the foreboding problem of waste disposal from nuclear technology of the 21st century. It is of the greatest importance to know the exact path that the waste will travel before it is placed in the ground. Toxic waste must not be allowed to invade and contaminate aquifers which are being used for municipal water supply, and water developers must be cautioned not to set up new well sites along the flow paths of the contaminating waste. If the projected path of toxic waste is assumed to be directly down the regional gradient, without taking into account the local variations in gradient due to formations such as buried stream channels and fault breccias, the projected flow paths may be tens of miles away from the true flow path. Once an error in calculating a flow path is made and the waste is dumped, it is essentially impossible to retrieve or reroute the waste even though it may be on a course which will ultimately destroy a city's water supply. Often it may take

ten or twenty years before the toxic waste reaches its unknowing target, but once the damage is done it is likely to be over one-hundred years before the contaminated aquifer is running pure again. It is this enormous time factor which causes any errors to be critical ones, and necessitates exacting study of the hydrologic characteristics of the subsurface in order to minimize the chance of any errors.

### EXPERIMENT 3

Model experiments were performed for the purpose of discovering any possible relationship between the hydraulic gradient and the paths of flow in a saturated confined medium. The small horizontal refraction model (Figure 3) was used for this purpose by operating it under a variety of gradients. The experiment showed that the flow pattern in this model remained constant, regardless of the hydraulic gradient imposed upon it. It was desired, however, to perform a further test on this relationship using a model believed to be more conducive to a change in the flow paths due to a change in the hydraulic gradient.

Figure 5 is a picture of the small horizontal model built for this purpose. The medium formed in the shape of a  $90^\circ$  arc of 2 in. width has three times the permeability as the encompassing medium. An ink reservoir was set at the entrance to the permeable arc from which an ink flow band moved through the arc until it finally refracted across the interface into the encompassing medium. Due to the gentle curvature of the interface between the arc and the encompassing medium, it was believed that an increased gradient might allow the flow band in the arc to move further down the curving interface before refracting across it. This,

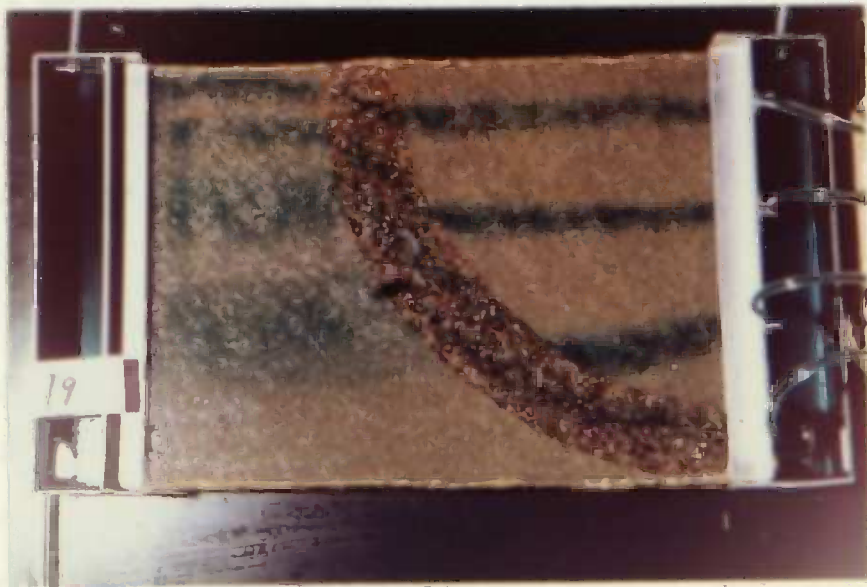


Figure 5. Photographs of an arcuate refraction model taken before and after the movement of ink flow bands through the system.

however, was not the case, as the flow path remained the same under all gradients.

It can be concluded that in confined saturated flow the hydraulic gradient does not effect the flow paths within the medium. This is a logical situation since it is actually the various boundaries within an aquifer which determine the flow paths. These boundaries include the impermeable bedrock, the upper saturated surface and any changes in lithology within the aquifer. Changes in the hydraulic gradient only change the flow paths insofar as they change the boundaries. When the hydraulic gradient is changed in an unconfined aquifer, the shape of the free surface changes accordingly. Since this free surface is in effect a flow boundary, such a change will effect the configuration of the flow paths. In a confined aquifer, however, a change in the hydraulic gradient is not accompanied by a change in the upper flow boundary, since this boundary is kept constant by the confining member. The piezometric surface above the aquifer is changed, but this does not act as a flow boundary; therefore, no boundaries are changed and the flow paths remain constant.

While experimenting with the arcuate refraction model an interesting observation was made. The velocity of flow in the highly permeable arc was more than twice the velocity of flow in the encompassing medium. In the model shown in Figure 3, however, the velocity of flow in the highly permeable member "b" was only slightly greater than that in the encompassing members "a" and "c", although the ratio of the permeability of the highly permeable medium to the surrounding medium was twice as large as that in the previously mentioned model. This puzzling situation

can be made clear when one realizes that increased permeability in a portion of an aquifer may have two different effects on the flow in the aquifer. The first effect is that the increased permeability may result in a very low hydraulic gradient, and have little effect on the velocity of flow. This will be true when the highly permeable member is everywhere bounded up gradient by a relatively low permeable member and when its cross sectional area is large in relation to the cross sectional area of the entire saturated thickness. Under these circumstances, the rate of flow through the high permeable medium cannot exceed the rate of flow through the low permeable medium. This situation is illustrated in Figure 3 where everywhere along the interface between members "a" and "b" the permeability increased down gradient. The gradient in member "b" becomes so low that it can be considered nearly an equipotential surface, however the velocity of flow in the medium is not greatly increased.

The second effect of an increase in permeability is that the velocity of flow may be greatly increased, while the hydraulic gradient in it will not be appreciably lowered. This can occur when the highly permeable member is partially bounded up gradient by a member whose permeability exceeds its own. This affords an ample supply of water to the highly permeable member, thus eliminating the necessity for a decrease in hydraulic gradient. This case is illustrated in Figure 5, where a portion of the highly permeable arc was bounded up gradient by the recharge area whose permeability was infinite. In this model, the velocity in the arc was much greater than in the surrounding medium, but the hydraulic gradient as shown on the flow net in Figure 6 was not

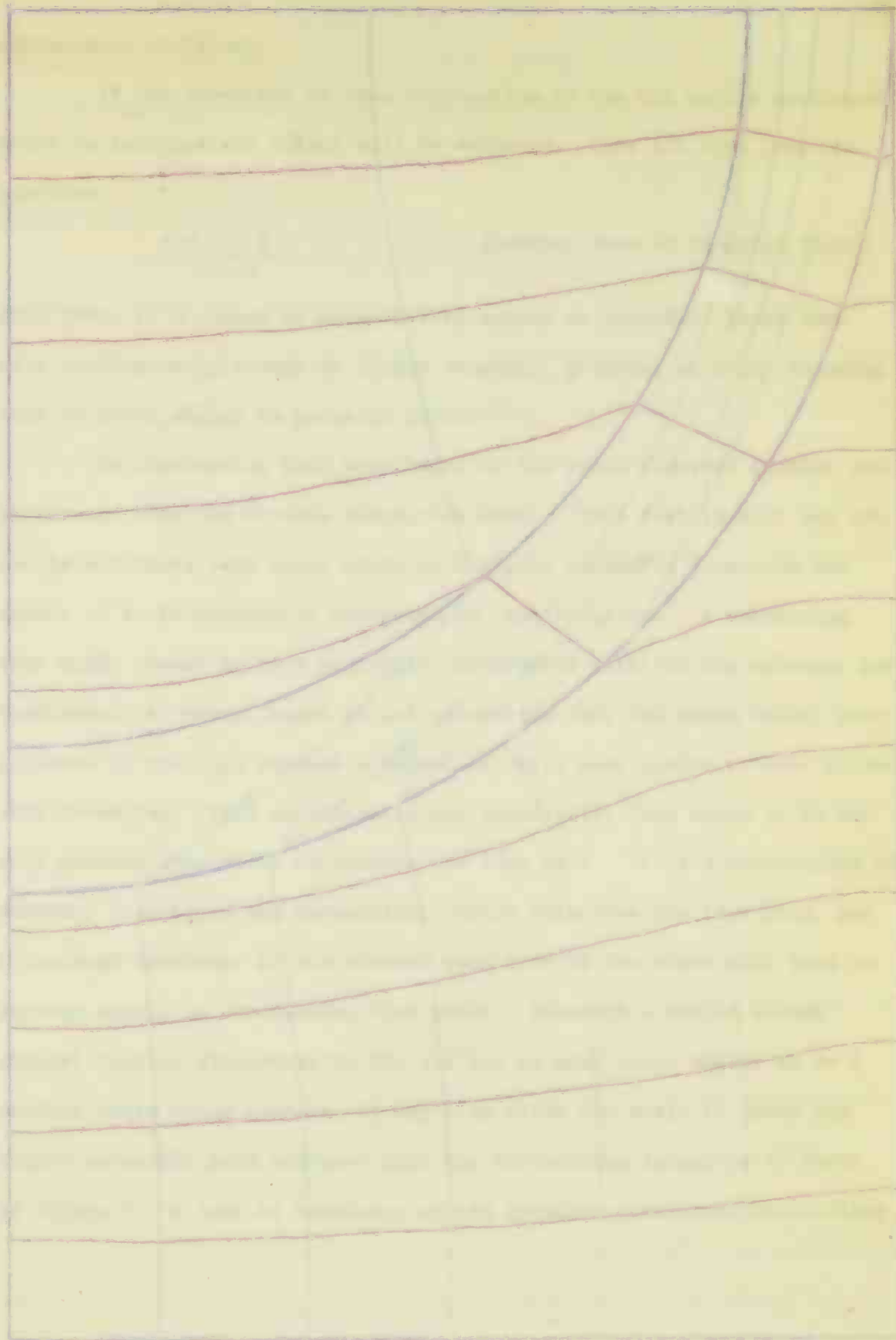


Figure 6. Flow net diagram of the arcuate refraction model in Figure 5.

Model Boundary

Flow Line

Scale = 1/2

Equipotential

appreciably different.

If the situation is some combination of the two models mentioned above an intermediate effect will be achieved. This all ties into the equation

$$P = \frac{V \theta}{I} \quad (\text{another form of equation (4.1)})$$

When there is a change in permeability across an interface there must be a corresponding change in either velocity, gradient or both, assuming that no major change in porosity occurs.

An interesting fact beneficial to the waste disposal problem can be learned from the arcuate refraction model. This fact is that one can not in all cases dump toxic waste in a highly permeable formation and expect it to be constantly contained in that formation. A shoestring sand might appear to be a perfectly predictable path for the movement and confinement of waste, based on the assumption that the waste water, once injected in the high permeable formation, will seek always to move within this formation. This situation is not necessarily true since it is not only permeability which determines the flow path. It is a combination of boundary conditions and permeability which determine the flow path, and a thorough knowledge of one without some idea of the other will lead to serious errors in determining flow paths. Although a buried stream channel leading ultimately to the sea may in many cases appear to be a perfect waste water conduit, it may also allow the waste to leave the highly permeable path and move into the surrounding formation as shown in Figure 5. A lack of knowledge of the boundary conditions controlling

the hydraulic gradients along the buried stream channel could lead to the destruction of an adjacent fresh water aquifer.

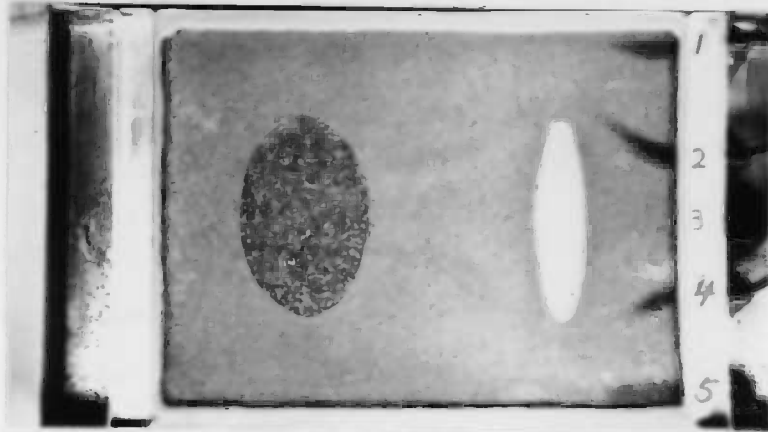
#### EXPERIMENT 4

A model experiment was performed in order to study the flow patterns around and through lenses of different lithologies. Figure 7 shows ink flow bands moving through a "small horizontal lens model" with three rock units of different permeability. The oblate lens on the right had a coefficient of permeability of less than one USGS unit. The elliptical lens on the left had a coefficient of permeability of 10,000 USGS units, and the encompassing medium had a permeability of 2000 USGS units. It is interesting to note (Figure 7C) that flow band No. 3 in the center bifurcated, completely wrapped around the oblate lens and then reunited into a single flow band and continued toward the second lens. Flow lines No. 2 and 4 were forced outward by the effect of the impermeable lens, but were then attracted toward the center of the second lens because of its great permeability and large capacity for transmitting water. As the flow lines left the second lens they again spread due to the decreased carrying capacity of the encompassing medium.

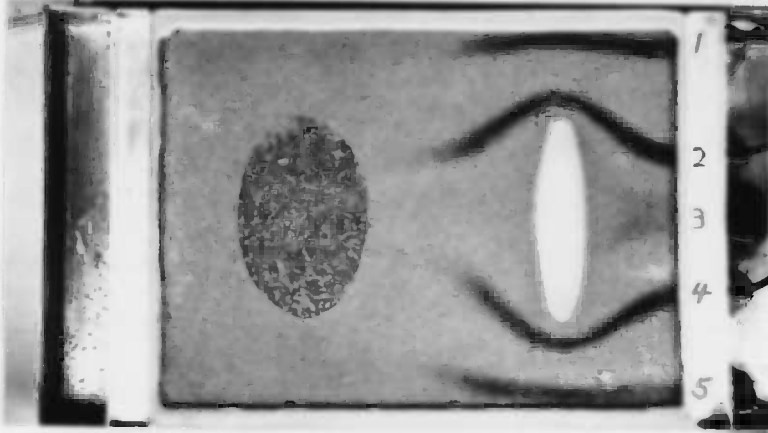
Prior to the completion of this model, many persons believed that a small area behind the impermeable lens would be a dead area with no flow moving into or out of the area. This model experiment supports the fact that there are no dead spots or stagnation zones in saturated laminar flow.

There is, however, a point of no flow called the stagnation point which may occur within a flow system. According to hydrodynamic law, a

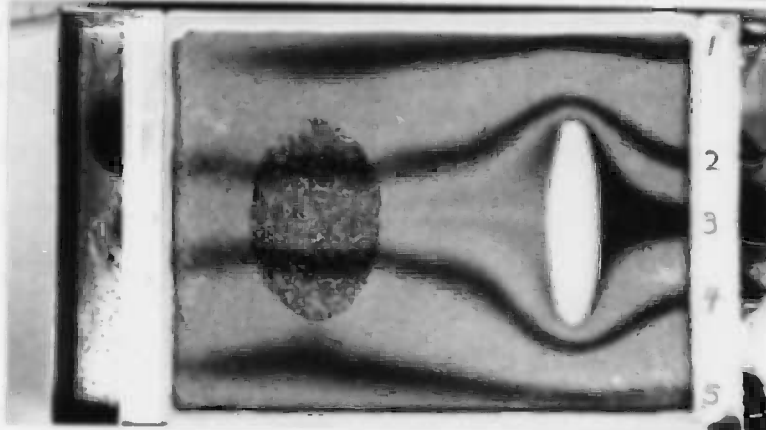
A



B



C



D

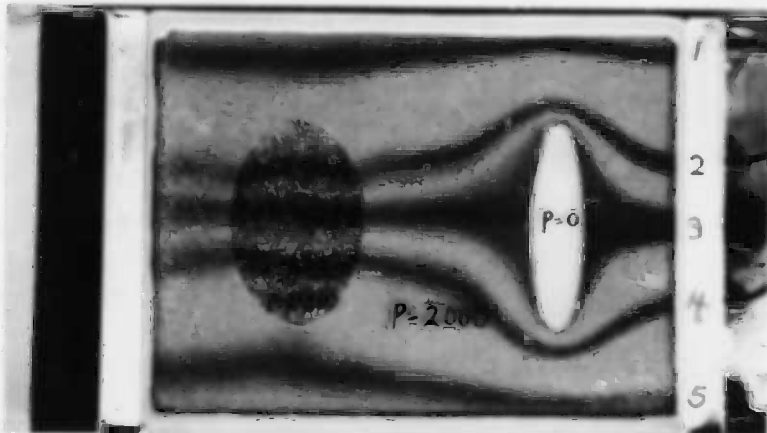


Figure 7. Photographic history of a horizontal lens model. The pictures were taken at the following times after the entrance of ink: A at 6 min., B at 18 min., C at 34 min. and D at 44 min.

flow line can not change its direction by means of a sharp angled turn unless it crosses a permeability interface; there must be some curvature to any turn made within a homogeneous medium, if the equation of continuity (2.1) is to be satisfied. When flow bands bifurcate or unite around some boundary condition such as the impermeable lens, in Figure 7, or a cone of depression of a pumping well, they require a point around which they can pivot in order to make turn with some curvature. If there were no point of stagnation to use as a pivotal point, the flow bands moving along the boundary conditions would have to move through every increment of the porous medium which would necessitate a sharp angular turn. Since a sharp angle turn may not occur without crossing an interface we know that the point of stagnation must exist. This stagnation point is probably represented by only a single molecule of water, but this theory has not yet been proven. With the exception of these stagnation points, when a hydraulic gradient is imposed upon a system, all the water in the system will flow, however, the velocity of the water movement is not necessarily constant throughout the porous medium. This can be seen in Figure 7 where, although all the ink was injected into the model simultaneously, the flow bands outside of the first lens traveled at greater rates than band No. 3 which was in front of this lens. In this case, the water behind the impermeable lens flowed very slowly, and was replaced by more flowing water in accord with the equation of continuity.

The change in thickness of flow band No. 3 as it moved around the first lens is of considerable interest (Figure 7). It was a thick band, both in front of the lens and behind it, but as it rounded the

corner it was very thin. In order for this to occur in homogeneous media, the velocity of flow must be much greater where the line is thin than where the line is thick, in order to satisfy the continuity equation

$$Q = A \theta V \quad (2.5)$$

The flow net diagram of this model (Figure 8) adequately designates these velocity variations by the changing dimensions of the flow net elements. Within a single medium, the velocity is greatest in the narrowest elements and lowest in the widest elements.

A great deal can be learned from this model in regard to the proper placement of wells seeking uncontaminated water. Many mistakes have been made in the placement of wells in areas of known toxic waste disposal. One common misconception is that the shadow of a low or impermeable formation such as an igneous plug or stock, down gradient from a point of waste disposal, offers a water supply safe from contamination. This model indicates that this so called shadow area only offers a delay rather than an escape from the inevitable contamination. In contrast to this observation is the excellent possibility of obtaining relatively uncontaminated water at some distance to the right or left of the high permeable lens. When such a lens occurs directly down gradient from the location of the waste disposal, it may have the effect of concentrating the waste fluid in a small cross section of flow, leaving the area to the sides of it uncontaminated and therefore capable of supplying potable well water.

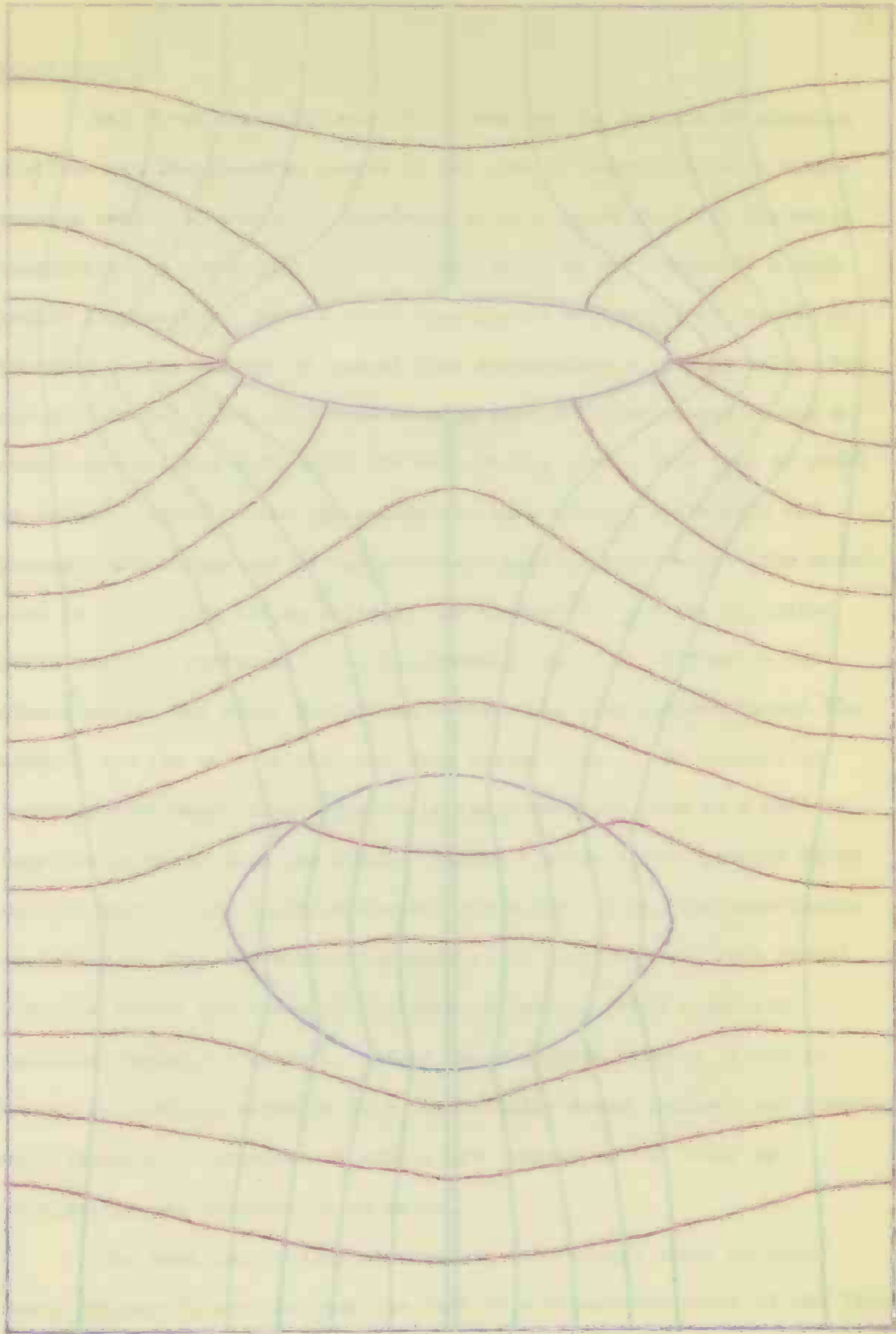


Figure 8. Flow net diagram of the horizontal lens model in Figure 7.

Flow Lines

Equipotential Line

Model Boundary Line

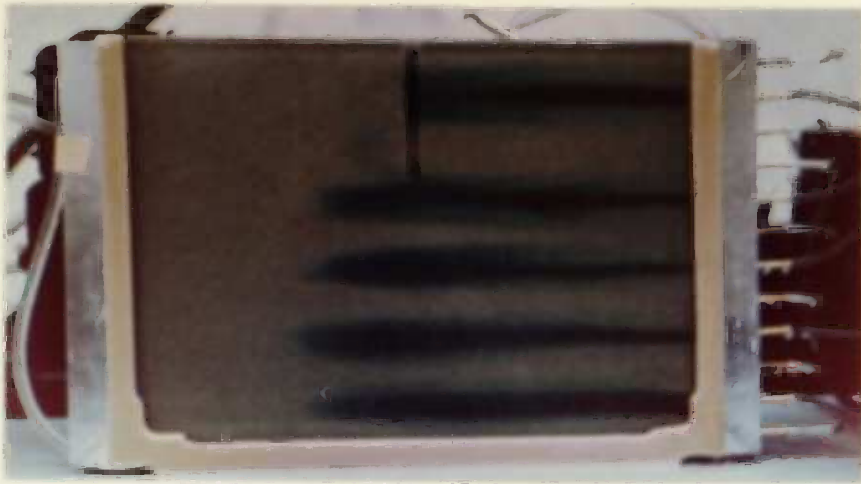
Scale = 1/3

## EXPERIMENT 5

The first vertical model built was for the purpose of studying the flow net displacement caused by the cone of depression of a single pumping well. It should be mentioned at this point that all the wells constructed in the models used for this study do not represent a true radial flow system. Only a three dimensional sand model is capable of yielding a true analogy of radial flow surrounding a pumping well. For visual flow net study of a true pumping well it is necessary to use a radial sector sand model with the well at the apex. This type of model is rather limited in its application to more complex hydrologic and geologic situations and is therefore not used in this study. The models used in this study are essentially two dimensional and the so called wells actually represent infinite channels toward which flow is two dimensional. The basic difference between the flow pattern toward the channel and the well is that the down stream side of the channel is supplied with water from below while the downstream side of a well is supplied by water from the sides. Figure 9 shows a flow pattern which matches that of the infinite channel situation. Since the experiments performed on this and succeeding models are not concerned with radial flow the author has taken the liberty of calling these simulated infinite channels, "wells". All of the phenomena studied in the so called well models occur in both the infinite drain channel and pumping well situation, therefore no errors are imposed on the study by considering the channels to be wells.

The most interesting observation made in the study of this model (Figure 9) was the complete lack of a transition phase of the flow

A



B



C



Figure 9. Photographic history of a small vertical well model. The pictures were taken at the following times: A at 23 min. after the entrance of ink, B at 2 min. after pumping began which was 24 min. after entrance of ink and C at 10 min. after pumping.



Figure 9 (continued). Photographic history of a small vertical well model. The pictures were taken at the following times: D at 6 min. after pumping stopped, pumping had continued for 11 minutes, and E at 25 min. after pumping stopped.

bands as they appeared before pumping, and, as they appeared after pumping had taken place for a few minutes. At almost the very instant the well began to pump, all the particles of water within the radius of influence of the well acquired a new vector of motion. There was no realligning of old flow bands because the old flow bands ceased to exist when pumping began. Each particle of water was on its own to take its place in the new net similar to individuals in a marching band when a new formation is imposed.

The change in the flow net is dependent upon the water level in the pumping well. Any change in boundary conditions in the system, such as drawdown in a well will be felt throughout the system, resulting in adjustments of the pressure distributions in accordance with the new boundaries. The speed with which these adjustments occur can be determined by the Theis non-equilibrium equilibrium equation (34)

$$s = \frac{114.6 Q}{T} \int_Z^{\infty} (e^{-u/\mu}) d u \quad (11)$$

$s$  = drawdown at any point, in feet

$Q$  = rate of discharge of the well in gallons per minute

$T$  = coefficient of transmissibility, in gpd per ft

$$Z = 1.87 \frac{r^2 S}{T t}$$

$r$  = distance between pumped well and point of observation, in feet

$S$  = coefficient of storage, dimensionless

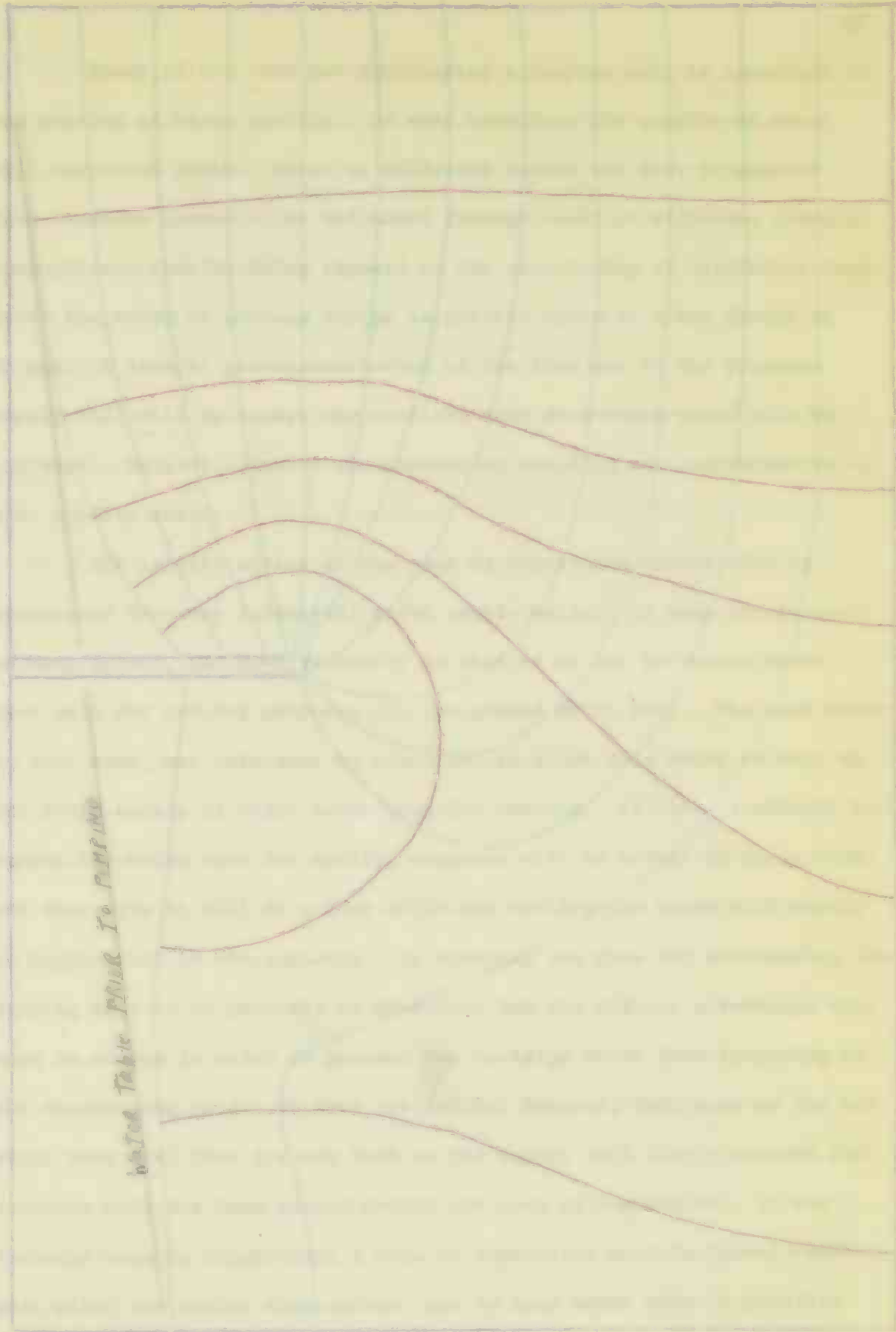
$t$  = time the well has been discharging in days

$\mu$  = a dimensionless quantity varying between the limits given

This equation was derived upon the simplifying assumption that the removal of water from an aquifer is exactly analogous to the removal of heat from a metal plate, for which the equations are already known.

Figure 9a shows a "small vertical well model" twenty-three minutes after the entrance of the ink; the flow bands have moved partly across the model under a small hydraulic gradient prior to the start of pumping. It must be mentioned here that variations in the thickness of the flow bands in Figure 9a are not due to velocity changes but rather due to adjustments in the ink input made by the experimenter in order to finally arrive at a neat thin flow band. Figure 9b shows the flow bands two minutes after pumping began in the small well at the center of the model. The existing pressure field was modified quickly to conform to the new boundary conditions.

The coloring matter began moving slowly along an infinite set of new stream lines which, intersected the lines of the old pattern at finite angles, they finally stabilized in a pattern coinciding with the actual stream lines determined by these new boundary conditions as shown in the photograph (Figure 9c) and the flow net diagram (Figure 10). When the pump was removed the curved flow lines moved horizontally as a unit (Figure 9d) until the ink was flushed out of the model and only the horizontal bands appeared (Figure 9e). Here an almost instantaneous change in the vectors of motion of the water particles took place because the reaction time is very fast in small models. In the nonpumping situation all the vectors were approximately equal, hence the old flow bands appeared to move as a unit.



Water Table Head To Pumping

Figure 10. Flow net diagram of the small vertical well model in Figure 9.

Flow Line

Equipotential Line

Model Boundary Line

Scale = 1/2

Study of the flow net surrounding a pumping well is important to the problem of water quality. In many locations the quality of water will vary with depth. Water at different depths may have originated from separate source areas and moved through rocks of different chemical composition, thereby being exposed to the solutioning of dissimilar ions. Often the water at certain depths is potable while at other depths it is not. A careful pre-determination of the flow net of the proposed supply well will delineate the vertical zone from which water will be captured. This will insure the chances of avoiding any contamination by poor quality water.

The lateral extent of the cone of depression should also be determined for many industrial water supply wells. In some areas, such as Long Island, New York, industry is obliged by law to return water used only for cooling purposes, to the ground water body. The used water is very warm, and care must be taken not to allow this water to heat up the fresh supply of water being used for cooling. If this is allowed to happen the water used for cooling purposes will be warmer to begin with and therefore it will do a less efficient cooling job which will result in higher cost to the industry. By studying the flow net surrounding the pumping well it is possible to determine how far distant a recharge well must be placed in order to prevent the recharge water from returning to the discharging well. It does not follow, however, that none of the hot water used will find its way back to the supply well simply because the recharge well has been placed beyond the cone of depression. If the recharge rate is significant a cone of impression will be formed which will alter the entire flow system, and in many cases make it possible

for the hot water to return to the discharge well. When the quantity of recharge is small, however, it may not significantly alter the flow pattern set up by the discharge well. Care must be taken to determine these factors prior to the permanent installation of the wells in order to prevent costly errors.

#### EXPERIMENT 6

An interesting experiment with a "large vertical model" involved pumping two wells simultaneously in order to observe the mutual interference of the flow nets surrounding the two wells. The model is shown in Figure 11 and its flow net is shown in Figure 12. It contains two horizontal clay layers 24" long, 1" thick and 4" apart. These layers were formed in the model to add a complexity to the flow net, but are not particularly relevant to the discussion which follows. In this experiment it was possible to observe the phenomenon of the ground water divide which is an imaginary surface of zero potential separating ground water movement in opposite directions. This surface can be seen as it formed, but once the flow lines moved on both sides of it, it could no longer be exactly defined; its formation is shown in Figure 11. The flow band was first seen to curve around into the first well, then a portion of the flow band began to move toward the second well, and it was finally seen to have reached the second well. Therefore, we have a unified flow band which divided into two parts and proceeded to flow in opposite directions. The position of this divide can be accurately drawn by the observer as he watches the original formation of the flow band. The position of the ground water divide and the flow lines on both sides are shown

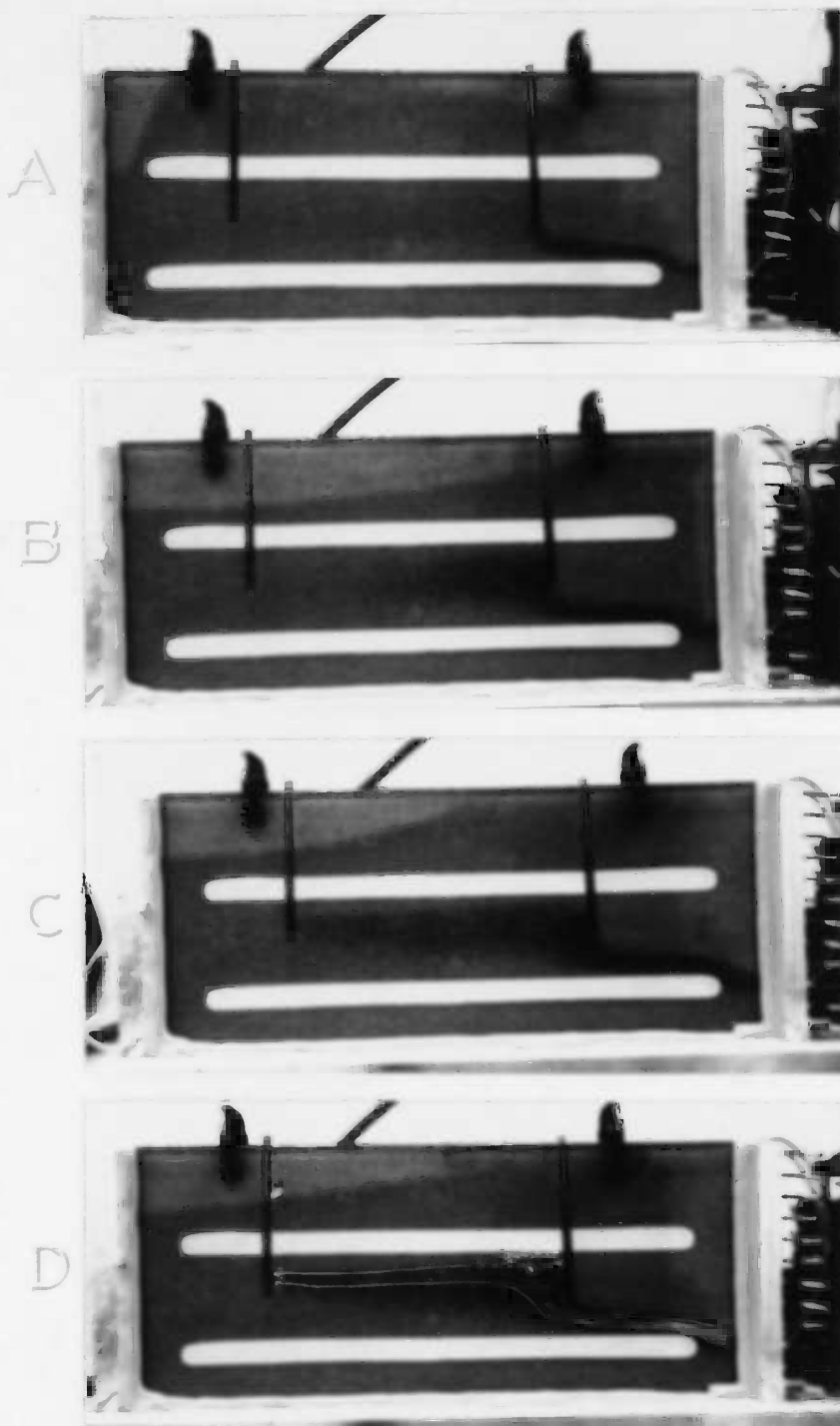


Figure 11. Photographic history of a large vertical double well model. The pictures were taken at the following times after the entrance of ink: A at 6 min., B at 16 min., C at 26 min. and D at 28 min.

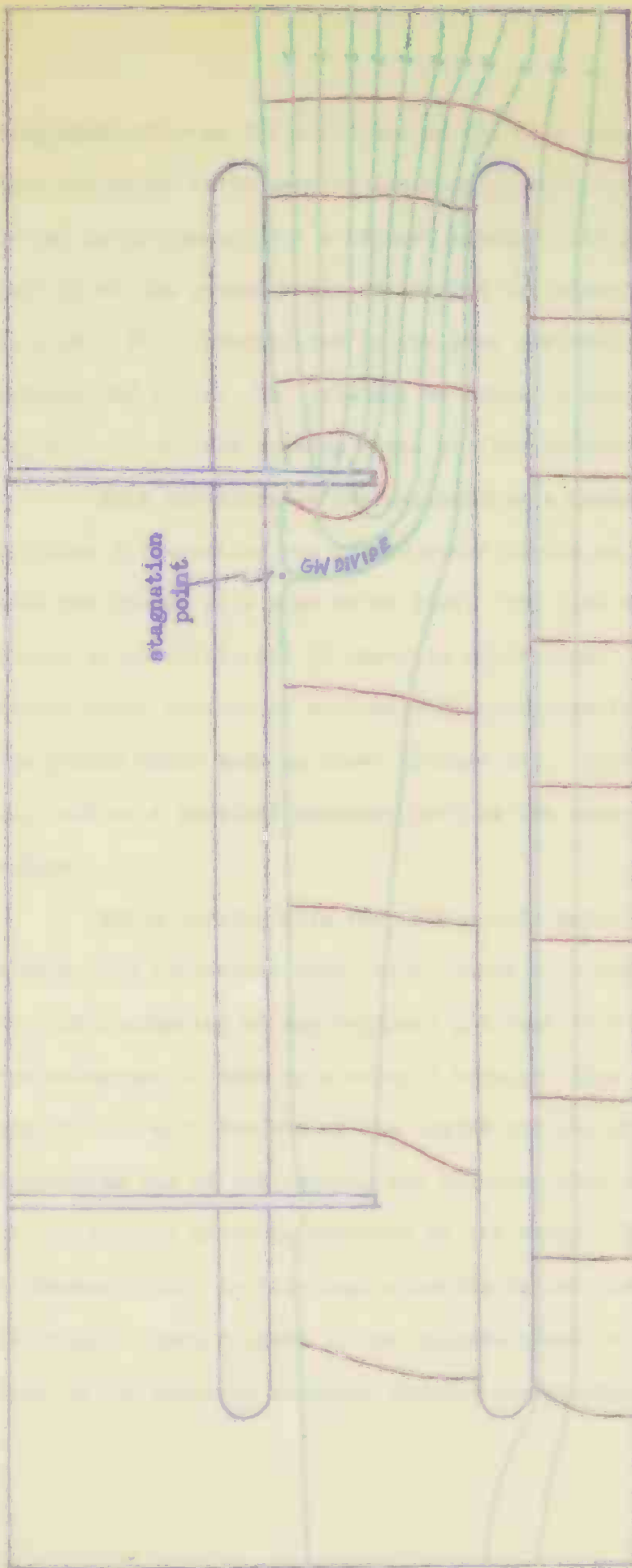


Figure 12. Flow net diagram of the large vertical double well model in Figure 11.

Model Boundary      Equipotential Line      Flow Line

Scale = 1/3

diagrammatically on the model and on the flow net (Figures 11 and 12). When the water table between two pumping wells can be seen in a model, or can be determined for a natural aquifer, the position of the intersection of the ground water divide and the water table can be easily located. This intersection is the peak position of the water table between the wells. The gradient on opposite sides of this peak is in opposite directions causing water to flow to both wells at the same time.

This investigator has encountered a number of diagrammatic sketches illustrating the ground water divide as shown in Figure 13. Here the divide is a line of no flow. The flow on opposite sides of the divide is parallel, but in opposite directions. This flow pattern cannot exist because it necessitates equipotential lines ending within the ground water body as shown (Figure 24). Equipotential lines can only end on a physical boundary such as the water table or an impermeable medium.

While working with the double well model, it was discovered that errors were introduced into calculations of discharge by using a straight line approximation of the regional gradient ( $I = \text{gradient} = \frac{h}{L}$ ). This approximation is made by drawing a straight line between the hydraulic head at the upstream end of the region and the hydraulic head at the downstream end of the region, and assuming that the length of this line is the average distance traveled by the water. The value of  $h$  (head difference) used in this approximation is the correct value, but the value of  $L$  (path length) is the minimum possible value, since a straight line is the shortest distance between two points.

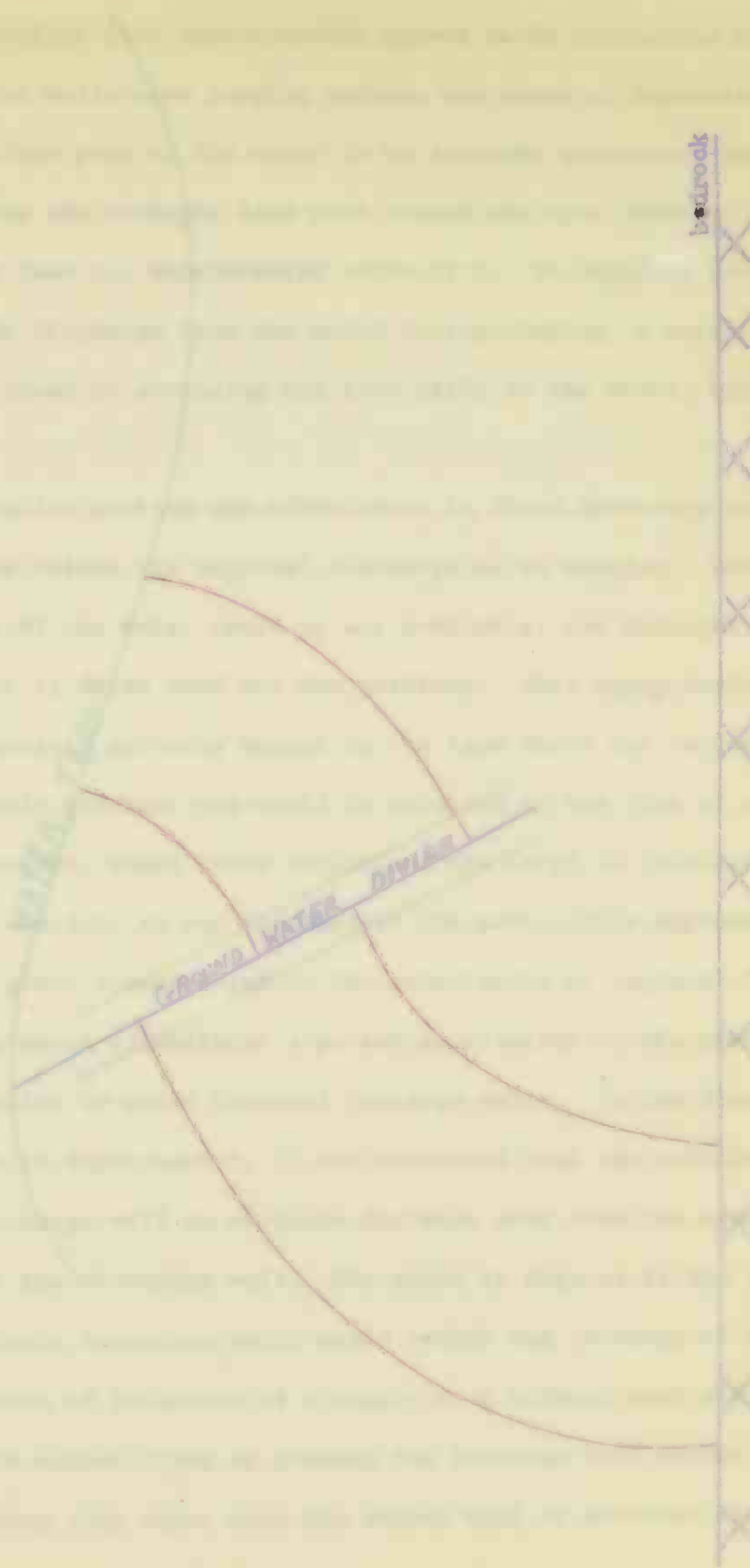


Figure 13. Flow net diagram illustrating an incorrect representation of a hypothetical ground water divide.

Boundary Line

Equipotential Line

Flow Line

A straight line approximation proved to be inaccurate in the model when the wells were pumping because the cones of depression caused the average flow path of the water to be somewhat tortuous. This departure from the straight line path caused the true value of  $L$  to be much greater than the approximated value of  $L$ . In order to correctly calculate the discharge from the model during pumping, a more realistic value of  $L$ , found by averaging the flow paths in the model, had to be used.

A similar problem may often arise in field hydrology when it is desired to calculate the regional discharge of an aquifer. When an accurate map of the water table is not available, the straight line approximation is often used for the gradient. This approximation will yield a reasonably accurate answer in the case where the variations in the water table gradient are small in relation to the size of the entire aquifer. However, where these variations are large in relation to the size of the aquifer, as was the case in the model, this approximation may lead to gross inaccuracies in the calculation of regional discharge.

This model illustrates a potential solution to the problem of back circulation in waste disposal recharge wells. In the discussion of this problem in Experiment 5, it was mentioned that the solution was to place the recharge well an adequate distance away from the area of influence of the discharge well. The model in Figures 11 and 12, however, shows a geologic situation which would permit the recharge of waste water within the area of influence of a supply well without back circulation. This could be accomplished by placing the recharge well screen below the lower confining clay layer when the supply well is screened only above

the clay. The recharge well could be very close to the supply well, but as long as it is screened only below the lower layer very little danger of contamination exists. If the well to the left of the model was screened below the lower clay layer rather than above it, any water recharged through it would have very little chance of being drawn back to the discharging well at the right. The low permeability of the clay layer will prevent the waste water from being drawn through the clay and back into the supply well. Once the waste has moved down gradient beyond the confinement of the clay layer it will be past the area of influence of the supply well and therefore will no longer have access to circulate back to the well.

#### EXPERIMENT 7

One of the most recent experiments performed with a "large vertical model" is shown in Figure 14. The upper layer in the model is a coarse medium having a permeability of 10,000 USGS units, the second layer has a permeability of 100 USGS units, the undulating bottom medium has a permeability of 5 USGS units, and the encompassing medium has a permeability of 2,000 USGS units. The purpose of studying this model was to learn what effect a highly permeable layer would have on partially confined water beneath a low permeable layer. This model was run both under pumping and non-pumping conditions. The model is first shown under nonpumping conditions (Figures 14b and 14c) as the ink illustrating flow paths moved through the model. It is readily seen that the highly permeable layer drew a large proportion of the total flow into it because of its great capacity for transmitting water. It offered the path



Figure 14. Photographic history of a large vertical lens model. The pictures were taken at the following times: A at 0 min., B at 7 min. and C at 51 min. after entrance of ink, D at 10 min. after the start of pumping in the two wells. Pumping began 52 min. after the entrance of ink.

of least resistance and most of the flow follows this path (Figure 15). Beneath the low permeable layer, however, very little of the flow is affected. Most of this flow remained beneath the lower layer, although a small percentage passed through it. In Figure 14d, the flow bands are seen ten minutes after pumping was initiated from the two wells drilled in the highly permeable layer. The partially confined flow beneath the low permeable layer was greatly affected by the high permeable layer, and was nearly all drawn to it.

Two wells screened only in the media directly below the high permeable layer were constructed and pumped at the same rate as the first two wells, but were not able to draw the partially confined flow up through the low permeable confining member.

After considerable study of this type of phenomenon, Muskat (26) derived the equation

$$\frac{Q}{Q_0} = \frac{\frac{K_1}{K_2} \text{Log } \frac{r_e}{r_w}}{\text{Log } \frac{r_0}{r_w} + \frac{K_1}{K_2} \text{Log } \frac{r_e}{r_0}} \quad (12)$$

for a system containing two adjacent concentric annular regions of permeability  $K_1$  and  $K_2$ . This system is the type encountered when a well is drilled into a pocket or facies of rock of greater or lesser permeability than the overall surrounding aquifer.

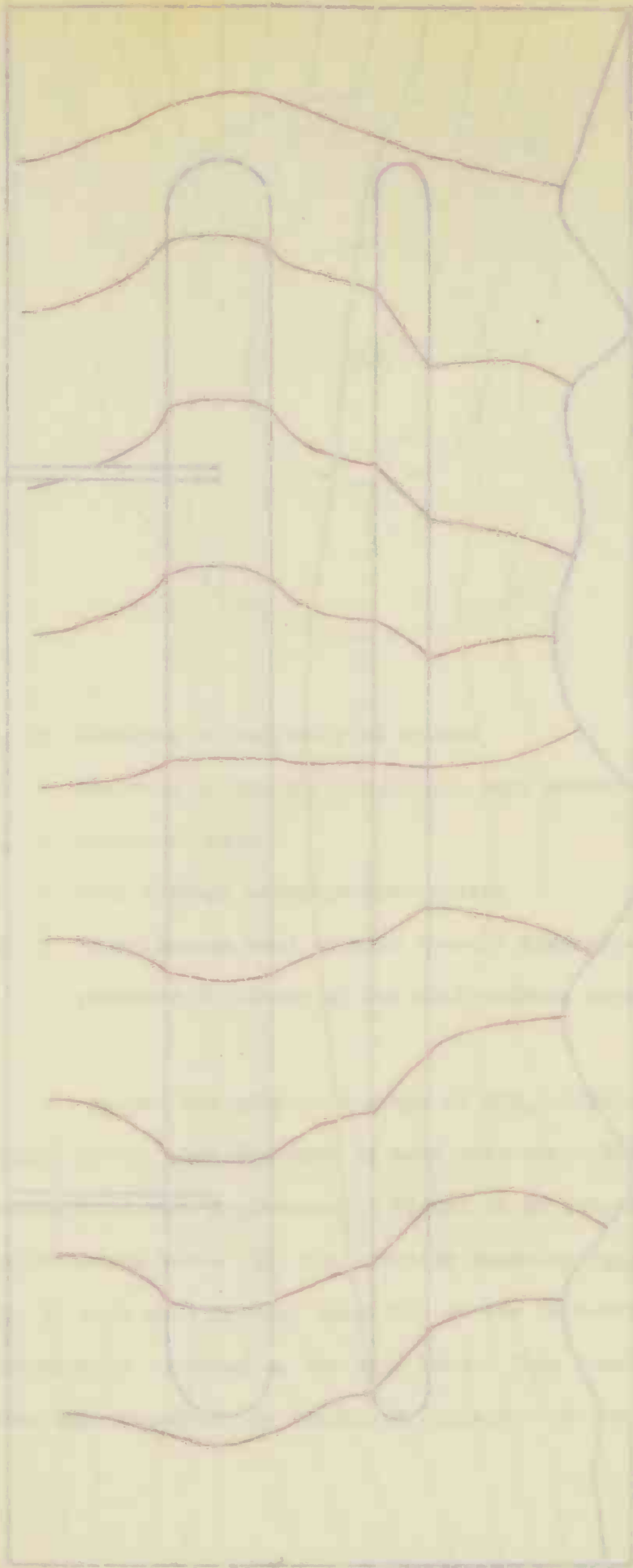


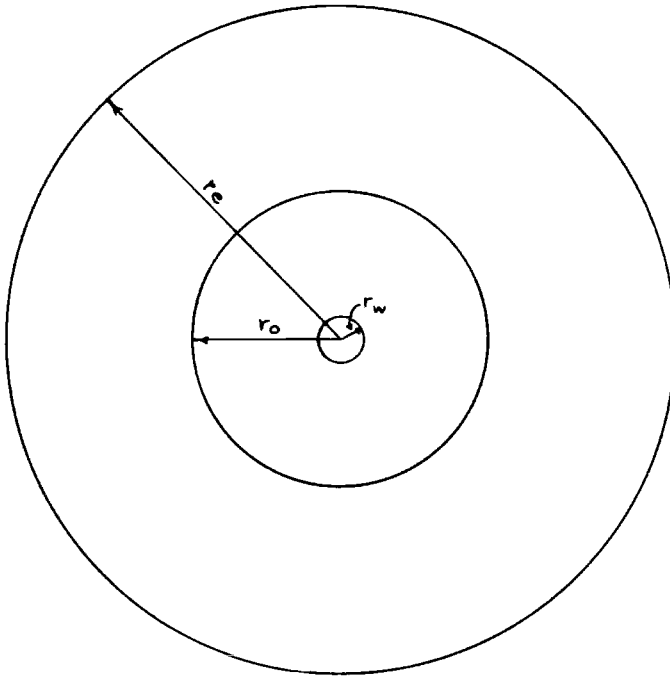
Figure 15. Flow net diagram of the large vertical layer model under nonpumping conditions as shown in Figure 14.

Model Boundary

Equipotential Line

Flow Line

Scale = 1/3



- $r_e$  = distance to extremity of system  
 $r_o$  = distance to extremity of inner rock member  
 $r_w$  = radius of well  
 $Q$  = flux through inhomogeneous system  
 $Q_0$  = flux through sand of same overall dimensions and under the same pressure differential but with uniform permeability  $K_2$ .

Muskat has plotted a graph of  $Q/Q_0$  versus  $K_1/K_2$  for various values of  $r_o$ , when drawdown is held constant. The resultant series of curves have been reproduced in Figure 16 of this paper. A study of these curves shows that the specific capacity (volume rate of discharge =  $\frac{Q}{s}$  drawdown) of a well is very sensitive to the permeability of the rock immediately surrounding the well bore. This result is understandable when one considers the localized character of the pressure drop



Figure 16. Variation of the production capacity of a well as a function of  $K_1/K_2 =$  (the permeability within the annulus of radius  $r_0$ ) / (permeability from  $r_0$  to 500 ft.).  $Q/Q_0 =$  (production capacity of well in sand where  $K_1/K_2 \neq 1$ ) / (production capacity of well in sand with permeability =  $K_2$  everywhere); well radius =  $1/4$  ft.

surrounding a well in a radial flow system.

Localized deposits of highly permeable material are not often found in nature, therefore, it is common practice to artificially construct a highly permeable region around a well by means of gravel packing. This is accomplished by drilling an oversized hole and placing the well casing in the center of the hole and gravel in the remaining volume of the hole. This creates a highly permeable annular region surrounding the well, which, in accordance with Muskat's equation 5-11, yields an increased specific capacity.

The wells, pumping from the highly permeable layer in the author's model utilized this layer as a well gallery which essentially increased the effective area of influence of the well. This illustration is of importance to those who are concerned with ground water development, because it indicates in this type of aquifer, the possibility of capturing deep, partially confined ground water flow through the use of well-placed shallow wells.

The model discussed in this experiment offers an interesting contrast to the model in Figure 11 with respect to its response to the back circulation of waste water. Once again in this model there is a lower confining clay layer as in the previous model, but in this model it cannot always be counted on to prevent the back circulation of waste water recharged beneath it. Figure 14 shows that when the pumping rate is high in the high permeable layer near the top of the model, flow may be drawn through the lower clay layer. This infers that stratification is no assurance of keeping out contaminants. The strength of pumping relative to the regional movement of ground water and the material from

which the pump is drawing are major factors. The most precise study possible must be undertaken in order to accurately predict the effects of the geologic elements upon the hydrodynamic system.

### EXPERIMENT 8

One of the most interesting ground water flow patterns found in nature is the one surrounding an effluent stream. Two of the first plexiglass models were built for the purpose of studying this flow pattern. The model shown in Figure 17 shows a porous consolidated medium 30 in. long and 12 in. high at each end sloping down to a small channel near the center of the model which represents the cross section of an effluent stream. The model is 1" thick inside and is encased in 1/2" plexiglass, with the built-in end tanks at each end. The ink discharge system utilized in this model is the perforated, buried brass tube from which all the flow lines are originating. In this model, water was recharged into both ends of the model and discharged only from the simulated stream by means of a tube tapping the stream from behind the model. The water table in the model was nearly even with the rock surface on either side of the stream. Figure 17 shows the ink flow bands after they moved from the left recharge tank into the stream. All the flow bands are not shown on the right side of the model, but they were nearly a mirror image of the left side.

The most difficult concept for most people to understand is why the flow lines near the bottom of the model turn upward and flow in a vertical path toward the stream. The answer to the problem is that the equipotential lines beneath the stream become horizontal as they connect



Figure 17. Photograph of an effluent stream model showing flow bands moving through a porous medium of isotropic permeability.

points of equal hydraulic head on opposite sides of the stream, as shown in the flow net diagram (Figure 18). The ground water flow must cross these equipotentials at right angles and hence move in a vertical direction.

The effluent stream situation represents what might be considered a natural well. In a man-made well, an area of low hydraulic head is produced by pumping, thereby causing the ground water to flow from the surrounding areas of high hydraulic head to the low head at the well. The effluent stream also represents an area of low head, but is a function of the topography and rainfall characteristics which have caused a high water table to form around the topographically low stream channel. The water moving from high hydraulic head to low hydraulic head, moves out of the ground into the stream.

The presence of equipotential lines, lying horizontally one beneath the other, below an effluent stream was demonstrated in the model as follows. Two wells were drilled in the effluent stream channel, and were screened at different depths, the water levels in the wells rose to different heights above the level of the stream itself. The deeper of the two wells had the higher water level. The flow net diagram (Figure 18) verifies this result by showing that the deeper wells have higher water levels because the hydraulic head increased with depth beneath the effluent stream.

The model in Figure 17 contains a homogeneous medium having constant permeability throughout the model. This resulted in a set of flow bands which followed smoothly curving paths. Figure 19 shows a model of an effluent stream similar to the one in Figure 17, but with

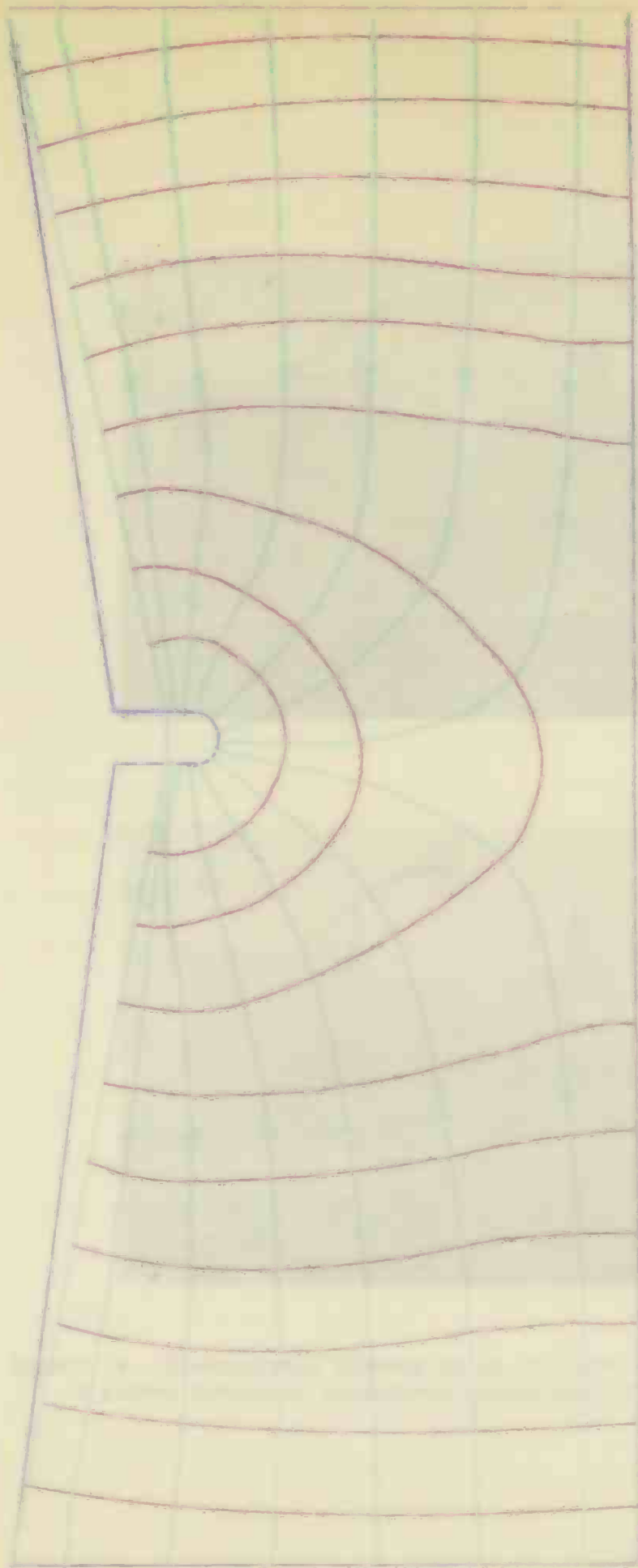


Figure 18. Flow net diagram of effluent stream model shown in Figure 17.

Model Boundary Line

Equipotential Line

Flow Line

Scale = 1/3

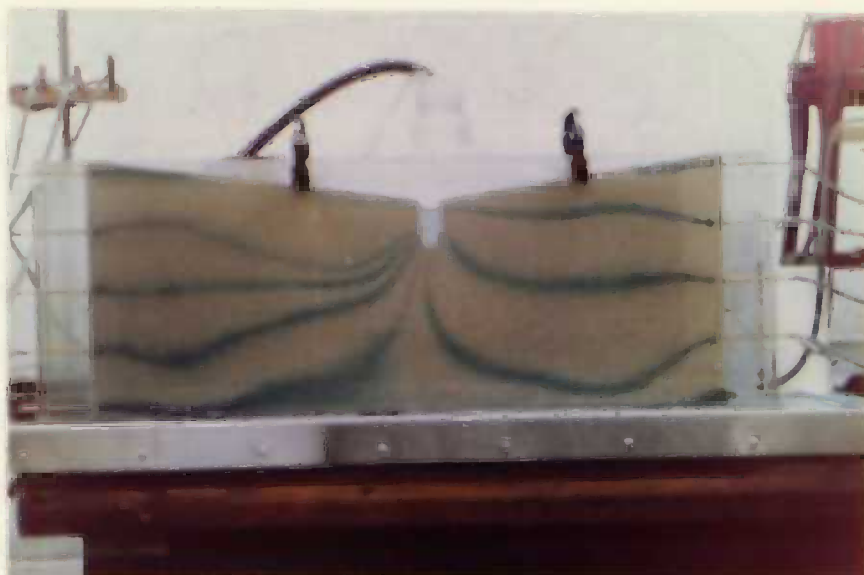


Figure 19. Photographic history of an effluent stream model containing a porous medium of anisotropic permeability.

variations in permeability. The consolidated medium was the same homogeneous sand, but it was packed into the model unevenly. The variations in packing caused variations in permeability, which in turn cause the erratic tortuous paths of the flow bands (Figure 19). Although the first effluent stream model was more convenient for flow net studies, the flow pattern of an effluent stream may be much less predictable when the permeability is not constant (Figure 19) which is often the case in nature.

The flow nets obtained in this experiment have a high degree of symmetry. This level of symmetry is rarely achieved in nature. A natural effluent stream may be recharged more from one side than from the other, entirely from one side, or in fact obtain water from one side of the stream and discharge some of it into the ground water body on the other side of the stream. All of these results can be obtained in the models used in this experiment by merely adjusting the hydraulic gradients occurring on the opposite sides of the simulated stream.

Some interesting legal disputes have arisen from improper interpretations of information regarding the hydrodynamic system of the effluent stream. Wells drilled to any depth on the bank of an effluent stream will yield water levels higher than that of the stream. This information has been used as evidence to prove that the ground water and stream water were unconnected. Once the party favoring this idea can establish it as a fact in court, it is very simple to obtain a court decision stating that no action taken upon one water body could possibly have any effect on the other water body. Such a stand might be taken by a ground water user attempting to prove that he could not possibly be

depleting a surface water user's supply by pumping. A similar argument would be put forth to show that a ground water user could not be contaminating the surface water stream by discharging waste down his well. This model shows this type of thinking to be completely in error. The ground water and surface water in this system are directly connected and all court judgments should be made accordingly.

The flow net of this model in Figure 18 shows that the flow through the zone at the impermeable basement beneath the stream channel is extremely slow. This fact proves to be very important in streams, approaching the sea, which are subject to onshore winds and salt water tides. The salt water may move up the stream, raising the water level and thus temporarily reversing the ground water gradient. The salt water then moves into the ground water body and eventually sinks to the bottom of the formation beneath the stream, due to the high density of the salt water. A salt water mound is thereby formed beneath the stream channel. This mound may have a long lasting detrimental effect on water supply wells in close proximity to the stream channel, tapping the deep portion of the aquifer. The very slow movement of ground water through the zone will take a long time to wash all of the salt out of the ground water body. A town's municipal water supply can be temporarily destroyed by this phenomenon. This problem can be avoided by placing water supply wells a safe distance from the bank of any stream subject to salt water tides.

## EXPERIMENT 9

One of the more important structural features in the study of ground water hydrology is the fault. Faults may represent impermeable boundaries to ground water flow, or in other situations, they may represent brecciated areas of exceedingly high permeability. Figure 20 shows a model simulating a normal fault, the consolidated medium is 30 in. long, 12 in. high and 1 in. thick. The members on the right side of the fault have been displaced downward from their adjoining members on the left side. Line xx' represents an erosion surface occurring after the fault, after which member "f" was deposited and then the entire structure was tilted to the left. The lower portion of the fault zone is occupied by a thin layer of coarse gravel simulating a fault breccia having a permeability of 9,000 USGS units. Members "a", "c" and "e" are effectively impermeable while all other members have a permeability of 1,500 to 2,500 USGS units. Figure 20 shows the model, as ink flow bands are moving through it. The lower flow band was forced to move downward into the model due to the effect of the dipping impermeable member above it. When it reached the fault breccia zone most of the flow moved rapidly out of the lower confining conditions through the brecciated zone into the unconfined aquifer above. Once out of the fault zone the flow band continued through the remaining portion of the model. The fault breccia served as a natural conduit for the water, because it was the only passage open to the confined ground water flow. Notice how the flow lines in Figure 21 converged as they passed into the fault zone and then began to diverge as they emerged from the fault zone.



Figure 20. Photographic history of a fault model illustrating the movement of ink flow bands under a hydraulic gradient of 3.3%. The pictures were taken at the following times: A at 1.5 min., B at 14.2 min., C at 25.6 min. and D at 55 min.

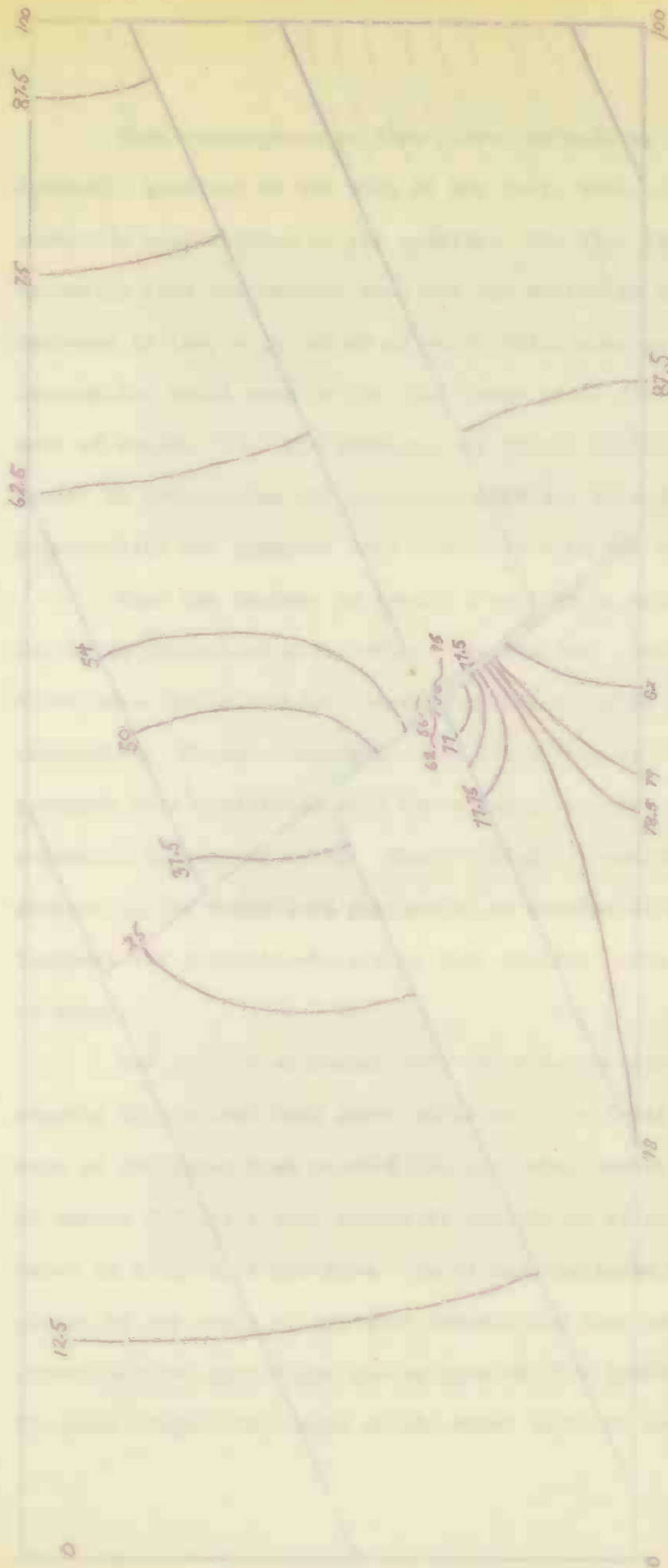


Figure 21. Flow net diagram of the fault model shown in Figure 20.

Equipotential Lines, values as shown from 100% to 0%

Flow Line

Model Boundary

Scale = 1/3

This convergence of flow lines, as well as the steepening of the hydraulic gradient at the neck of the fault zone, is caused by the geometric constriction of the aquifer. The flow lines converge of necessity into the smaller area and the hydraulic gradient steepens in response to the large volume of water which must move at the same rate through the small area of the fault zone as it did through the larger area of member "b". The permeability of the fault breccia is also a factor in determining the hydraulic gradient through it, since permeability and gradient vary inversely with one another.

When one desires to locate a well in an aquifer, he should look for large unconfined areas within the aquifer. Small confined areas offer interfering boundary conditions which result in low specific capacities. Highly convergent flow lines (Figure 21) often infer the presence of a restricted area which can only offer a poor production potential to pumping wells. Where a highly brecciated fault zone is present in the unconfined portion of an aquifer it may effectively increase the transmissability of that aquifer, thus offering a good source of water.

The portion of member "b", which was downstream from the fault breccia is confined both above and below. The fault breccia transmitted most of the water from beneath the confining member ("c"). This portion of member "b" was a zone typically thought of as containing stagnant water in a state of non-flow. As it was mentioned previously, there cannot be any areas of non-flow beneath the free water surface within an interconnected hydrologic system upon which a hydraulic gradient exists. Pictures (Figure 22) taken of the model under an increased hydraulic

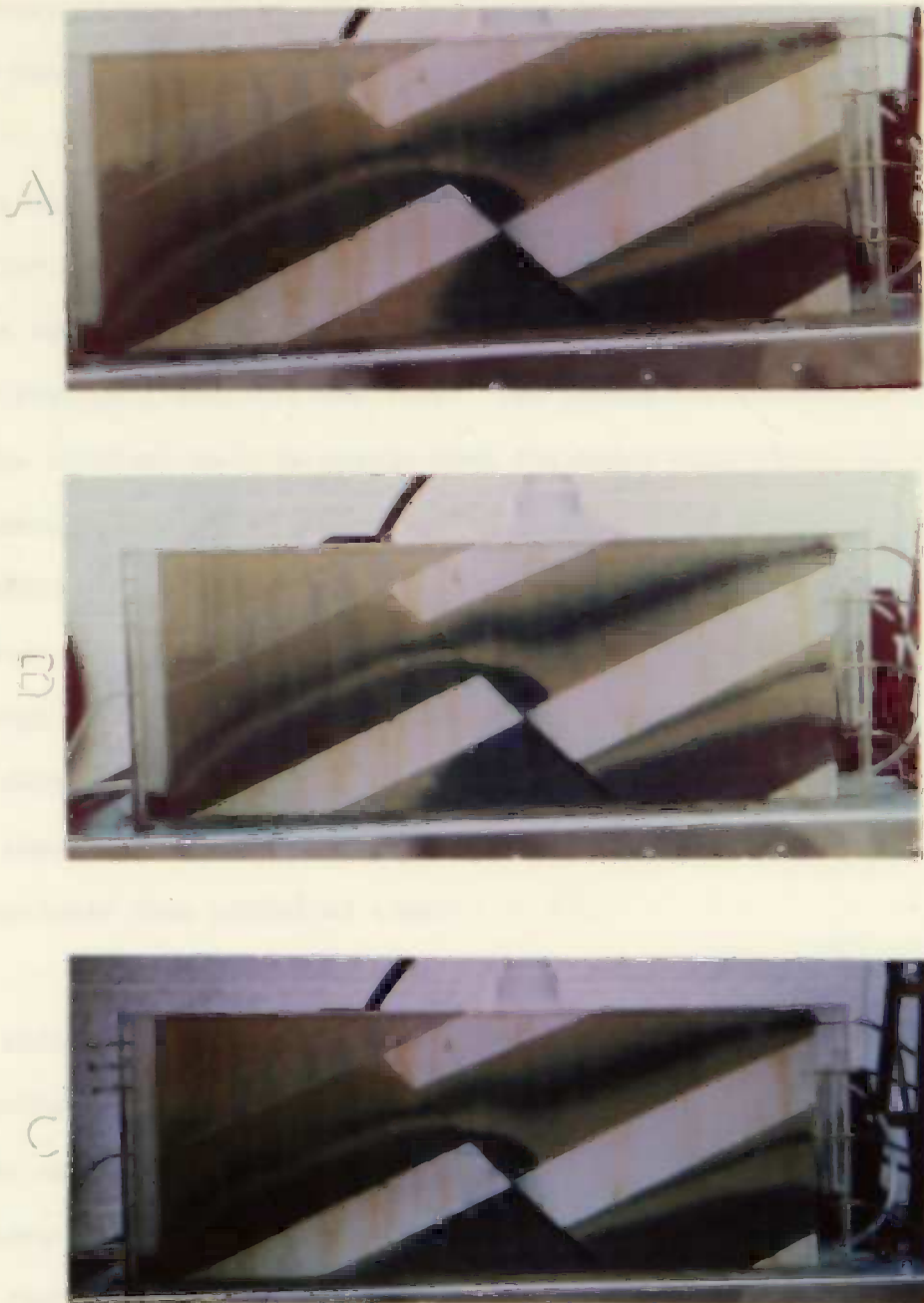


Figure 22. Photographic history of the fault model illustrating the movement of flow bands under a hydraulic gradient of 33%. The pictures were taken at the following times: A at 120 min., B at 130 min. and C at 140 min.

gradient showed that ground water flow was moving into and out of this zone, although at an extremely slow rate as compared to movement within the rest of the model. Under the increased gradient of 33%, the upper flow band took only nine minutes to traverse the entire model.

The flow net of the model (Figure 21) clearly depicts the flow lines as they move in and out of this confined zone, however, the quantity of flow is so small and the hydraulic gradient is so low that extra flow lines and equipotentials, beyond the normal density, had to be drawn in this area to illustrate the flow. The reason for the low flux of water in the confined zone is simply that the water will always attempt to take a combination of the shortest and most permeable path from high to low hydraulic head, thereby, bypassing the less permeable and longer routes. However, as it has been stated before, some water must continuously move through these latter areas in order to satisfy the law of continuity. The result is that there can be no completely stagnant zones, but there are zones where a complete change over in existing water requires an excessively long period of time.

The fault model discussed in this experiment is of interest to the mining industry because it indicates the mechanics by which a hydrothermal ore vein may be formed within a fault breccia. The ground water moves through the rock up gradient from the fault, and may dissolve certain minerals out of these rocks. As the water approaches the fault, the flow lines converge, thus concentrating the quantity of mineral ions in solution that pass through the rock per unit time. As the water moves up through the fault breccia it encounters a decrease in temperature in accordance with the normal geothermal gradient. The

decrease in temperature may produce a state where the fluid is saturated with the dissolved minerals, thereby causing some mineral content to be precipitated out of solution and collect on the surfaces of the fault breccia. The concentrated flux of ground water, containing dissolved solids, through the fault offers a large exposure to precipitation of mineral matter which may ultimately result in a highly concentrated ore vein.

#### EXPERIMENT 10

With the increasing decline of ground water levels throughout the country, a great deal of work has been initiated in the area of artificial recharge in hopes of halting this decline. One of the most popular means of artificial recharge in use today is the recharge pit. The pit is essentially a hole in the ground into which water is poured in hopes that the water will infiltrate the sides and bottom of the pit and then recharge the main ground water body. Recharge pits have been constructed in a variety of shapes in hopes of finding the optimum shape for the maximum recharge rate possible. Generally, the question of shape has been refined down to a question of whether a large or small portion of the wetted perimeter of the pit should be bottom area. The extreme cases in this argument are represented by the rectangular or square pits which have a large bottom area, and the wedge shaped pits which have little or no bottom area.

General practice has shown that the wedge shaped pits allow a larger recharge rate. The most popular reasons for this are as follows: (1) the existence of a greater permeability in the horizontal direction

than in the vertical direction, causing the side area of the pits to be of greater value as a recharge surface than the bottom, (2) the existence of excessive silt which collects evenly over the bottom of a rectangular pit, but concentrates primarily at the apex of a wedge shaped pit. In the case where the ground water recharge mound is built up above the base of the recharge pit, this experimenter believed that greater recharge occurred from the wedge shaped pit for reasons hypothesized as follows.

All flow, originating from a recharge pit at the top of a ground water mound, will ultimately arrive at the extremities of the mound, since these extremities represent points of low hydraulic head relative to the hydraulic head at the top of the mound. All flow must move down the hydraulic gradient, in other words from high hydraulic head to low hydraulic head. The rate at which the flow will proceed from the top of the mound to the extremities of the mound will depend on the average path length which the flow follows, if all other variables such as permeability, cross sectional area, and hydraulic head difference are kept constant. This follows from the equation

$$Q = P \frac{h}{L} A \quad (2.11)$$

Therefore, the inclined side area of a recharge pit will allow a faster rate of recharge than will the horizontal bottom area because the inclined side area allows the water to follow the shortest possible path length to the extremities of the ground water mound. The reason for this is that since all flow must originate in a direction perpendicular to the perimeter of the pit (the pit being an equipotential surface), the inclination of the sides of the wedge shaped pit can be

constructed in such a way that most of the flow is initiated on a nearly straight line path toward the extremities of the mound. Flow from the horizontal bottom area of a pit, however, must begin its path vertically downward and then at some later point begin turning toward the extremities of the mound. This results in a more tortuous path than that taken from the inclined sides and hence a lower rate of recharge. It should be mentioned here that in a pit of any shape where the water table has reached the bottom of the pit, some of the flow must of necessity move vertically downward in order to maintain saturated flow throughout the mound. The rate of this flow from the middle of the pit is very slow, due to the very long path length it must travel. Therefore only a very small surface area of the pit is needed to supply flow to this portion of the mound, and the entire horizontal bottom area of a square pit would normally be in excess of the amount of surface area needed for this purpose.

In order to test this hypothesis the experimenter constructed two models (Figures 23 and 24), which were alike in every respect except for the shape of the single recharge pit that each contained. The models have a 1/2 in. plexiglass case containing consolidated media 30 in. long, 12 in. high and 1 in. thick. The media in both models are identical in every respect as to their hydrologic character such as permeability and porosity. Centered at the top of each model is a recharge pit. The model in Figure 23 shows a wedge shaped pit whose top width is 6 in. and whose sides are 5 in. long. The model in Figure 24 shows a rectangular pit whose sides are 2 in. high and whose bottom is 6 in. wide. Both of these pits have a wetted perimeter of 10 in. within the porous media,

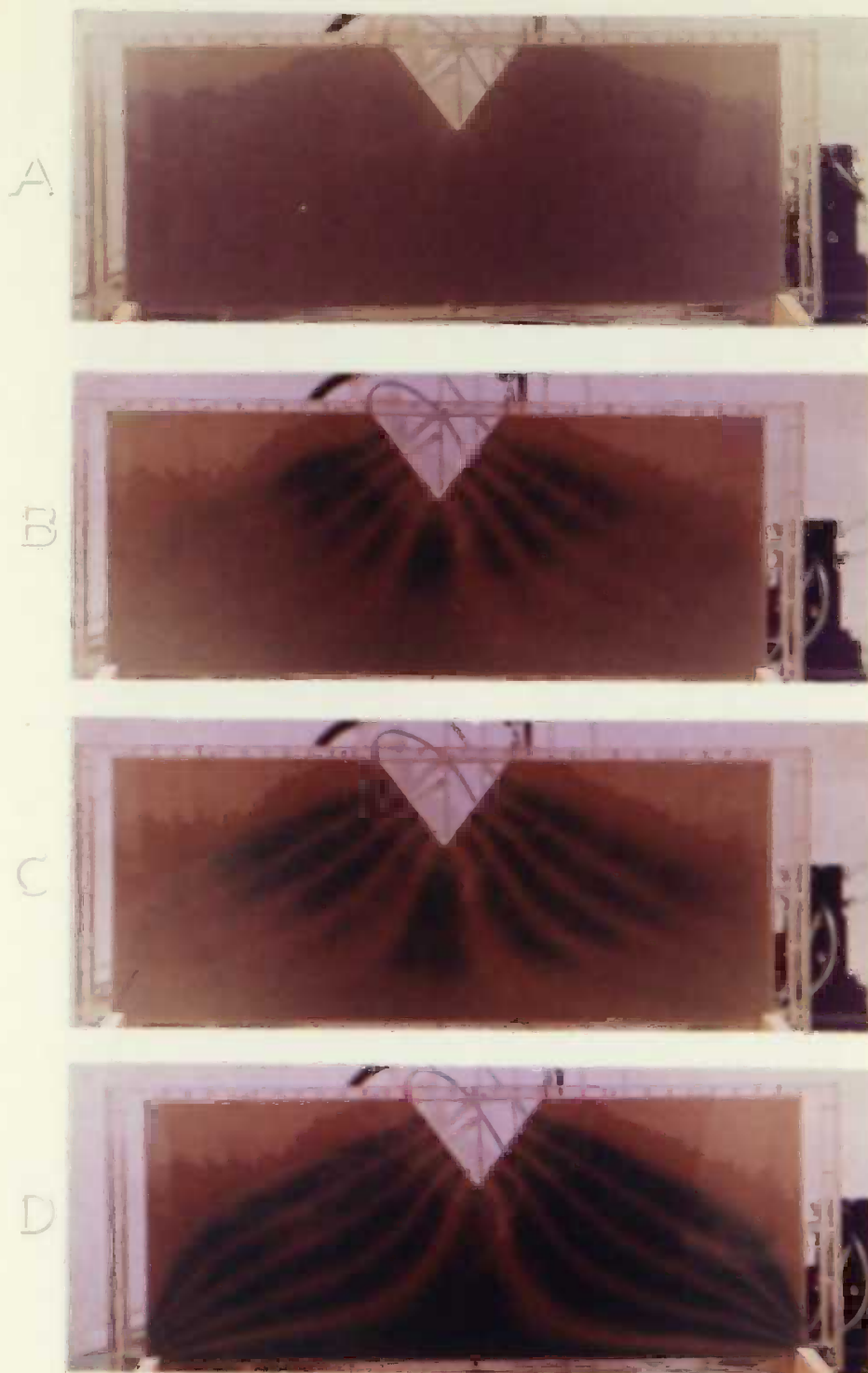
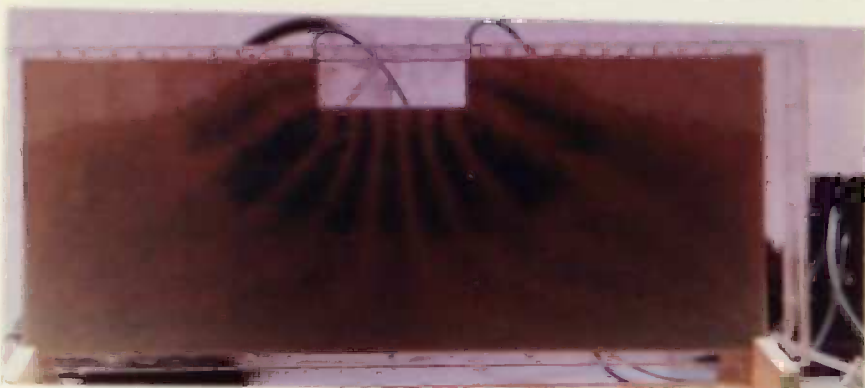


Figure 23. Photographic history of a recharge model containing a wedge shaped pit. The pictures were taken at the following times after the entrance of ink: A at 0 min., B at  $1\frac{1}{2}$  min., C at  $2\frac{3}{4}$  min. and D at  $18\frac{3}{4}$  min.

A



B



C



D

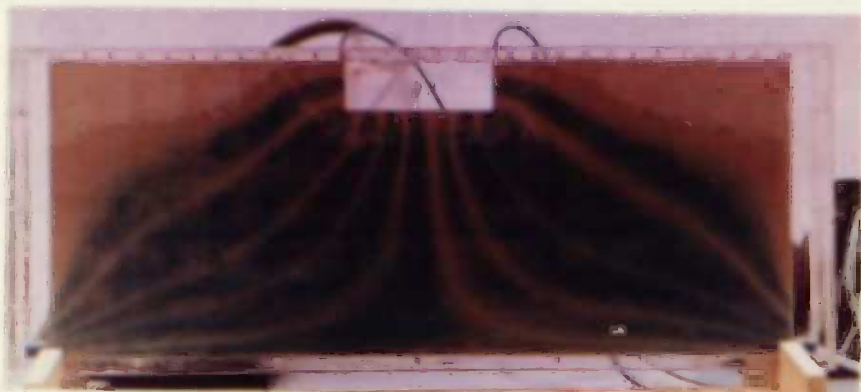


Figure 24. Photographic history of a recharge model containing a rectangular-shaped pit. The pictures were taken at the following times after the entrance of ink: A at 0 min., B at 1-1/2 min., C at 3 min. and D at 26 min.

and a volume of 12 cubic inches. Geometrically, therefore, they are alike in every respect except for their shape. An ink injection tube was imbedded in the porous media along the perimeter of each pit, with perforations for the introduction of ink flow bands at the center of the perimeter of each pit and at positions 1 in., 2 in., 3 in. and 4 in. from the center point of the perimeter along both sides of the pit. This resulted in 9 ink outlets symmetrically placed in both models. The models were recharged in the pits and discharged at the bottom of their right and left end tanks. The recharge was maintained at such a rate that the water level in both pits was kept exactly at the top of the pit. Therefore the hydraulic head difference between the recharge pit and the discharge points in the end tanks was expected to be the same in both models.

Figure 23 shows the ink flow bands as they moved through the ground water mound beneath the wedge shaped pit. Figure 24 shows the ink flow bands as they moved through the ground water mound beneath the rectangular pit. The configuration of the flow bands in Figures 23 and 24 are very similar, but they do illustrate the validity of the hypothesis stated by the author that the flow lines emanating from the bottom of the rectangular pit are more tortuous than those emanating from the sides of the wedge shaped pit. The actual difference, however, was very slight. The average path length of the flow bands from the rectangular pit was only 3% greater than the average path length of the flow bands from the wedge shaped pit. The rate of discharge as expected was also 3% greater in the wedge shaped pit than in the rectangular pit.

Although the author's hypothesis was correct, it was by no measure statistically significant and certainly does not prove the superiority of the wedge shaped pit over the rectangular pit. The difference in original flow directions of water leaving the pits of various shapes is evidently adjusted to the flow in the ground water mound without there being a significant difference in path length. The greater the size of the ground water mound in relation to the size of the recharge pit, the smaller will be the path length difference due to the shape of the pit. It is expected that in nature the path length difference will be even less than the 3% figure arrived at in the models, since the ratio of the size of the ground water mound to the size of the recharge pit within the models was very small relative to what normally occurs in nature.

The flow net diagrams of the wedge pit model and the rectangular pit model are shown in Figures 25 and 26, respectively. The exact position of the free water surface (water table), as determined by piezometer tubes attached to the rear of the models, is shown in these diagrams. The free water surface did not reach the top of either pit, but it is higher in the wedge shaped pit. It was of great interest to follow the movement of ink flow bands above the free water surface. They appeared to follow a laminar flow path nearly parallel to the water table, and at some positions assimilated into the saturated ground water body itself. This is illustrated by the uppermost ink flow band in Figure 24.

This author concludes that large differences in recharge rates between wedge shaped pits and rectangular pits built in material of similar geology can probably be ascribed to one of the reasons mentioned

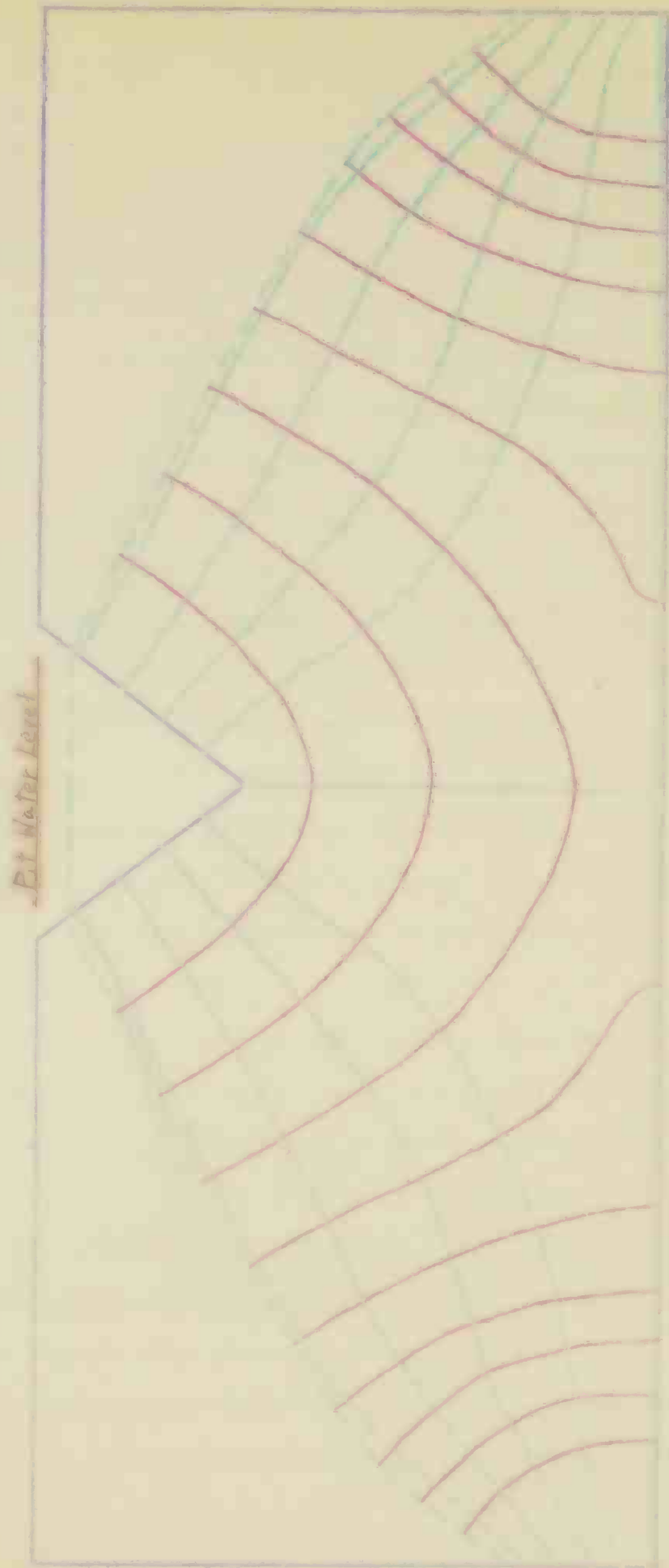


Figure 25. Flow net diagram of the recharge model containing a wedge shaped pit as shown in Figure 23.

Model Boundary Line

Equipotential Line

Flow Line

Free Water Surface

Scale = 1/3

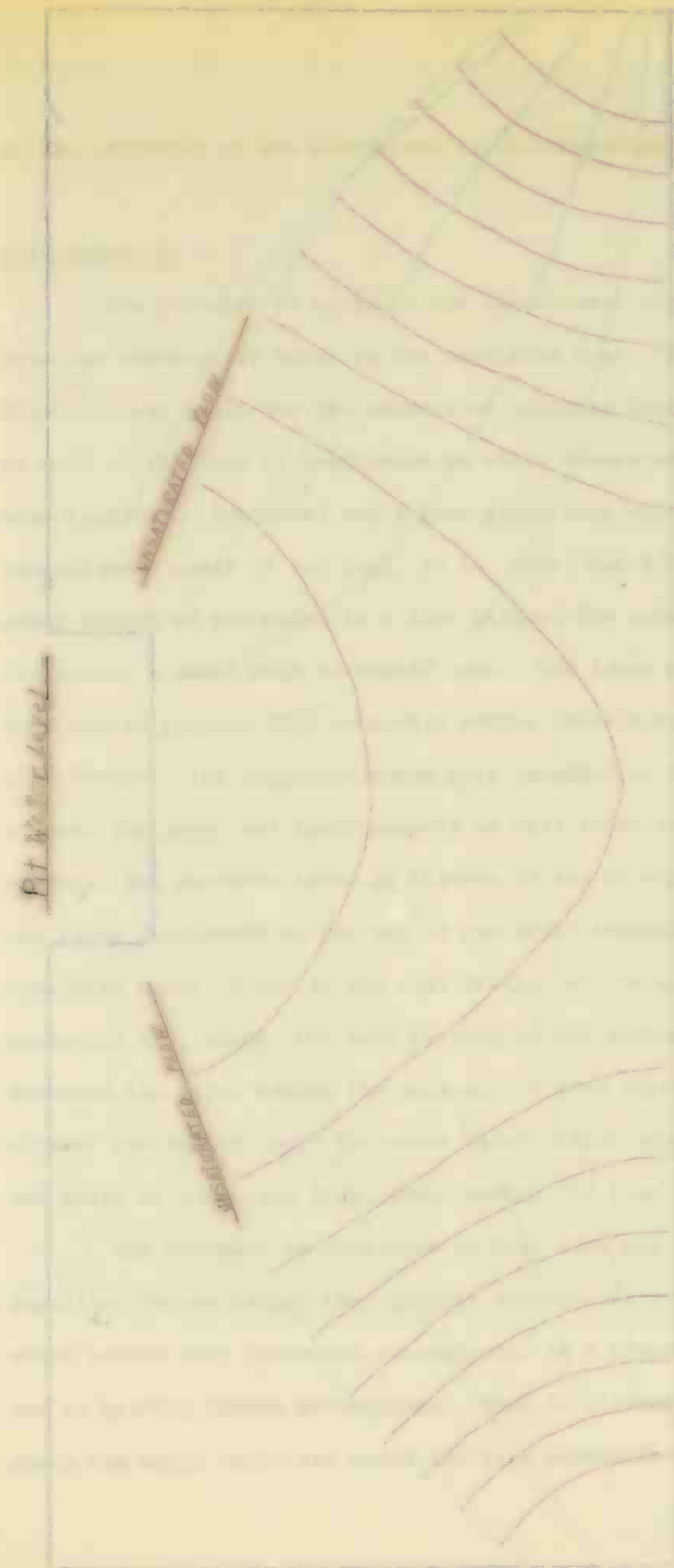


Figure 26. Flow net diagram of the recharge model containing a rectangular shaped pit as shown in Figure 24.

Model Boundary Line

Equipotential Line

Flow Line

Free water surface

Scale = 1/3

at the beginning of the discussion on this experiment.

#### EXPERIMENT 11

The movement of water in the unsaturated zone differs greatly from the movement of water in the saturated zone. The model shown in Figure 27 was built for the purpose of studying these flow differences, as well as the area of confluence in which saturated and unsaturated flow come together. The model has a plexiglass case which contains a consolidated media 31 in. high, 18 in. wide, and 1/2 in. thick. The upper member of the model is a fine grained low permeable medium containing a small high permeable lens. The lower member of the model is a coarse grained high permeable medium containing three low permeable clay layers. Ink injection tubes were imbedded in the model at the top of both the upper and lower members as well as at the sides of the lower member. The pictures shown in Figures 27 and 28 were taken while water was being introduced at the top of the model through a perforated rain simulator tube. Prior to the infiltration of the water the model was perfectly dry, hence, the mere wetting of the medium by the clear water darkened its color making the unsaturated flow visible in the pictures without the use of ink. The water first infiltrated the top of the media and moved as a wetting front down through the fine grained upper member.

The movement in this zone is very slow and subject mainly to the capillary forces rather than gravity forces. Only when a quantity of water became very large and concentrated in a single area did movement due to gravity become predominant. This is illustrated in Figure 27d where the water collected above the high permeable lens until its weight



Figure 27. Photographic history of an infiltration model as clear water infiltrates into the dry porous medium. The pictures were taken at the times shown in the photographs.

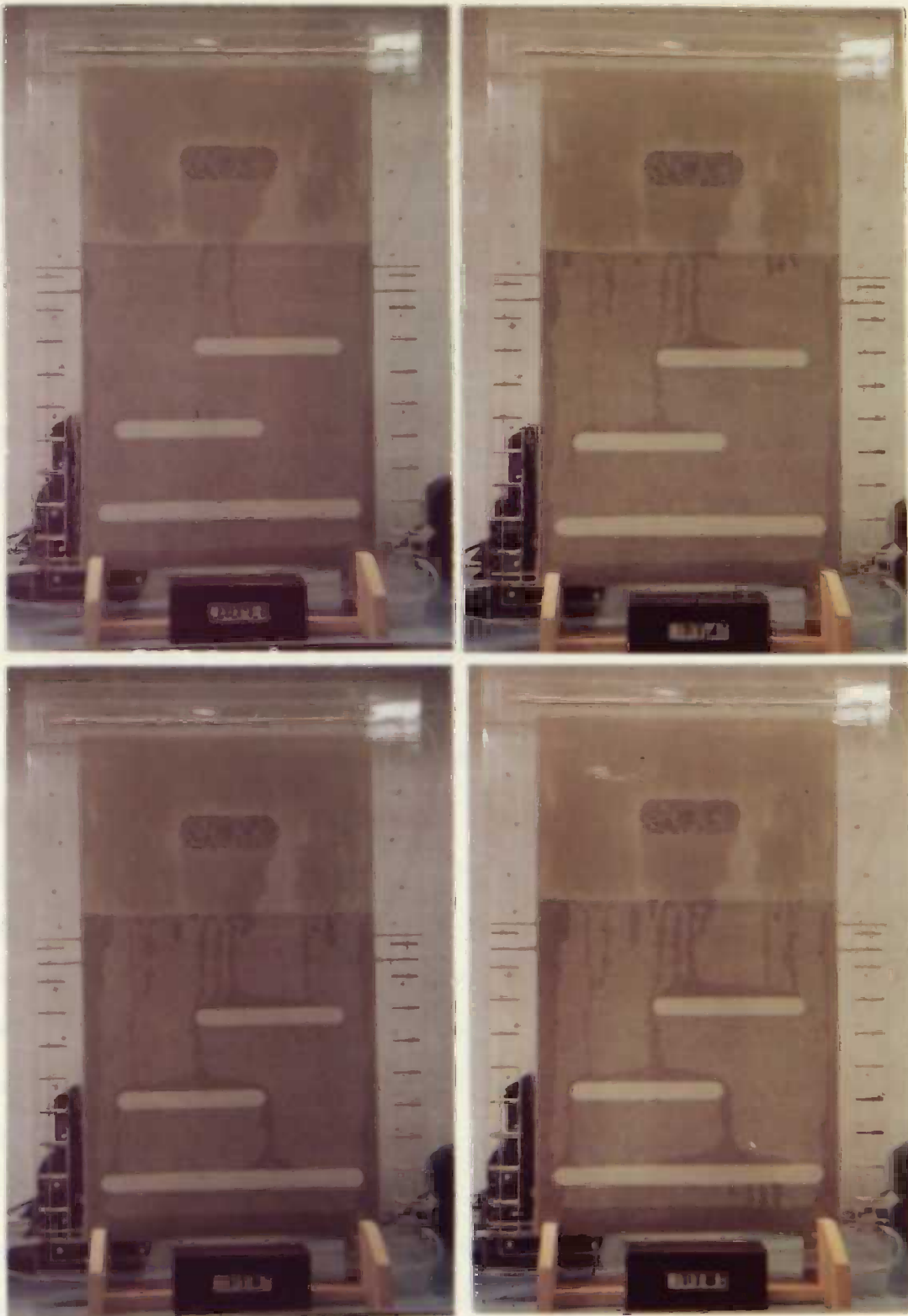


Figure 28. Continuation of photographic history shown in Figure 27 of an infiltration model as clear water infiltrates into the dry porous medium. The pictures were taken at the times shown in the photographs.

was great enough to pull it directly through the lens in opposition to the higher capillary forces acting around the lens.

It should be noted here that the simulated rainfall rate was so high in this experiment that some of the rejected recharge ran down the sides of the consolidated media. The capillary forces along the sides of the media pulled some of this moisture into the medium which accounts for the darkening of the medium along the entire length of its sides. Part of this runoff which did not immediately drain from the bottom of the model, also accounts for the darkening of the bottom two inches of the lower member.

When the infiltration rate is low and the quantity of water moving through the fine grained media is very small, the unsaturated flow will be controlled by a balance between gravity forces and capillary forces. Under these conditions a coarse grained high permeable medium, possessing small capillary forces, when surrounded by a fine grained medium, possessing large capillary forces, will act as a low permeable barrier to the capillary movement of water, causing most of the water to move around it. This effect is illustrated in Figures 29 and 30 where the small quantity of green ink introduced at the top of the upper member is seen to move around the high permeable lens rather than through it.

Figure 28a shows the model as the unsaturated flow began to enter the coarse grained lower member. Notice that the movement was no longer along a wetting front propagating downward evenly throughout the model. It moved down in thin vertical streams at only a few places. This was because the capillary forces were stronger in the upper member than in

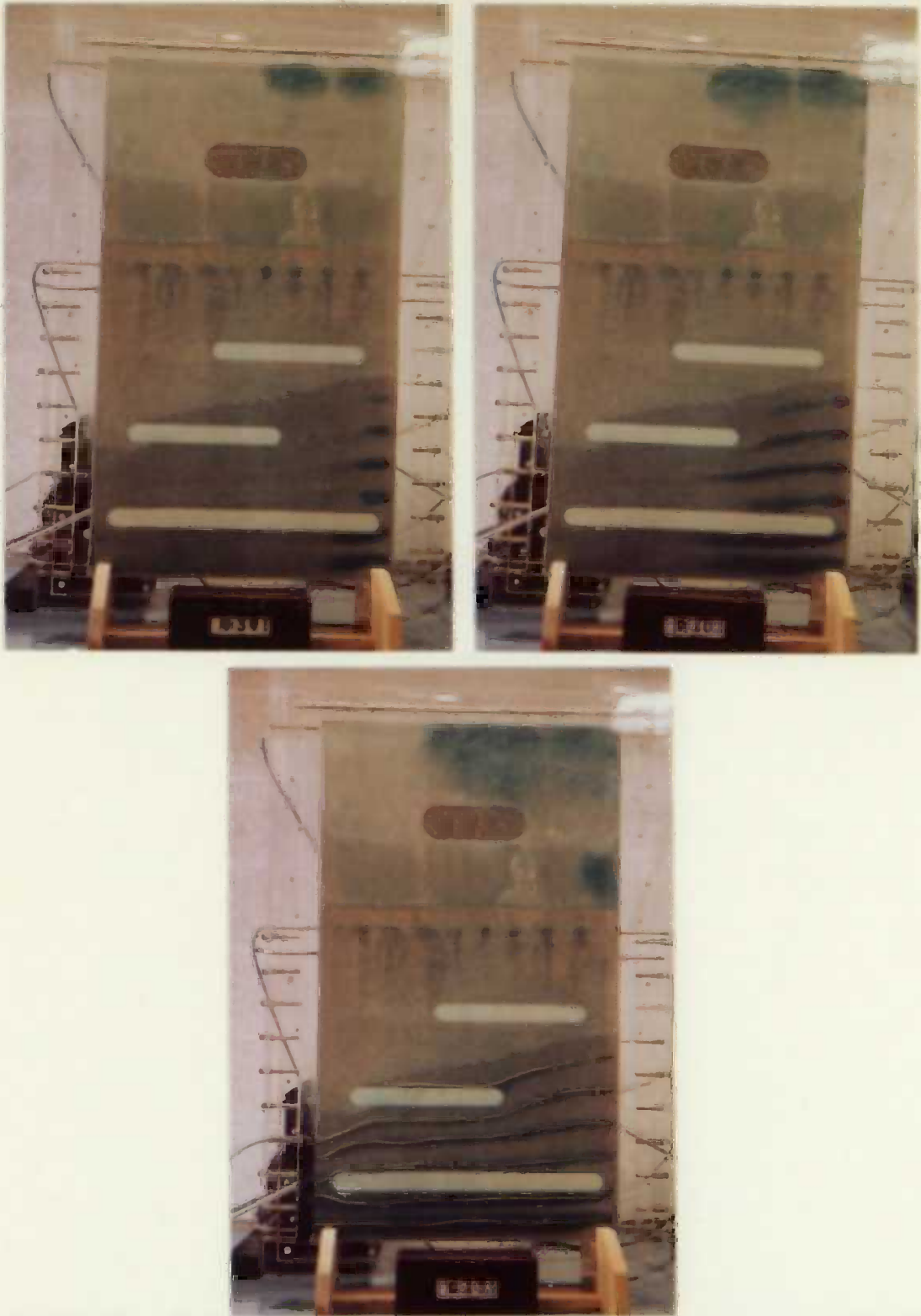


Figure 29. Photographic history of the infiltration model as ink is injected into the unsaturated zone in the fine grained medium and the saturated zone in the lower coarse grained medium. The pictures were taken at the times shown in the photographs.

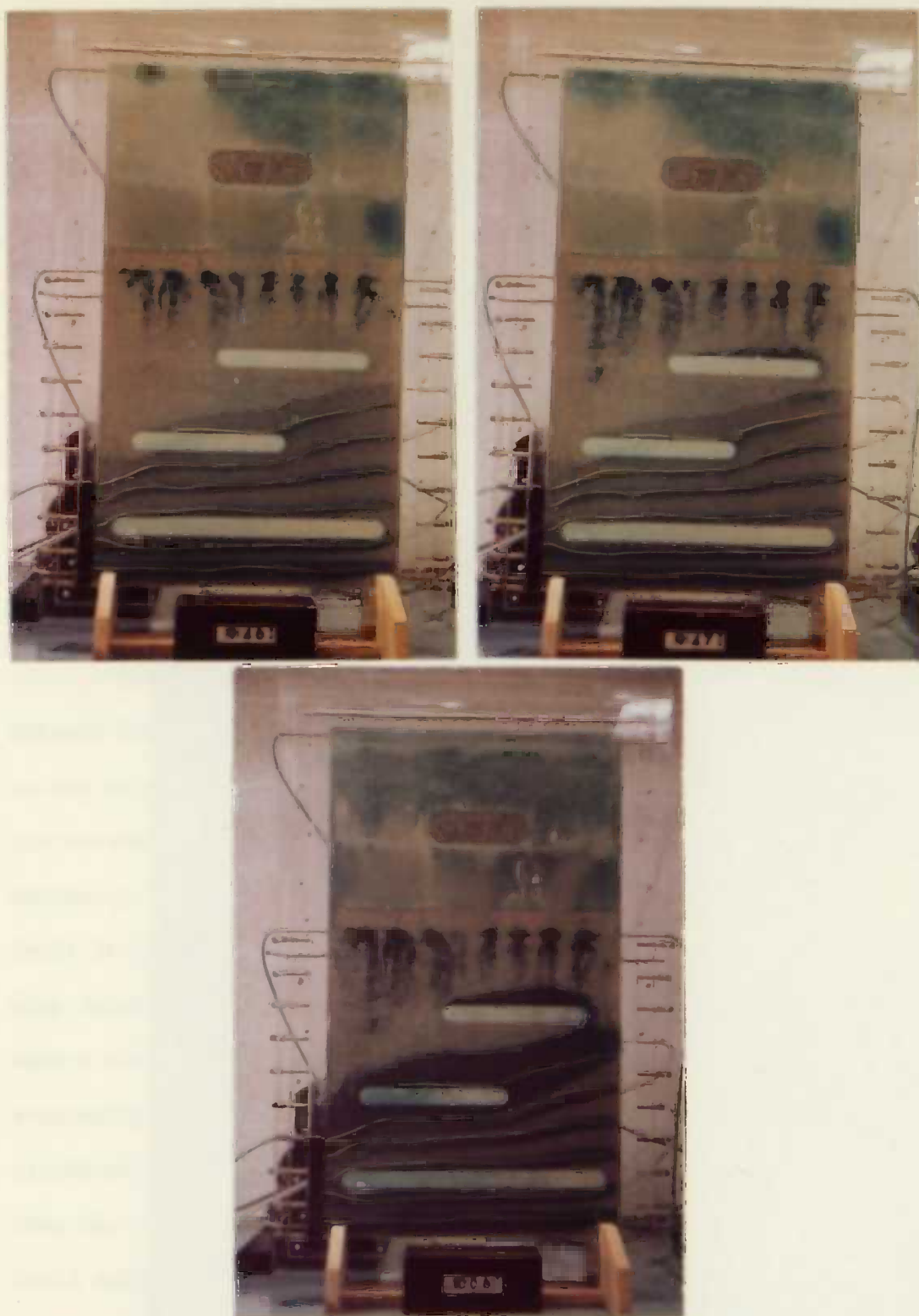


Figure 30. Photographic history of the infiltration model as ink is injected into unsaturated zone of the coarse grained medium. This is a continuation of Figure 29. The pictures were taken at the times shown in the photographs.

the lower member. The water was held back from the lower member until the accumulated mass of water had a great enough weight to overcome the capillary forces tending to retain the water in the upper member. The water then broke through at a few points along the interface and began to stream into the lower member. The vertical stream remained thin in the lower member because of the high permeability which allowed a small area of the lower member to drain a large area of the upper member. Once a stream has broken through the interface, the same path will be followed by the succeeding flow of water because the cohesive attraction of water molecules and the capillary attraction of the wetted tube will tend to draw the water along the already dampened path.

The movement of water then continued into the lower member (Figure 28) and eventually there was a build up of perched water tables on the three clay layers within this member. It is interesting to note the movement of some water through the lowest clay layer in spite of its extremely low permeability, (Figure 28d). Water will move through a clay layer in the unsaturated zone more readily than it will move through a clay layer in the saturated zone. This is true because in the unsaturated zone a large head of water can be built up on the clay which may eventually drive the water through the clay (as in Figure 28d). In the saturated zone, however, the normal hydraulic gradients are so small that the resulting hydraulic heads are not adequate to drive more than a small quantity of water through the clay layers.

In the next experiment with this same model water was pumped into the right end tank and discharged from the left end tank in order to maintain saturated flow within part of the lower member. Water levels

in the two end tanks were kept at constant elevations. Ink flow bands were then allowed to move through the saturated ground water body (Figure 29). Yellow lines were drawn on the model face over the flow bands, which can be used as reference in studying later changes in the flow paths. Ink was next injected into the model (Figure 30) at the top of the lower member, simulating recharge water which had already arrived at this depth. Figure 30b shows the recharging ink as it began to build a perched water body on the uppermost clay lens. The flow system soon reached a steady state (Figure 30c). We have now seen the confluence of unsaturated and saturated flow within the ground water flow system. Notice that the recharge mound built on top of the original water table superimposed a new hydraulic gradient over the flow moving beneath it. This new gradient resulted in changes to the original flow net within this area. This is clearly evidenced by the changes in the positions of the flow bands which were originally directly beneath the yellow lines. They have been slightly depressed below their former positions. This illustrates the fact that all water which reaches the water table of the saturated ground water body becomes an integral part of that body which acts as a single hydrodynamic system. This author has encountered ground water flow diagrams showing recharge water running off the water table in the same manner as water runs off a duck's back; in such a case, it was as though two separate flow systems coexisted. It is important to realize that this is not true. Hydrologists should clearly understand what actually does happen to unsaturated flow as it reaches the water table, and what affect the addition of this unsaturated flow has upon the saturated flow system. This model will aid in such an

understanding.

It is interesting to note in this model study, the different effects that a clay layer may have upon the position of the water table. A gentle sloping water table may intersect a clay layer in such a way that the surface of the water table actually refracts across the clay layer. When the aquifer material both above and below the clay layer is more permeable than the clay layer, the slope of the water table will be steeper in the clay than in the surrounding aquifer. This will result in what appears to be a step in the water table. The elevation of the water table will vary greatly on opposite sides of the portion of the clay layer through which the water refracts. This phenomenon is illustrated in Figure 29c where the water table refracted across the middle clay layer near the left side of the model. The exact position of the water table has been checked in this situation by introducing ink at the top of the free water surface in the recharge tank at the right and watching this ink flow along the surface of the water table. The presence of this refracted water table was verified in this manner. This phenomenon probably accounts for a large number of the anomalous differences found in water table elevations measured at locations in close proximity to one another.

Another interesting effect brought about by the intersection of a clay layer and the water table is illustrated in Figure 31. Here the uppermost clay layer, being almost completely impermeable, did not allow water to pass through it. The portion of the saturated flow which was deflected onto the clay layer moved above it until it reached the extremity of the clay layer and was able to move down to the main ground



Figure 31. Photograph of the infiltration model showing a perched water body on the upper most clay lens, being recharged by water from the saturated zone.

water body. A perched water table was produced on top of the clay, which was entirely fed by water from the zone of saturation rather than from unsaturated flow descending from above. In nature, if the clay layer is very long or the ground water gradient very steep, the main ground water body may lie well below the clay layer at its extremity.

The final experiment performed with this model was for the purpose of studying the movement of water in the capillary fringe above the water table. A small blip of ink was injected into the area just above the water table at the right hand side of the model. The blip first moved upward due to the capillary attraction, and then as it neared the limit of elevation to which the capillary forces could draw it, it began to move down the slope of the capillary fringe. The velocity of the movement within the capillary fringe was found to vary inversely as its distance above the water table. This result checks closely with the measurements obtained by Mavis and Tsui (23) for flow in the capillary fringe. The motion of the water in the capillary fringe, parallel to the hydraulic gradient of the water table, is a result of the superimposition of a hydraulic gradient upon the capillary forces.

The study of movement of water in the unsaturated zone is of increasing interest to people involved in waste disposal as well as those in geochemistry. The movement of waste in the fine grained unsaturated zone may be largely lateral as well as vertical. Lateral flow will continue until the capillary forces are balanced by the gravity forces and the water again begins to move downward. Where lateral movement is not taken into account the waste water moving through the ground may end up in some totally unexpected place. Further

work is needed in this area on the effects of size and strength of recharge impulses as well as the continuous or discontinuous manner in which they are applied. The problem of lateral movement, for example, is quite likely to be more serious where continuous recharge is applied at excessive rates. The vertical path downward may become clogged leaving open only the lateral direction for the movement of fluid. Light discontinuous recharge bursts, on the other hand will necessitate less lateral movement.

Clay lenses may also be a means of diverting unsaturated flow far from the point of recharge before it reaches the ground water body. The direction of saturated flow from the point at which the waste water finally reaches the water table may be quite different from the direction of flow from the position on the water table directly below the point of waste disposal. For these reasons careful analysis must be given to the potential movement of fluid in the unsaturated zone when it is desired to dump wastes at the ground surface through pits and spreading areas rather than directly into the saturated ground water body by means of wells.

Geochemists are particularly interested in the alteration and weathering which goes on in the unsaturated zone. Many of them believe that the vast majority of chemical changes to subsurface rocks occur in the unsaturated zone rather than the saturated zone, because the gases of the atmosphere are present to aid in the chemical reactions. With this in mind one can speculate that chemical alteration will be concentrated where water flow is concentrated in the unsaturated zone such as around the margins of low permeable barriers. Clay lenses such

as those in the infiltration model divert most of the water moving down above them, to their periphery. Here a larger than normal concentration of flow may occur favoring the alteration, leaching or solutioning of the formation. D. K. Hamilton (10) implies that this has occurred in some of the Kentucky limestones.

### EXPERIMENT 12

Perhaps the most interesting of all ground water phenomena is the artesian well. In order to study this phenomena the author constructed a model (Figure 32) which represents the classic hydrogeologic situation giving rise to the occurrence of artesian wells. It closely resembles the cross section of the great Dakota sandstone which is an important artesian aquifer in the midwest. This model shows a limb of a fold which has been truncated, causing the different formations to outcrop at a high elevation. The left portion of the model represent the lowlands area lying at some distance from the uplands or mountainous region, illustrated by the right hand portion of the model. The consolidated medium within the plexiglass case is 30 in. long, 11 in. high at the extreme right and 6 in. high at the extreme left, while being 1 in. thick. Members 1 and 5 have permeabilities of 1,200 USGS units, members 2 and 4 have permeabilities of less than 1 USGS unit, while member 3 has a permeability of 10,000 USGS units. A simulated strike slip fault has been constructed in the model at the vicinity of well C<sub>5</sub>. Fault breccia occurs along the plane of the fault where it passes through members 2 and 4.



Figure 32. Photograph of an artesian well model showing water levels in three wells under static water level conditions.

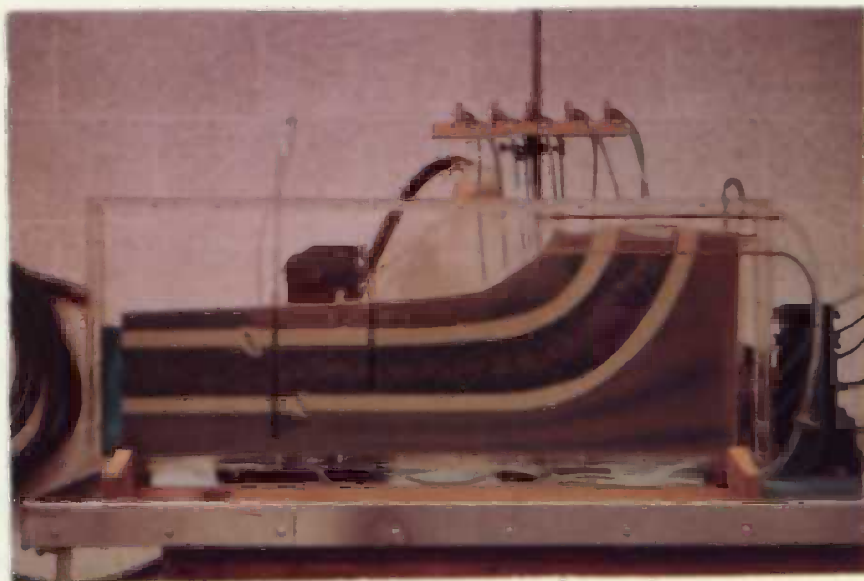


Figure 33. Photograph of an artesian well model showing ink flow bands, while well C<sub>5</sub> is being pumped.

The model is recharged by two methods. Water is pumped into the right end tank and maintained at a higher level than the water in the left end tank, resulting in the flow of water through member 5. At the same time recharge by rainfall is simulated by means of a perforated recharge tube set above the high area to the right. Under these conditions members 3 and 5 are confined aquifers, being confined by members 2 and 4, respectively. Member 1 is an unconfined formation with a free water table. The model contains three wells each being screened in only a single member. Well  $A_3$  is screened in member 3, well  $B_1$  is screened in member 1 and well  $C_5$  is screened in member 5.

Wells  $A_3$  and  $C_5$  are both artesian wells according to the following definition: An artesian well is a well within which the water from a confined aquifer rises above the bottom of the confining bed. This is due to the fact that the water level in these aquifers at their source areas are above the elevation of the aquifer at the location of the wells. This excess head differential between the source area and the well location pushes the water up the well bore to a position above the top of the aquifer. The water level will not rise up to the level of the water in the source area because some of the potential energy is transformed into work done against friction during the transmission of the water through the aquifer. The water level is higher in well  $A_3$  than in well  $C_5$  because well  $C_5$  is further down gradient from the source area. The reader might notice at this time that if wells  $A_3$  and  $C_5$  were cut off at ground level, well  $A_3$  would flow, but well  $C_5$  would not. Therefore we have two artesian wells, but only one flowing well. It is a common misconception that all artesian wells must flow above the ground level,

however, there is no basis for this in the standard definition of an artesian well, as previously stated.

One of the most interesting occurrences observed in this model, was the decline in the water level in well A<sub>3</sub> with time, while there was no concurrent change in the water level at the source area. This puzzling situation was finally accounted for by the author when he discovered the progressive accumulation of trapped air within member 3. The air was evidently exsolving from the water within the aquifer. The trapped air bubbles caused an air block which lowered the effective hydraulic head at the source area, which in turn lowered the entire piezometric surface.

Figure 33 shows the model after ink flow bands have been allowed to flow through its entire length. Well C<sub>5</sub> was being pumped at the time this picture was taken. The fault to the right of well C<sub>5</sub> in member 4 acted as a leak in the confining layer and allowed water to be pulled out of the upper aquifer into the lower aquifer and thence into the well. This situation results in what maybe called a leaky aquifer. The more common leaky aquifer situation referred to in most of the literature is attributed to an area of the confining bed where the permeability is sufficiently high to allow water to move through it into or out of the confined aquifer when a sufficient head difference occurs between the artesian aquifer and the unconfined water table above the confining layer. This situation becomes of increasing importance when the piezometric surface of the artesian aquifer is lowered by pumping, to a position where the water table head is capable of driving large quantities of water through the confining layer.

Figure 33 also shows that the artesian flow in member 3 is leaking into member 1 through the fault in member 2. A natural ground water mound being recharged from below has been created here. A situation such as this occurring in nature would make an excellent location for shallow low capacity pumping wells.

### EXPERIMENT 13

The subsidence of the earth's surface surrounding an artesian well has posed a problem to ground water engineers for many years. Many theories have been presented to explore this phenomenon, but only one is now commonly accepted. The accepted theory can be stated as follows: When water is pumped from an artesian well, the piezometric surface, or the confined water pressure level, is lowered in the vicinity of the well, perhaps extending a radius of many miles. This decrease in water pressure within the confined aquifer removes a portion of the pressure which was supporting the rock overburden lying above the confined aquifer. The system is then out of equilibrium because the pressure exerted by the rock overburden now exceeds the combined supporting pressures of the aquifer skeleton and the water. The result is that the aquifer skeleton is further compressed by the overburden. The compression of the aquifer skeleton therefore allows the earth's surface around the well to subside.

This is a difficult phenomenon to study in the laboratory because enormous rock pressures are involved. The artesian well model (Figure 33) does not demonstrate subsidence, because the slight piezometric drawdown combined with the large modulus of compression of the rock will not result in a measurable quantity of subsidence.

Because of the great interest in this subject the writer decided to depart from his true hydrodynamic models, and construct what might be considered a mechanical model which would illustrate the principles described previously in the accepted subsidence theory. Figure 34 shows the model which was constructed for this purpose. The model case is made of 1/2 in. plexiglass having inside dimensions of 33 in. x 12 in. x 4 in. Member 1 is a consolidated porous medium having a permeability of 2,000 USGS units. Member 2 is an unconsolidated porous medium consisting of fine particles of cellulose sponge having a very low modulus of compressibility, and a permeability of about 100,000 USGS units. The sponge is surrounded by a thin plastic membrane which acts as a confining layer around the aquifer. The sponge aquifer leads up into a plexiglass cylinder 10 in. long and 2 in. in diameter at the top of the right side of the model. This tube allows the water pressure within the model, to be built up to a level greater than the main body of the model would allow. Member 3 is made of 3 layers of consolidated lead shot representing the rock overburden. Well A is an artesian well screened only in member 2. The model is recharged through the plexiglass cylinder connected to member 2. The white line drawn on the model in Figure 34a marks the elevation of the bottom of the overburden prior to the commencement of pumping in Well A. Figures 34b and 34c shows the subsidence of the upper surface as the well is pumped and the piezometric level is decreased.

The pressure of the overburden was no longer balanced by the opposing pressure of the water and aquifer skeleton. The overburden compressed the sponge skeleton until the reaction pressure exerted by

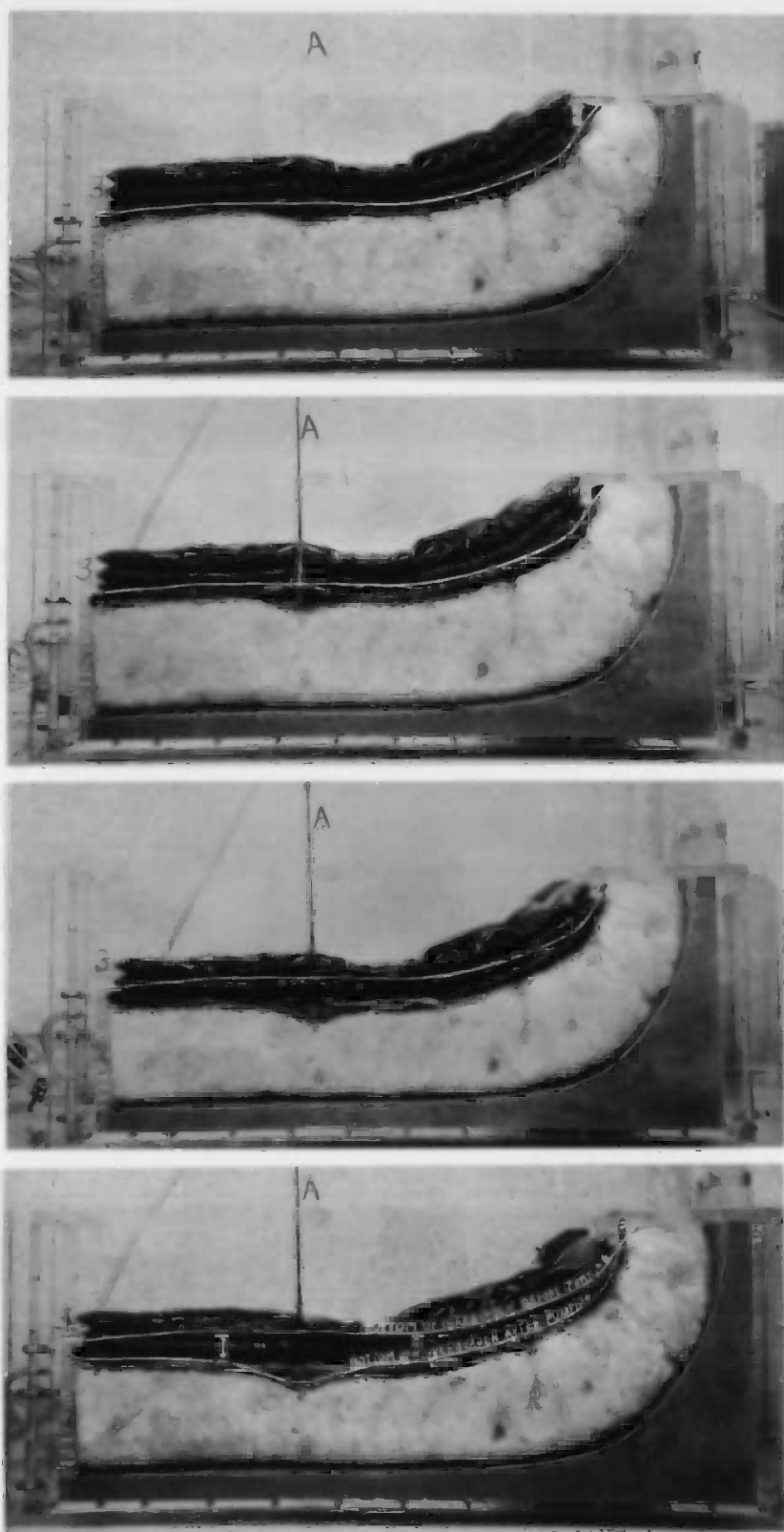


Figure 34. Photographic history of an artesian subsidence model before, during and after pumping in well A. The white line represents the bottom of the overburden before pumping.

the sponge skeleton was increased by an amount equal to the decrease in water pressure caused by the pumping well. When this adjustment was completed, the system was again in equilibrium.

Due to the small extent of the aquifer, the cone of depression in the piezometric surface reaches the source area of the aquifer, therefore subsidence occurs throughout the entire length of the model. When the water level at the source area was maintained at a constant elevation, the resultant cone of depression was too shallow to allow measurable subsidence, because of the enormous permeability of member 2.

Under natural conditions the greatest amounts of subsidence probably occur when the cone of depression reaches the source area. Small depressions in the piezometric surface of artesian aquifers may result in no measurable subsidence. This is particularly true in areas where the overburden is in the form of consolidated layers of rock. This overburden has a horizontal tensile strength which tends to impede the subsidence of the overburden in any local area. The portion of the overburden overlying the depression cone will be partially restricted from subsiding by the tensile strength of the adjoining overburden whose supporting pressure has not been decreased.

Although this model is not a true analogy to nature, it still has value in allowing an observer to visually study a physical phenomenon.

EXPERIMENT 14

One of the most practical aspects of the study of ground water flow is the information obtained about the various configurations of the water table brought about by the pumping of water table wells. The best way to observe variations in the water table is by means of observation wells which are essentially unaffected by the capillary forces present at the water table within the porous medium.

The model shown in Figure 35 contains 31 wells which accurately measure the position of the water table within the model. The model case is made of 1/2 in. plexiglass having inside dimensions of 33 in. x 12 in. x 3 in. The medium at the extreme right of the model is impermeable and is intended to represent the subsurface portion of an igneous mountain front. The remaining medium within the model has a permeability of 2,000 USGS units. The left end tank of the model is intended to represent the cross section of a stream channel into which water is recharging while the sloping top surface of the porous consolidated medium is intended to represent a tributary channel capable of leading runoff from the mountain front to the main stream channel. All of the wells have 1/4 in. diameters. (The four deepest wells are screened at their lowest 6 in., while the rest of the wells are open only at the bottom.) A small red bead of wax was placed in each observation well so that the water level would be clearly visible within the wells.

Figure 36 shows the model before and after well B had been pumped for a long enough period to achieve a steady state condition. Notice here the definite effects of the boundary conditions upon the cone of



Figure 35. Photograph of a cone of depression model with its static water level drawn in white.



Figure 36. Photograph of the cone of depression model after pumping in well B had reached a steady state. The cone of depression is drawn in black.

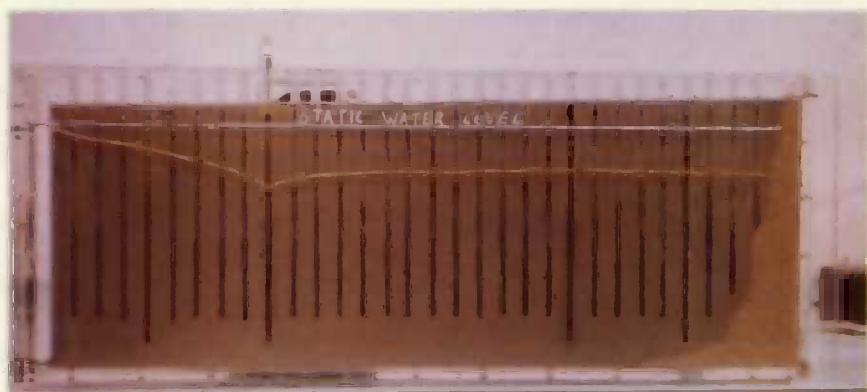


Figure 37. Photograph of the cone of depression model after pumping in well A had reached a steady state. The cone of depression is drawn in yellow.



Figure 38. Photograph of the cone of depression model after pumping in wells A and B had reached a steady state. The existing multiple cone of depression is drawn in red, while the individual cones of depression of wells A and B (as shown in Figure 36 and 37) are drawn in yellow and black, respectively.

depression, which has been marked by a black line on the model. The limb of the cone to the right of the well was almost flat, due to the effect of the impermeable boundary to the right. The well was unable to take water from storage beyond this impermeable barrier and hence, was forced to take an increased amount of water from storage in front of the barrier, which resulted in a lowering of the cone of depression in that area. The cone of depression at the left of the well extended to the surface of the recharging water. At that point, it ceased to grow because it induced recharge from the end tank, thus eliminating the necessity of drawing any further water from storage within the aquifer and enlarging the cone of depression. This is exactly what happens in nature when a well pumping near an influent stream extends its cone of depression to the edge of that stream. Figure 37 shows the model after well A had been pumped for a long enough period to achieve steady state conditions. The surface of the cone of depression is drawn in yellow on the face of the model. Once again, the effects of the two boundary conditions are evident. In this situation, the effect of the recharging end tank was more intense than the effect of the impermeable barrier, because well A was closer to the end tank than the barrier.

In a multiple well system where surface recharge and evaporation are negligible the drawdown at any point within the area of influence is the sum of the individual drawdowns of each well in the multiple well system. This fact has been proved in this model. When wells A and B were pumped simultaneously, the resultant cone of depression was the sum of the individual cones. Proof of this fact can be seen in Figure 38, which shows the model after wells A and B had been pumping long enough

to reach the steady state condition. Both wells were pumped at the same rates at which they were pumped in Figures 36 and 37, respectively. The black line on the model in Figure 38 represents the individual drawdown caused by well B as shown in Figure 36, while the yellow line represents the individual drawdown caused by well A as shown in Figure 37. The red line on the model represents the drawdown caused by the simultaneous pumping of the two wells. It is readily obvious that the vertical distance between the red line and the static water level represented by the white line is equal to the sum of the vertical distances between the yellow and white lines and the black and white lines.

This same model can be used to study artificial recharge by wells which is coming into common practice in many areas today. It is important to understand the effects of this recharging water upon the shape of the water table. It has been theoretically proved that the cone of impression brought about by a recharging well, will be a mirror image of the cone of depression formed by pumping the well at the same rate as it is recharged. An experiment was performed in this model to verify this relationship and the results are shown in Figure 39. The model is first shown without any pumping; the white line represents the static water level. Well B was then pumped and allowed to reach the steady state (Figure 39b). Pumping was then stopped until the water level recovered to the static position, at which time the well began recharging at the same rate that it had been discharging. Figure 39c shows the model after the steady state condition had been reached. Notice that the cone of impression drawn in red above the static level is the mirror image of the previously formed cone of depression drawn in red beneath the static level.

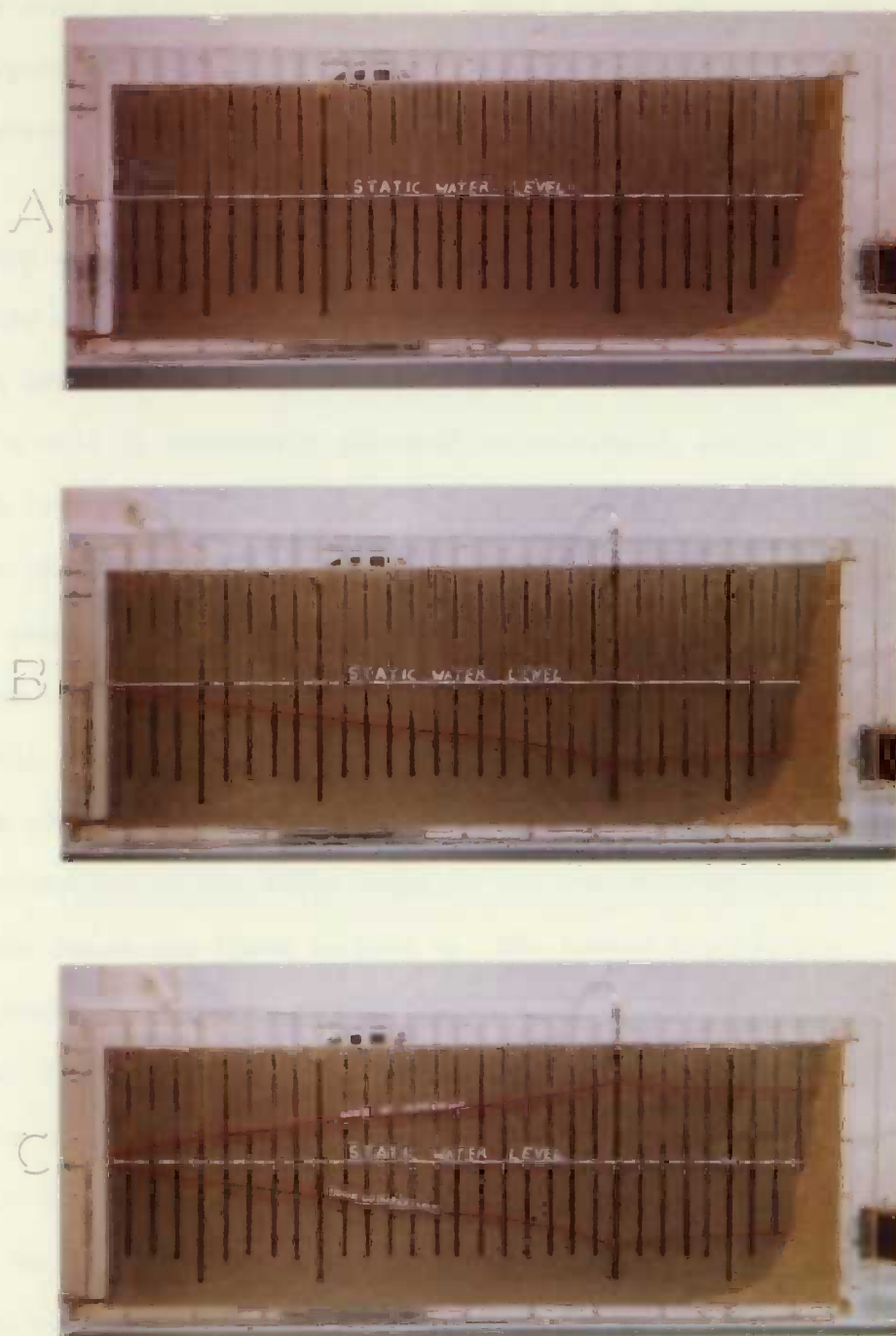


Figure 39. Photographs of the cone of depression model (A) under static water level conditions, (B) after pumping in well B reached a steady state, (C) after recharging into well B reached a steady state.

This model can also be set up with some of the wells discharging while other wells are recharging. These very different water table configurations can be produced and studied. Figure 40 shows such a situation with well B recharging and well A discharging.

It is a common misconception that the drawdown level within a pumping well represents the level of the water table contiguous to the outside of the well casing. This is not necessarily true and may lead to an incorrect interpretation of the elevation of the water table. When a well is improperly screened or developed, the entrance losses may be so large that the water level in the well does not rise as high as the water table. This fact was demonstrated in the model when water levels were compared in two wells pumping at the same rates but having different screen length. Well A and the observation well immediately to the right of well A were pumped at separate times at exactly the same rate. The cones of depression produced by the two wells were nearly identical with the exception of the water level in the pumped observation well, which was far below the level in well A. The reason for this is that well A is screened in over half of the aquifer and allows the water to enter along normal flow paths. The observation well, however, is open only at the bottom and therefore causes the water to take a circuitous path into the well. This extra path length necessitates that an additional amount of work be done against friction in moving the water to the well. Thus, there is a resultant energy loss in the system known as the entrance loss. It shows up simply as a lowering of the water level in the pumping well. There is almost a direct relationship between the percentage of the well casing which is screened in the aquifer, and the drawdown in the well for



Figure 40. Photograph of the cone of depression model with well B recharging and well A discharging. The resultant water level is drawn in red.

constant values of  $Q$ . This is adequately explained by Todd (37) in Chapter 4 of his textbook, Ground Water Hydrology.

By the use of this same model, it is possible to observe a way in which mountain runoff water may recharge a ground water basin. Figure 41 demonstrates this effect. The model is first shown as green runoff water begins to slowly infiltrate into the subsurface along the foot of the mountain front. The following pictures show how the recharging water moves as a front through the saturated aquifer. This is often the case in nature where the ground water has an underground outlet from the basin. It is an extremely slow process in nature and becomes complicated by the fact that there may be many other areas of recharge within the basin. It is however worthy of study in even its simplest form.

The cone of depression model has a number of important implications in applied hydrology. The most obvious fact illustrated by the model is the advantage of placing a pumping well as near as possible to a source area.

Under natural conditions prior to development by wells, most aquifers are in a state of dynamic equilibrium; which essentially means that natural discharge is equaled by natural recharge, and the quantity of water in storage remains essentially constant. When wells tap an undeveloped aquifer a new discharge is superimposed upon the previously stable system. This must be balanced by an increase in natural recharge, or a decrease in natural discharge or a decrease in storage, or a combination of all three. The system is temporarily in a state of nonequilibrium until discharge from it again equals recharge. The

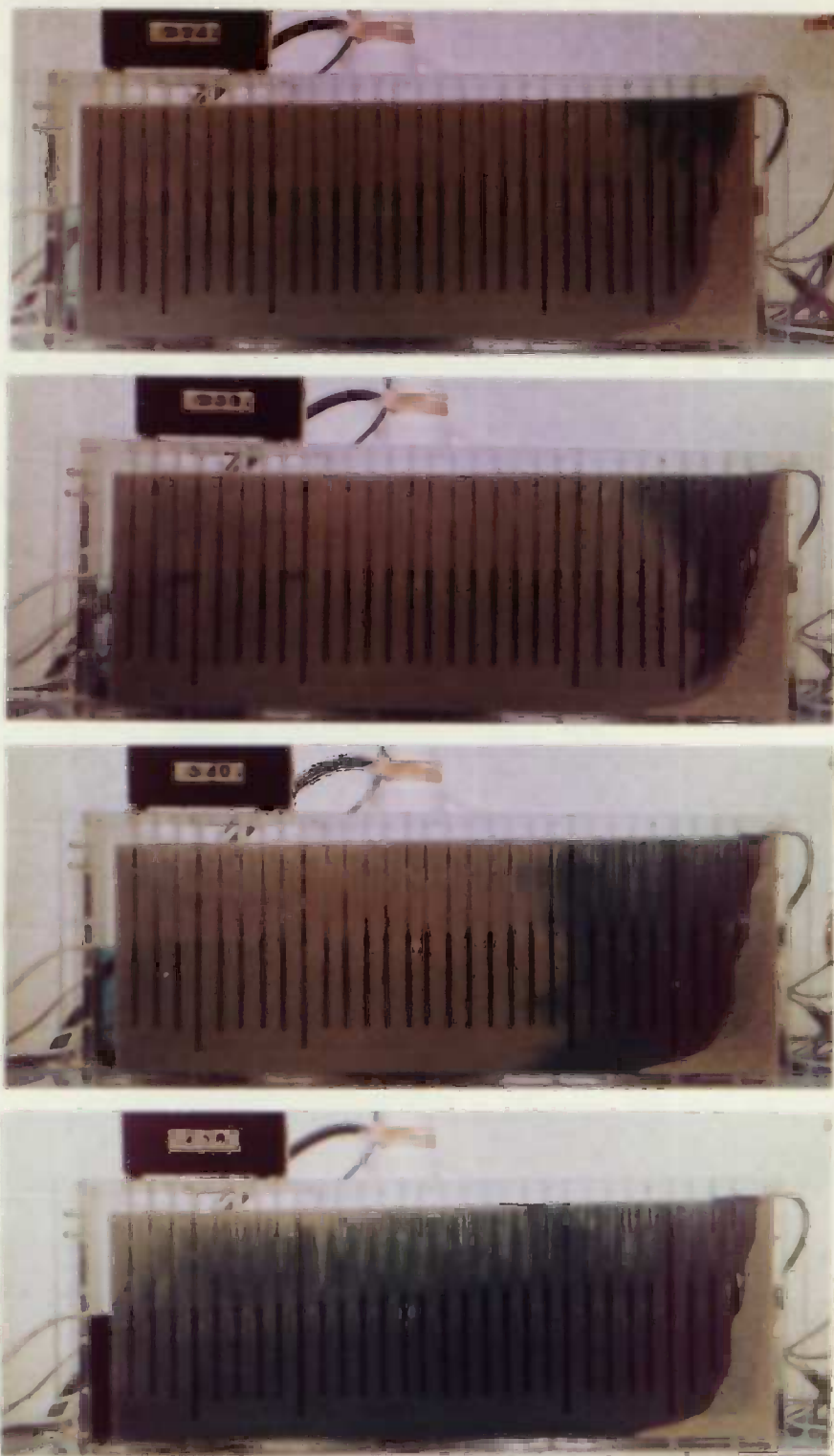


Figure 41. Photographic history of the cone of depression model, as green runoff water infiltrated into the subsurface of the porous medium.

ultimate cone of depression of a pumping well is the mechanism by which the recharge and discharge are again caused to be equal. When the cone of depression reaches a recharge area where previously recharge was being rejected, it causes the natural recharge to be increased by means of the steepened gradient. When the cone of depression reaches the discharge area it decreases the gradient and hence decreases the quantity of natural discharge. When a well is placed close to an area of rejected recharge such as a stream or swamp, its cone of depression rapidly reaches the recharge area, inducing increased natural recharge. Only a very shallow cone of depression is required in this case as can be seen in well A (Figure 37). When a well is placed far from the recharge area, it will take longer for the cone of depression to reach it and hence a deeper cone will result as in well B (Figure 36).

This model also points out an important fact to the mining industry. Namely, that it is possible to dewater portions of a mine without pumping water out of the mine excavation itself. Wells can be located in a circle around the excavation which will produce a multiple cone of depression completely eliminating any natural discharge into the excavation. In this model wells A and B (Figure 38) can be used to dewater the rock between them after which a dry excavation can be dug.

Probably the most important concept illustrated by this model is the idea that all the ground water within a single set of hydrologic and geologic boundaries is part of a single hydrologic system. Any action such as pumping imposed at one point in the system will have far reaching effects through out the whole system. Let us assume that wells A and B are owned by farmers A and B respectively. Farmer A must realize

that when he pumps his well it will effect the water level at the well of farmer B. Likewise farmer B must realize that when he pumps his well it will effect the well of farmer A. A subsurface aquifer along its areas of surface water recharge and discharge is a large integrated system which must be jointly controlled and operated by all the water users if the optimum benefits of its water supply are to be gained.

## CHAPTER VI

### CONCLUSIONS

The models discussed in this paper are hydrodynamically analogous to natural situations when the problems studied are effectively two dimensional, or when a three dimensional flow system can be accurately viewed along a two dimensional cross section.

Basic research with these scale models has aided in a visual affirmation of the following set of previously conceived principles of laminar ground water flow.

1. Saturated ground water flow must obey the "equation of continuity" as stated by Muskat (26).
2. Within the zone of saturation ground water flows from high hydraulic head to low hydraulic head.
3. The velocity of saturated ground water flow varies directly with the hydraulic gradient and inversely with the porosity in accordance with Darcy's Law (Eq. 3.8).
4. With few exceptions, ground water moves along laminar flow paths, which permits very little physical mixing of ground water.
5. Ground water flows contiguous to all impermeable boundaries within the zone of saturation.

6. Within a given set of boundary conditions, when the law of continuity is satisfied, ground water will seek paths of least resistance represented by rock of highest permeability.

7. Ground water will refract across a permeability interface in a direction that will allow it to remain in highly permeable material as long as possible, and in a direction that will allow it to pass out of low permeable material as soon as possible.

8. Areas of total stagnation may not occur within a saturated system upon which a hydraulic gradient has been imposed.

In summary, the following applications are emphasized:

(1) Models such as have been shown here can be constructed to simulate many known geologic and hydrologic situations and, therefore, can be used as a tool in applied research.

(2) Visual empirical experiments of the type described here will enable persons involved in ground water planning and development to better understand the phenomena of the dynamics of laminar flow in ground water systems.

(3) This simple, straightforward approach to the solution of ground water problems could aid in removing the mystery and confusion surrounding ground water movement, and will perhaps help to educate the student, layman, and lawmaker.

Proper warning should be given however, of the possibility of oversimplifying a problem by means of these models. The ground water systems are controlled by boundaries. Where improper boundaries are built into a model, a completely erroneous non-analogous flow system may be achieved. Great care and patience must be applied to see that

misconceptions are not spread in this manner.

Another problem which can arise with this type of model is the fascination which one can acquire for the flow patterns. No hydrologist should become too preoccupied with the configuration of streamlines that he loses sight of the reason why he is studying these flow lines. Practical study of the streamlines in a flow net lead to interpretation of the permeability of the porous media. Further interpretation leads to the determination of boundary conditions controlling the ground water movement. With this information the hydrologist is equipped to designate the optimum locations for the acquisition of ground water from pumping wells, and to predict the future effects of pumping on the ground water body.

In conclusion, the author offers the following evaluation of model studies as expressed by Barnes (2).

Model studies are neither a mechanical process for grinding out the right answers nor are the findings mere approximations of the truth because dynamic similarity is imperfectly attained. Significant results from model studies are to be expected only where experience and judgment derived both in the laboratory and in practical design and construction are brought to bear on the work.

## BIBLIOGRAPHY

1. Babbitt, H. E., and D. H. Caldwell, The free surface around, and the interference between, gravity wells, University of Illinois Eng. Exp. Sta. Bull. 374, Urbana, 60 pp., 1948.
2. Barnes, G. E. Compilation of reports on hydraulic model studies, Bull. 20, Univ. Iowa Studies in Eng., Iowa City, pp. 131-141, 1940.
3. Baumann, P., Ground-water movement controlled through spreading, Trans. Amer. Soc. Civil Engrs., vol. 117, pp. 1024-1074, 1952.
4. Boulton, N. S., The flow pattern near a gravity well in a uniform water-bearing medium, Jour. Inst. Civil Engrs., vol. 36, pp. 534-550, 1951.
5. Corey, A. T., CE 269, Fluid Mechanics of Porous Solids, Course Outline. Colorado State University, Fort Collins, Colorado, 1959.
6. Dachler, R., Grundwasserstromung, J. Springer, Vienna, 141 pp., 1936.
7. d'Andrimont, R., Note preliminaire sur une nouvelle methode pour etudier experimentalement l'allure des nappes aquiferes dans les terrains permeables en petit, Annales Soc. Geol. Belgique, vol. 32, Liege, pp. M115-M120, 1905.
8. d'Andrimont, R., Sur la circulation de l'eau des nappes aquiferes contenues dans des terrains permeables en petit, Annales Soc. Geol. Belgique, vol. 33, Liege, pp. M21-M33, 1906.
9. Hall, H. P., An investigation of steady flow toward a gravity well, La Houille Blanche, vol. 10, pp. 8-35, 1955.

10. Hamilton, D. K., Some solutional features of the limestone near Lexington, Kentucky, Economic Geology, vol. 43, no. 1, pp. 39-52, Jan-Feb 1948.
11. Hansen, V. E., Complicated well problems solved by the membrane analogy, Trans. Amer. Geophysical Union, vol. 33, pp. 912-916, 1952.
12. Hansen, V. E., Unconfined ground-water flow to multiple wells, Trans. Amer. Soc. Civil Engrs., vol. 118, pp. 1098-1130, 1953.
13. Harder, J. A., T. R. Simpson, L. K. Lau, F. L. Hotes, and P. H. McGauhey, Laboratory research on sea water intrusion into fresh ground-water sources and methods of its prevention--final report, Sanitary Eng. Research Lab., Univ. Calif., Berkeley, 68 pp., 1953.
14. Hele-Shaw, H. S., Stream-line motion of a viscous film, Rep. 68th Meeting British Assoc. for the Advancement Sci., pp. 136-142, 1899.
15. Horner, W. L., and W. A. Bruce, Electrical-model studies of secondary recovery, in Secondary recovery of oil in the United States, 2nd ed., Amer. Petroleum Inst., New York, pp. 195-203, 1950.
16. Hubbert, M. K., Theory of scale models as applied to the study of geologic structures, Bull. Geol. Soc. Amer., vol. 48, pp. 1456-1520, 1937.
17. Hubbert, M. K., Entrapment of petroleum under hydrodynamic conditions, Bull. Amer. Assoc. Pet. Geol., vol. 37, pp. 1954-2026, 1953.
18. Hubbert, M. K., The theory of ground water motion, Jour. Geol., vol. 48, pp. 785-944, 1940.
19. Kellogg, F. H., Investigation of drainage rates affecting the stability of earth dams, Trans. Amer. Soc. Civil Engrs., vol. 113, pp. 1261-1309, 1948.

20. Kirkham, D., Artificial drainage of land: streamline experiments, the artesian basin--I, Trans. Amer. Geophysical Union, vol. 20, pp. 677-680, 1939.
21. Kirkham, D., Pressure and streamline distribution in water-logged land overlying an impervious layer, Proc. Soil Sci. Soc. Amer., vol. 5, pp. 65-68, 1940.
22. Lamb, H., Hydrodynamics, Dover, New York, 738 pp. 1879.
23. Mavis, F. T., and T. P. Tsui, Percolation and capillary movement of water through sand prisms, Bull. 18, Univ. Iowa Studies in Eng., Iowa City, 25 pp., 1939.
24. Mills, R. V. A., Experimental studies of subsurface relationships in oil and gas fields, Economic Geology, vol. 15, pp. 398-421, 1920.
25. Mills, R. V. A., Relations of texture and bedding to the movements of oil and water through sands, Economic Geology, vol. 16, no. 2, pp. 124-141, 1921.
26. Muskat, M., The flow of homogeneous fluids through porous media, McGraw-Hill, New York, 763 pp., 1937.
27. Nemeth, E., L'importance de la loi de filtration de Darcy a la lumiere des resultats de quelques essais sur modeles reduits, International Geodetic and Geophysical Union, Symposia Darcy, Publ. 41, Assoc. Int'l d'Hydrologic Scientifique, vol. 2, pp. 116-127, 1956.
28. Nomitsu, T., Y. Toyohara, and R. Kamimoto, On the contact surface of fresh- and salt-water under the ground near a sand sea-shore, Mem. College Sci., Kyoto Imperial Univ., Ser. A, vol. 10, no. 7, pp. 279-302, 1927.
29. Pennink, J. M. K., Grondwater stroombanen, Stadsdrukkery, Amsterdam, 151 pp., 1915.
30. Potter, W. D., and M. V. Baker, Some of the factors influencing the behavior of perched water-tables at the North Appalachian Experimental Watershed near Coshocton, Ohio, Trans. Amer. Geophysical Union, vol. 19, pp. 393-402, 1938.

31. Skibitzke, H. E., Radioisotopes in the laboratory for studying groundwater flow. International Geodetic and Geophysical Union Assemblée Generale de Helsinki Assoc. Int'l d'Hydrologic Scientifique, pp. 513-523, 1960.
32. Stallworth, T. W., Quickly constructed model facilities seepage studies, Civil Eng., vol. 20, no. 7, pp. 45-46, 1950.
33. Rose, H. E., An investigation into the laws of flow of fluids through beds of granular material, Proc. Inst. Mech. Engrs., vol. 153, pp. 141-148, 1945.
34. Theis, C. V., The significance and nature of the cone of depression in ground water bodies, Economic Geology, vol. 33, no. 8, pp. 889-902, December 1938.
35. Theis, C. V., The source of water derived from wells essential factors controlling the response of an aquifer to development, Civil Engineering, pp. 277-280, May 1946.
36. Todd, D. K., Unsteady flow in porous media by means of a Hele-Shaw viscous fluid model, Trans. Amer. Geophysical Union, vol. 35, pp. 905-916, 1954.
37. Todd, D. K., Ground Water Hydrology, John Wiley and Sons, New York, 336 pp., 1959.
38. Wyckoff, R. D., and H. G. Botset, An experimental study of the motion of particles in systems of complex potential distribution, Physics, vol. 5, pp. 265-275, 1934.
39. Wyckoff, R. D., and H. G. Botset, and M. Muskat, Flow of liquids through porous media under the action of gravity, Physics, vol. 3, pp. 90-113, 1932.